# GHOST IMAGING FOR FINGERPRINTS WITH THE SELF - ASSOCIATIVE HOLOGRAPHIC MEMORY

Thesis for the Degree of Ph. D.
MICHIGAN STATE UNIVERSITY
ROLAND KRANZ
1974

This is to certify that the

thesis entitled

# GHOST IMAGING FOR FINGERPRINTS WITH THE SELF - ASSOCIATIVE HOLOGRAPHIC MEMORY

presented by

ROLAND KRANZ

has been accepted towards fulfillment of the requirements for

Ph. D. degree in Electrical Engineering and Systems Science

Richard J. Reid

Major professor

Date April 30, 1975

**O**-7639

. . . .

#### ABSTRACT

GHOST IMAGING FOR FINGERPRINTS WITH THE SELF-ASSOCIATIVE HOLOGRAPHIC MEMORY

Вy

#### Roland Kranz

A concept is presented for automatic latent fingerprint identification utilizing a holographic memory fingerprint file. The memory is termed as "self-associative" and is a memory in which recall is by ghost imaging, or code transformation. It is assumed that the input to the system, the latent print, is in transparency form, with the memory being in the form of photographic emulsion plane amplitude holograms. The process involves coherent spatial filtering, extended-reference-source coding, and storage of fingerprints, as well as variants, such as obtained due to excessive printing pressure, as Fourier-transform subholograms. The subholograms are spatially separated holograms containing the code-differentiated fingerprints recorded in superposition. Consecutive exposure spatial-frequency multiplexing is utilized in the recording process to maximize output discrimination. Coherent optical image processing parameters are examined in terms of the requirements for practical implementation. The important parameters in this case are shown to be the beam offset angle, the beam ratio, reconstruction positioning accuracies, and hologram efficiency. The proposed method is aimed at obtaining improved identification accuracy by utilizing multiple discriminant functions. This technique gives high density redundant storage, and identification is shown to be possible even if the latent print is imperfect or only a partial latent print is available.

# GHOST IMAGING FOR FINGERPRINTS WITH THE SELF-ASSOCIATIVE HOLOGRAPHIC MEMORY

Ву

Roland Kranz

## A THESIS

Submitted to
Michigan State University
in partial fulfillment of the requirements
for the degree of

DOCTOR OF PHILOSOPHY

Department of Electrical Engineering and Systems Science

#### **ACKNOWLEDGMENTS**

It is a pleasure to thank Professor R. J. Reid, the author's adviser, for guidance in the preparation of this dissertation, and for support throughout the graduate program. Appreciation is given to Dr. W. L. Kilmer for introducing the author to holography and the theories of associative recall. The author is indebted to the members of his committee, Drs. R. O. Barr, Jr., R. C. Dubes, J. S. Frame, and G. L. Park, for their help in making this work possible. All of the above have served and will continue to serve as an inspiration for personal and professional excellence. The author also would like to thank his wife, Aira, for deciphering the first rough draft, and his family for their interest, encouragement, and patience.

# TABLE OF CONTENTS

|      |                           |  | Page |
|------|---------------------------|--|------|
| LIST | OF T                      | ABLES  | v    |
| LIST | OF F                      | IGURES   | vi   |
| NOME | NCLAT                     | URE  | viii |
| Chap | ter                       |  |      |
| ı.   | INTR                      | ODUCTION   | 1    |
| II.  | MEMORIES AND FINGERPRINTS |  | 6    |
|      | 2.1                       | Memory Requirements In Automatic Fingerprint Processing and File Searching                                 | 6    |
|      | 2.2                       | · · · · · · · · · · · · · · · · · · ·  | 11   |
|      |                           | Associative Information Storage: CAM and Holographic   | 14   |
|      |                           | Previous Research In Holographic Assistance for Fingerprint Identification                                 | 19   |
| III. |                           | HOLOGRAPHIC MEMORY AND TWO-DIMENSIONAL RMATION PROCESSING  | 25   |
|      | 3.1                       | Holographic Techniques Applicable In Fingerprint Identification  | 25   |
|      | 3.2                       |  | 29   |
|      | 3.3                       |  | 37   |
|      | 3.4                       | Hologram Efficiency  | 44   |
|      | 3.5                       | •  | 48   |
|      | 3.6                       |  | 51   |
|      | 3.7                       | The Recall Variables: Latent Fingerprint Transparency and FTH Memory Frame, Filter, Positioning Accuracies | 55   |
|      | 3.8                       | The Extended-Reference-Source, "Ghost Imaging", or Self-Associative Holographic Memory                     | 59   |
|      | 3.9                       | Summary of Theoretical Considerations  | 63   |

| Chapter |   |  | Page |
|---------|---|--|------|
| IV.     | THE SELF-ASSOCIATIVE HOLOGRAPHIC MEMORY AND RECORDING/<br>RETRIEVAL OF FINGERPRINT DATA |  | 6.5  |
|         | 4.1   | Description of the Proposed Self-Associative Holographic Memory  | 65   |
|         | 4.2   | Capabilities of the Self-Associative Holographic Memory In Automatic Fingerprint Identification                              | 73   |
|         | 4.3   | Provisions for Accurate Latent Fingerprint Trans-<br>parency and FTH Filter Positioning In the Recall,<br>or Search, Process | 83   |
|         | 4.4   | ·  | 84   |
|         | 4.5   | Requirements On the Parameters of the FTH Self-<br>Associative Memory for Successful Retrieval of<br>Stored Data             | 89   |
|         | 4.6   | Summary of Design Considerations   | 99   |
| V .     | GENE  | ERAL SUMMARY, CONCLUSIONS, AND FUTURE RESEARCH   | 101  |
| APPE    | ENDIX   | VARIATIONS ON THE DESCRIBED SYSTEM   | 104  |
| BIBI    | IOGRA   | APHY   | 106  |
| REFE    | ER ENC E  | ES .   | 111  |

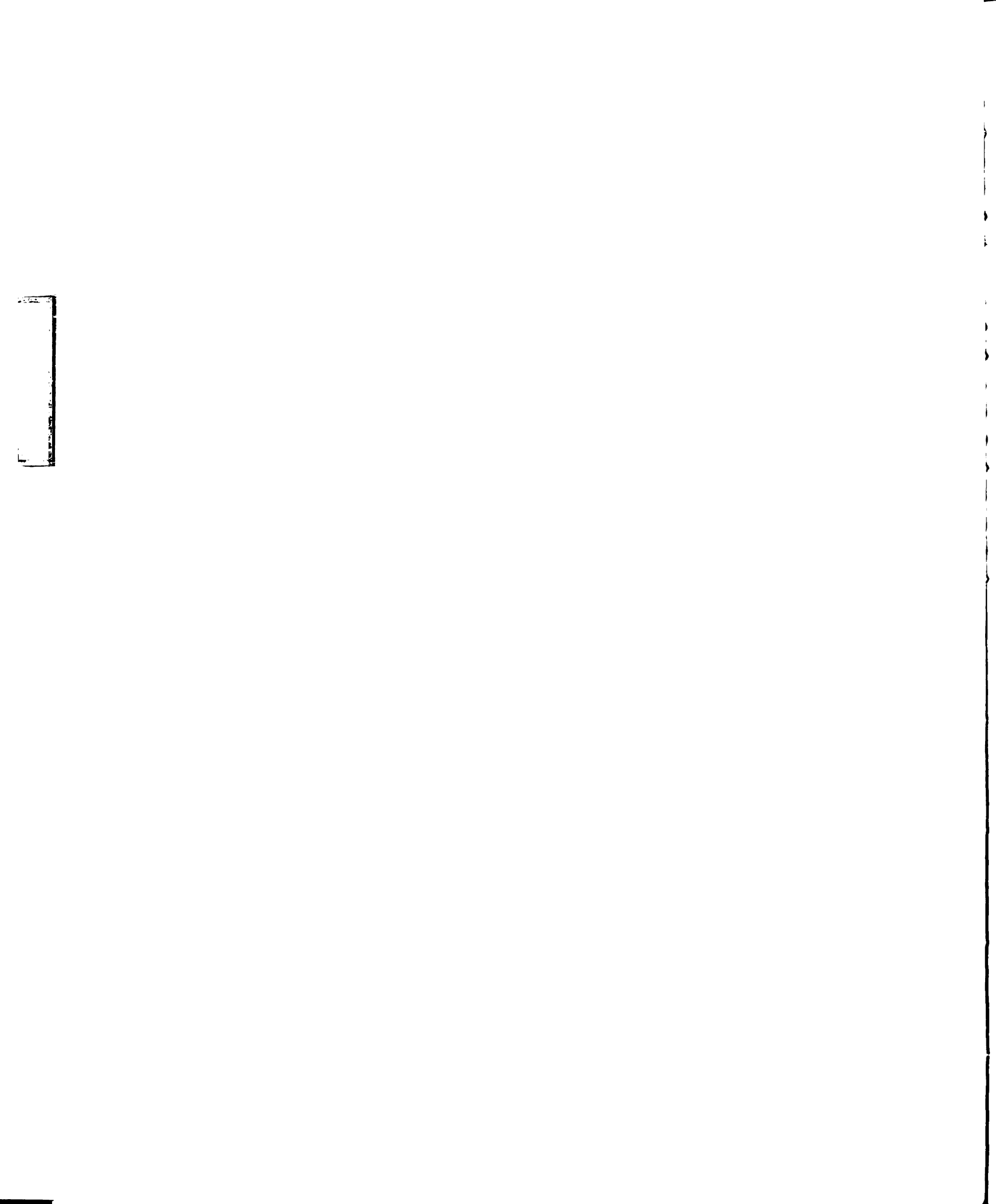
## LIST OF TABLES

| Table |  | Page |
|-------|--|------|
| 1.    | Holographic Memory Input Parameters          | 39   |
| 2.    | Holographic Memory Storage Medium Parameters | 40   |
| 3.    | Holographic Memory Recall Parameters         | 41   |

## LIST OF FIGURES

| Figure |   | Page       |
|--------|---|------------|
| 1.     | Latent Fingerprint Identification Utilizing the Self-Associative Holographic Memory   | 11         |
| 2.     | An Interference Method for Fingerprint Comparison   | 20         |
| 3.     | Forming the Optical Fourier Transform   | 27         |
| 4.     | Two-Dimensional Spatial-Frequency-Plane Filtering   | 28         |
| 5.     | An Interferometric Matched Filter Generator   | 31         |
| 6.     | Recording of the Interference Pattern Produced by Two<br>Plane Waves From the Same Coherent Source to Form a<br>Hologram              | 31         |
| 7.     | Generation of Two Real Images With a Fourier-Transform Hologram   | 35         |
| 8.     | Two Arrangements for Forming a Fourier-Transform Hologram (a) With a Lens, and (b) Without a Lens                                     | 36         |
| 9.     | Diffraction Efficiency as a Function of Offset Angle<br>Between Object and Reference Beams  | 47         |
| 10.    | Longitudinal Filter Displacement From the Frequency Plane   | 58         |
| 11.    | Forming the Extended-Reference-Source Fourier-Transform Hologram  | <b>6</b> 0 |
| 12.    | Output Plane Light Distribution From a Coherent Optical Matched-Filter Correlator Showing the Autocorrelation of an Oily Fingerprint. | 64         |
| 13.    | Twenty-seven Variants/Fingerprint, Ten-Finger File  | 66         |
| 14.    | The Rotation Variants   | 66         |
| 15.    | Consecutive Recording of (a) Fingerprint Variants and (b) Different Fingerprints In Superposition                                     | 67         |
| 16.    | Recording the Self-Associative Hologram: Functional Diagram   | 69         |

| Figure |  | Page |
|--------|--|------|
| 17.    | Hololens Search for a Fingerprint Match With a Latent Fingerprint Input: Functional Diagram          | 71   |
| 18.    | Searching Several Pages in Parallel by Use of a Compound<br>Structure of Beam Splitters              | 72   |
| 19.    | Recording the Self-Associative Hologram  | 75   |
| 20.    | The Self-Associative Hologram Physical Geometry  | 76   |
| 21.    | Recall With the Self-Associative Hologram  | 78   |
| 22.    | Total Object Transmittance O = Fingerprint Variant<br>Transmittance F + Its Array Code Transmittance | 85   |
| 23.    | Complex Amplitude Distributions In the Output Plane $P_3$  | 87   |



### NOMENCLATURE

- = spatial convolution
- 🗶 = spatial correlation
- ★ = complex conjugate

- cdo = tilt of the reference wave, or angle of the reference wave
   propagation vector which it makes in the y-z plane with the
   z-axis (with the object wave propagation vector parallel to
   the z-axis)
- 6 = offset angle, or angle that each of two interference pattern forming wave normals makes with the interference planes
- $\phi$  = phase
- a = fringe period
- **\beta** = code string
  - b = distance from the center of a fingerprint variant to the nearest point source of its array code in the y-direction of the input plane
  - D = code plate aperture
- $D(\beta_1, \beta_2)$  = hamming distance
  - c,d = object plane displacements
    - E = exposure
  - = hologram reconstruction efficiency
    - = intensity of a reconstructed wavefront/total intensity of the reconstruction beam
    - f = latent fingerprint
  - $f_1$  = focal length of the lens

F = stored fingerprint variant

F.T. = Fourier-transform

FTH = Fourier-transform hologram

F[] - denotes F. T.  $F[f(x,y)]=F(p,q)=\iint_{-\infty}^{\infty} f(x,y)\exp[+j(px+qy)]dxdy$   $F^{-1}[] - \text{denotes inverse } F. T.$ 

F<sup>-1</sup>[F(p,q)]=f(x,y)=
$$(\frac{1}{2\pi})^2$$
  $\int_{-\infty}^{+\infty}$  F(p,q)exp[-j(px+qy)]dpdq

Note: p,q chosen to be positive, with these functions being defined only at specific points in their respective planes

$$t(y_1) \longrightarrow T(q)$$

$$F(y_1) \longrightarrow F(q)$$

$$f(y_1) \longrightarrow f(q)$$

$$g = g(x_1,y_1) \longleftrightarrow G(p,q)$$
  
= signal = stored fingerprint variant (transparency)

h = filter impulse response

input = latent fingerprint (transparency)

k = beam ratio = reference beam intensity/object beam intensity at the hologram

1 = distance between planes  $P_1$  and  $P_2$ , Figure 5

L = signal length

 $L_c$  = extent of the code array in the y-direction

 $L_{\rm p}$  = maximum extent of a fingerprint variant in the y-direction

m = number of fingerprint variants superposed on one subhologram

MxN = two-dimensional code matrix of point sources

n = number of code points above threshold

 $n(x_1, y_1) = input noise$ "negative ridges" = transparent fingerprint ridges on opaque background to minimize background noise  $NxN = N^2$  cell subdivisions of a binary hologram plane N(p,q) = spectral density 0 = total stored information = stored fingerprint variant + its array code = spatial frequency variables (radians/unit distance) = distance variables in plane  $P_2$ , related to p and q by  $\xi = \lambda p f_1/2\pi$  and  $\chi = \lambda q f_1/2\pi$  with  $\xi$  parallel to x and  $\chi$  parallel to y P, = input, or object, plane  $P_2$  = Fourier, or frequency, plane  $P_3$  = output, or image, plane  $\Delta P$  = filter displacement normal to the optical axis r = r(x,y) = complex light amplitude transmitted by thehologram s = recording medium thickness  $S_{L}/S$  = discrimination ratio = autocorrelation coefficient/ cross-correlation coefficient t or  $t_A = amplitude transmittance$ =  $t_A(x,y)$ = transmitted complex field/incident complex field at each point (x,y)  $t_{o}$  = amplitude transmittance of the unexposed recording medium **↑** = exposure time  $V_{N}$  = visibility of  $N^{th}$  fringe pattern W = bandwidth of signal g w = code point spacing = distance variables in plane  $P_{i}$ 

#### CHAPTER I

#### INTRODUCTION

Law enforcement agencies have accumulated fingerprint records numbering in the millions. A major problem is the lack of a method of accurate automatic matching of a latent print discovered at the scene of a crime against this almost unlimited file. A holographic technique may provide the solution to this problem.

A "hologram" may be defined as a recording of the interference pattern of two or more coherent wavefronts, the object wavefront and a reference wavefront. The diffraction grating thus formed stores information. The recorded interference fringes serve as a "lens system" to form a virtual or real image of the object when the hologram is illuminated by the reference, or read-out, beam.

From an intuitive viewpoint a holographic storage medium that operates directly on the two-dimensional fingerprint seems to be most applicable as a high-access-speed memory. This dissertation thus proposes and investigates the feasibility of a self-associative, or "ghost-imaging", holographic memory for use as the main element in automatic fingerprint identification.

The self-associative holographic retrieval of information has been defined as "ghost" or "phantom" imaging by vanHeerden [1], Stroke [2], and Collier and Pennington [3]. This type of holographic memory is described here as "self-associative," following the nomenclature of Kohonen [4]. The self-associative memory is defined as a memory in which a stored pattern itself, or any part of it, can be used as the retrieval key. Further, this memory will have redundant storage;

that is, the memory will tolerate a large number of flaws that occur (1) in the memory medium, and (2) in the key information.

Experimental results for automatic character recognition using a self-associative method similar to the method proposed here are reported by Nakajima, et al., [5]. The process there is described as storage by use of the "code-transform hologram" technique.

Use of complicated sources or patterns, such as Chinese ideograms or fingerprints, as key objects has been suggested by Garbor and Stroke [6]. An application of the self-associative technique to character recognition has also been described by Gabor [7], and provides the major impetus for this dissertation.

The usual method of recording for holographic information storage involves associating the data with a simple reference beam. In Gabor's method the association is between alphabetic or numeric characters, or variants, and code words formed by an array of point sources. This method is also analyzed by Collier, et al., [8], and will be termed here as the "extended-reference-source hologram" technique.

The fingerprint data memory would consist of holographic storage of each fingerprint with variants, such as, for example, to account for slight rotations or variations in fingerprint pressure, in association with a point-source array code word. Several detection filters, i.e. fingerprints with their variants, would be recorded on each hologram in superposition by consecutive exposure.

In order to retrieve the stored fingerprint information the memory would be illuminated with the light beam transmitted by a transparency (or equivalent optical modulator) of a latent print. The latent print may possibly be a variant or fragment of a stored print. This would

then recall the stored fingerprint as well as its code. The code is a "ghost image," since it is not directly addressed, and is recalled by association with its particular recording print. Further processing by digital computer methods would proceed to give a complete identification file for the latent print. An outstanding property in terms of practical application of this system, and as found also in spatial filtering point-reference-source methods, is that the identification can be carried out even if only part of the latent print is available, as is usually the case.

The self-associative memory as considered here would be in the form of Fourier-transform holograms. The usual recording medium used to form this hologram is a photographic emulsion. Development of photographic film or plates is time-consuming. Thus, in order to realize real-time optical fingerprint storage, a suitable memory medium must be found.

Experiments to find possible permanent, erasable, holographic memory mediums are continuing, and involve consideration of such materials as photochromics, electrostatics, magnetics, and ferroelectrics [9], [10], [11]. A major requirement of the storage medium is read/write capability, as opposed to the read-only (ROM) property of photographic film-type optical memories.

Most storage system parameters reflect the particular memory medium utilized. For the present an implicit assumption is made that a "permanent" holographic storage medium is desired. It is therefore assumed that the fingerprint data is recorded in hologram form, with a laser providing a bright, highly coherent light source, and using a photographic film or plate archival memory medium. The use of a "thin"

emulsion is assumed, where the emulsion thickness is of the order of one recording light wavelength. High resolution photographic film has at present the highest sensitivity of any storage medium considered. Also, fast erasure may not be a requirement for fingerprint data storage.

The basic structure of an optical processor involves coherent spatial filtering. The input material is usually not in the form of a transparency, which implies that a photographic intermediary must be made before performing the coherent optical processing. This problem may be solved by the use of real-time incoherent-to-coherent converters as input transducers.

An approach to real-time optical information processing by use of a Pockels effect real-time electro-optic image modulator is discussed by Nisenson and Iwasa [12]. This on-line two-dimensional spatial light modulator would be utilized as an active filter as well as for direct input conversion. The converter function allows real-time introduction of hard copy into a coherent processor. Complex spatial filter systhesis would be by the usual two-beam interference hologram formation methods, by use of a transparency object.

A typical real-time optical modulator (made of Bi<sub>12</sub>SiO<sub>20</sub>) has a dark storage time of several hours, and a cycle time in milliseconds. A variation of this real-time method is proposed here utilizing a permanent plane hologram storage medium, instead of the image modulator store. The solution of real-time hologram spatial filter introduction into the system by imaging is not expected to be an insurmountable obstacle. This is not pursued here. For present purposes signal injection into the processor, corresponding to the stored fingerprint

file, is assumed to be accomplished by photographic film or plates.

Use of the self-associative holographic memory is discussed in Chapter II in terms of where it would fit in a memory hierarchy, as operating in a fingerprint data file-searching mode. Chapter III discusses different pattern processing techniques based on holographic information storage. A coherent optical image processing background is used to indicate the importance of involved parameters.

The chief obstacle of automatic fingerprint processing is print quality. The emphasis of Chapter IV is, thus, on analysis of the performance of the proposed self-associative holographic memory system when dealing with imperfect inputs. Parameters examined are the latent transparency and hologram positioning accuracies required for image formation, the effect of using a code word spatially modulated reference source instead of a point reference source, and allowances for retrieval key (latent fingerprint) imperfections.

The main purpose of this investigation is to explore the potential of a holographic memory, which is accessed by an extended-reference-source coding scheme, to give very high storage density, and a possible increase in accuracy over previously considered holographic techniques for fingerprint identification. The specific fingerprint processing step considered is that of matching a latent fingerprint against a tenprint file.

#### CHAPTER II

#### MEMORIES AND FINGERPRINTS

A system for rapid and automatic fingerprint processing is visualized as the basis for automatic verification, or authentication, of personal identity. To implement this system, operational requirements, and interfaces with present fingerprint storage systems need to be analyzed. Integration with, and modification to existing operations must be considered in terms of economy. Such factors as information transmission, fingerprint readers, and display requirements must be taken into account. A proposed memory must also be examined first from a feasibility viewpoint, with respect to the type of data to be stored.

The concern here is with the storage/retrieval process for fingerprint data. The discussion in this chapter therefore focuses on the
applicable memory technologies and methods in the memory hierarchy
which can be utilized for the establishment of a holographic memory
data file.

# 2.1 Memory Requirements In Automatic Fingerprint Processing and File Searching

The present prevalent fingerprint storage "memory" consists of card files. Fingerprint processing is a multi-step process. The first step, an initial classification by trained experts, offers enough information to route a fingerprint card received from law enforcement agencies across the nation to the appropriate section of files for searching. In this preliminary classification the ridge detail of prints is examined by skilled technicians through magnifying glasses.

Descriptive numerical and letter symbols for each individual finger are recorded in specified sequence.

The next step involves taking this completely classified set of prints, or print, and comparing it against cards with similar patterns in the master file. This comparison is again a manual process, and requires the checking of maybe hundreds of cards on file with prints closely resembling those being tested.

Currently the only generally accepted fingerprint classification technique is the Henry system and its derivatives [13]. In this system sets of usually five or all ten fingerprints are classified using only a few features of each print. That is, the identification and classification is based on the print "minutiae," which include loops, whorls, and arches.

The filing of fingerprint cards is generally by use of ten-finger classification schemes, such as the Henry system. The Henry system allows for 1024 major subcategories. In order to search a file efficiently, information from all ten fingers is required.

Most latent fingerprints, i.e. those left by criminals at the scene of a crime, are single prints. It has not been feasible to search a large ten-finger card file using the information from a single print. Special single fingerprint files of limited size have been established to enable a more efficient search with latent finger-print inputs.

A widely used single print classification system is the Battley system [14]. The Battley system is based on topological combinations of print features presented on a pictorial classification guide.

However, the Battley system has been found inadequate for the

-

increasingly larger files.

Fingerprint identification may also be linked to personal characteristics data in a special fingerprint file. Latent fingerprints are matched with fingerprints on file through a unique code. By entering a special code, related to any physical characteristics of the offender if they are known, the size of the search group can be reduced to a select group of classified fingerprints. A fingerprint file search that formerly took four or five hours can in this case be completed in fifteen to twenty minutes.

At the present time manual or semi-manual fingerprint file storage and search techniques are being eliminated. Data formerly on finger-print cards, police records, and photographs may now be found stored on files in a computer system. Most of this identification information is stored either on disc memory or on microfilm. Interaction between the computer and microfilm viewers is commonly accomplished through teleprinter terminals.

The new detective may actually be a computer system, but due to the sheer volume of offensive and arrest data, the mechanical limitations of the system tend to limit its utility. Using digital techniques, the first step for identification of a latent print is classifying the print by means of a computer as being a member of one or several groups. This reduced file is then examined visually, on a microfiche viewer or CRT printed code interface. The final positive identification still rests with a fingerprint analyst. To make computer techniques more effective, a more automatic fingerprint processing system is essential. Accuracy and speed are the important feasibility parameters.

The basic problem in attempting to duplicate the faculties of the human eye and brain by automatic-mechanical means is that the human makes allowances for inconsistencies. The human allows for such distortions as caused by dirt, physical growth, or rotation.

The most common imperfections are: ridge discontinuities, or gaps, and contiguous ridges. Contiguous ridges are caused by spreading of ink, skin oils, finger pressure, particles of skin, or by excessive inking or smearing during rolling of the finger. Other imperfections are due to lightly inked prints, thin ridges, excessive pore structure, such as enlargement due to illness, which appears as dotted or perforated ridges, and damaged or scarred fingers [14].

If a fingerprint is deformed by pressure or by the nature of the surface on which it is recorded, the detail is deformed very little. The identification by characteristic points is not affected. The topological structure of a fingerprint is invariant under distortions due to rolling, stretching of the skin, changes in the size of the finger, and translation or rotation of the print. Any effective automatic fingerprint identification system should therefore be based on topological matching. Also, any automatic single print interpretation technique should be able to extract all necessary identification information from each print.

The basic optical method which has been proposed to achieve automatic fingerprint identification is that of template matching, or optical correlation (see Section 2.4). Optical methods may circumvent the problems of feature detection, but face problems of print orientation, changes in size, and shape distortion. These variations do not affect the topological properties of the print. However, in the

fingerprint matching process, the correlation peak output response decreases as the input departs from the nominal. The latent print input must have a size, orientation, and quality comparable to the stored print. This "standardization" can be accomplished by several means, and one method is indicated in Section 4.1.

Improvements in linear density in magnetic-disc memories may slow the development of any new high density optical memory systems, such as those based on holographic storage. For a new memory technology to be competitive other advantages besides high density are also required.

The users of a fingerprint identification system are concerned with the retrieval of stored information. The ease, simplicity, and cost of using the retrieval apparatus becomes very important.

Holograms are difficult to record and very simple to retrieve. With archival holographic (read-only or ROM) storage the ease of recording is not particularly important since the recording activity may be limited to a few locations that specialize in recording. Far more fingerprint identification retrieval systems are required than recording systems. The self-associative holographic memory finger-print retrieval (matching) process is delineated by Figure 1.

The utilization of a fingerprint search system that processes and stores two-dimensional fingerprint data directly is supported by feasibility studies of the use of satellites to satisfy the data transmission needs of law enforcement agencies [15]. A satellite-based fingerprint transmission system using facsimile equipment for high-speed transmission of fingerprint images is considered technically feasible, and is recommended as the best solution to high volume data

transmission problems.

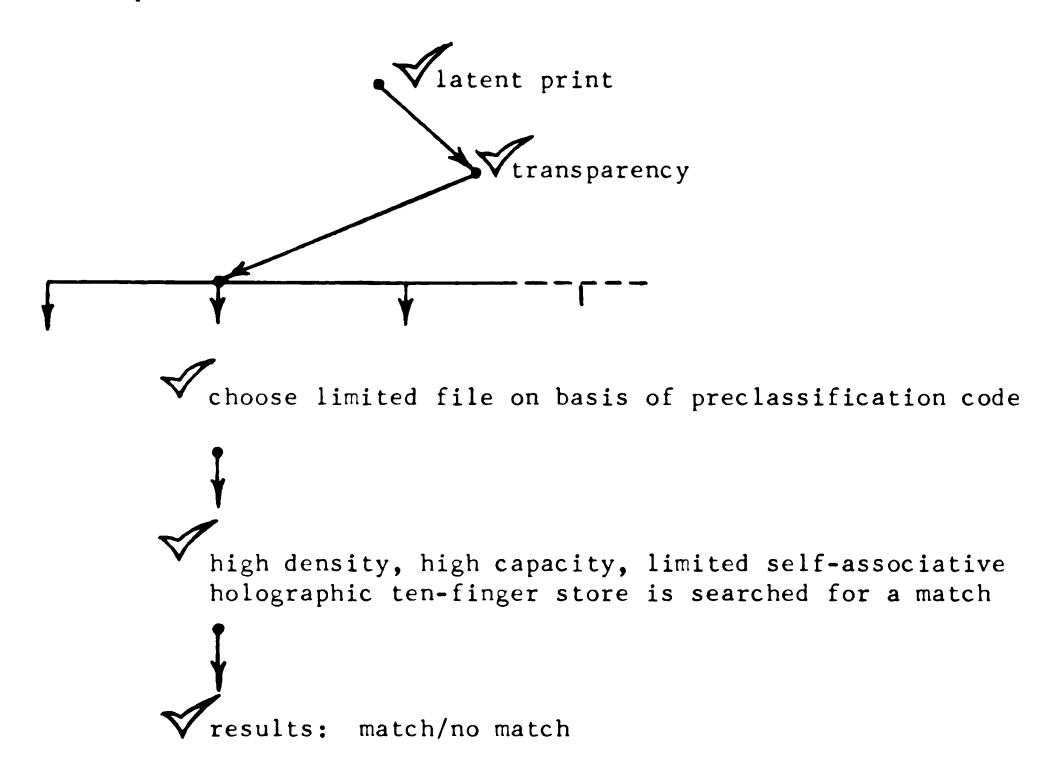


FIGURE 1. Latent Fingerprint Identification Utilizing the Self-Associative Holographic Memory.

A fully automated latent fingerprint identification system must handle prints which may be smudged, partially obscured or missing, or combined with other prints from the same person or different persons. The application of a holographic system to latent fingerprint identification will then depend on its ability to deal with the special set of problems provided by imperfect inputs. A useful hologram memory must have fast search speed and proven superiority in match/no-match retrieval accuracy.

# 2.2 The Memory Hierarchy

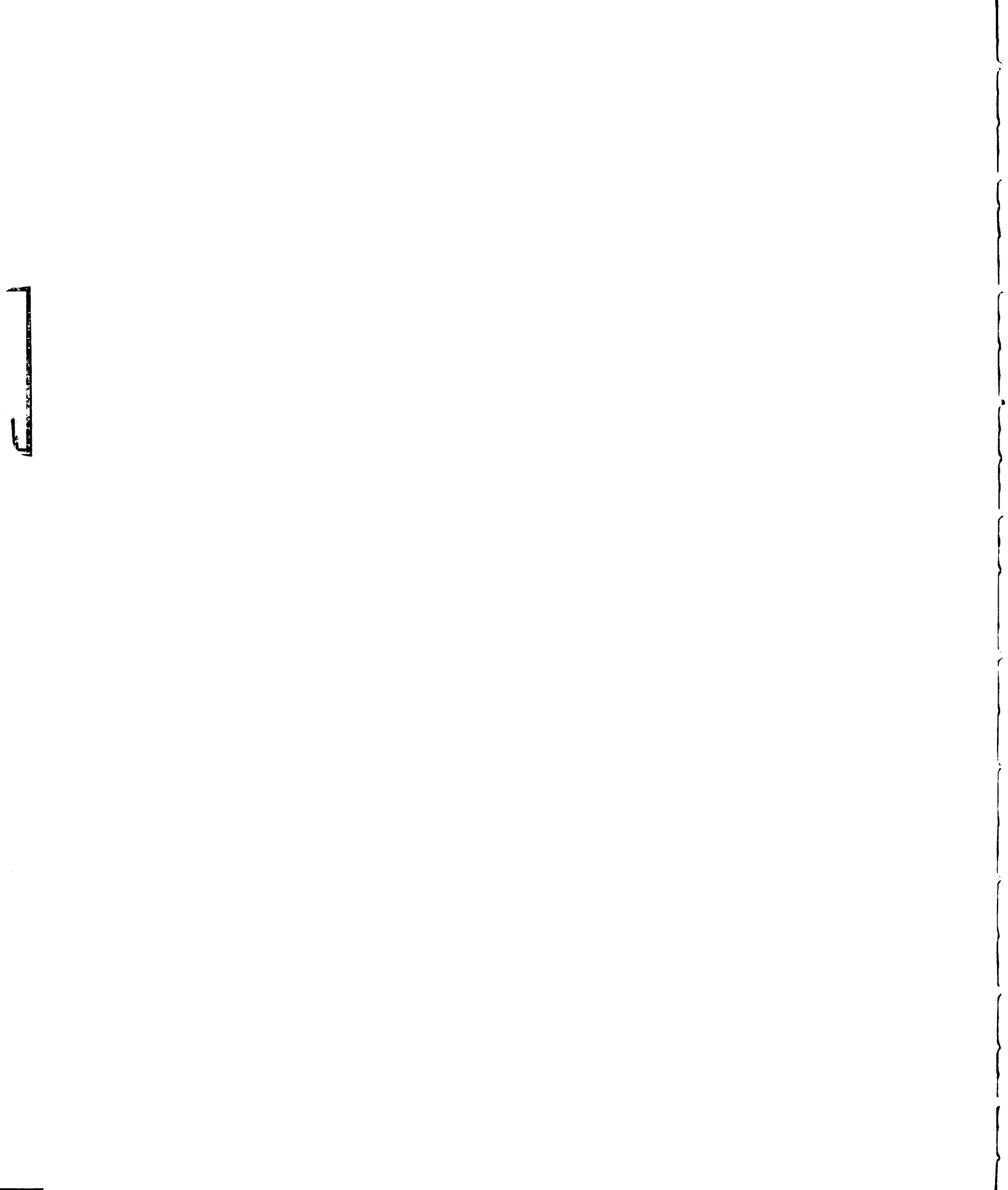
For a given cost, memory systems exhibit a trade-off between speed and capacity. Thus a computer may be equipped with several

memories which are used together in a coordinated way to form a hierarchy. Cost of the main memory is usually the deciding economic factor in the total cost of the computing system. Memory design becomes the guide to practicality.

Speed, cycle or access time, of the computer memory has been the criterion of computer performance because it has represented the advancing state-of-the-art. However, as with using IC's, for example, reliability and complexity should also be considered for design priorities. As expressed by N. DeWolf on IC's, "what needs to be looked at is the total economic justification" [16]. New system organizations, therefore, rather than further advances in circuit and memory speed, are expected to increase computer system computational capability.

Replacement of different categories of memories by future memories will most likely result from the batch fabrication advantages of the replacing memories. Significant advantages will be needed over the well established technologies, such as magnetic core, for new technologies to be economically feasible. Two cost factors should always be considered when developing a new approach: (1) will costs be reduced in the proposed application, and (2) low cost of the computer itself, so as not to negate the savings from the first factor.

Optical holographic memories may compete with core and semiconductor memories when used for main frame storage, with random-access,
read-write capability, and fast (1 sec or less) access time. Other
possibilities for the holographic memory are as a buffered memory with
random-access, read-write capability, and slow access time (of more



than 1 msec) to compete with discs and drums, as a read-mostly memory to compete with magnetic tape, or as an archival read-only memory, with high storage capacity ( $10^8$  bits or larger), to compete with microfilm.

The present experimental optical holographic binary memories combine the large capacity of mass storage, such as discs, with the short access times of bit-type memories such as cores and IC's, and at a cost much less than cores or IC's [17]. The low cost is justified by the basic simplicity of the optical memory.

Sufficient progress seems to have been made at the present time to indicate eventual realization of practical read/write holographic storage [18],[19]. However, a ROM for archival storage, using an array of permanent holograms, is more of a near-term possibility.

Optical methods of information processing are attractive due to the high spatial resolution and bandwidth existing at optical wavelengths. Extremely high densities of information can be handled, using the inherently high information capacity of the two-dimensional aperture. Ideally, the only restriction on information density is imposed by diffraction limitations.

All the information contained in the two-dimensional image(s) is processed in parallel utilizing coherent optical processing methods. This capability is needed for fast searching of a single latent finger-print against a ten-finger file.

The optical system's "instantaneous" results, however, are obtained only in the comparison process. This is preceded by either insertion of a personalized hologram card (in access control for example) or a lengthy search of a large print file. A comparison of digital vs. optical automatic fingerprint identification systems therefore must

also consider other parameters such as accuracy, degree of automation, etc.

### 2.3 Associative Information Storage: CAM and Holographic

Storage of information such that retrieval is by means of 'data' association requires a content-addressable memory or CAM. With a CAM, access is determined by the content of the word searched for. Use of the word "associative" is then more properly reserved for retrieval of information on the basis of 'ideas' or 'patterns.'

Content addressing gives a significant increase in speed and programming efficiency over location addressing if the data set is unordered, or if the data can be addressed by sets of reference properties. Search functions such as nearest neighbor and pattern recognition functions are examples of associative memory applications.

Associative processing becomes particularly efficient when the same computation must be applied to a large number of data sets, such as in comparing a fingerprint against a file.

Application of CAM's has been limited by the high cost of the more complex memory addressing hardware that would be required.

Also, no proven superiority of the CAM's for general purpose use has been exhibited. Associative hardware organizations as special-purpose auxiliaries to conventional computers seem to be justified, however, by a large range of possible applications.

Optical memory technology may be considered where there is a need for very large volume (order of  $>10^8$  bits) high density data storage. Automatic fingerprint identification system implementations using holographic techniques can be visualized with the memory medium

consisting of "holograms" or, for example, microfilm "aperture cards", and this point is further discussed in Section 2.4.

High density photographic (microfilm) storage can only be considered as an interim measure. Eventually the need for high density storage will exceed the limitations of microfilm storage devices.

Storage material, such as microfilm, with a requirement for virtually no surface defects rapidly becomes very expensive in large volume information handling and processing.

The very high bit-storage density inherent in optical techniques can be realized by holography in a simple manner, without demagnifying lenses and high precision alignments. This can be contrasted with the microfilm storage limitations of a requirement for precision readout optics, a storage material which is very sensitive to surface defects such as dust or scratches, and where duplication is complex and costly.

Comparing high-density microfilm storage to holographic recording, in terms of storage density utilizing the same recording material, shows that the plane hologram requires about eight times the recording surface to record a pattern of prescribed information content [20]. This is due to the difference in the effect of the limiting resolution of the storage medium for direct photography and holography. Holographic recording in plane, as opposed to volume, holograms does not present an advantage over direct photographic recording if high density of information storage is the only consideration. An advantage is gained if full recovery of information from a densely stored record is of primary importance.

Numerous techniques can be applied in forming holograms [21] - [23]. The off-axis reference beam method, as introduced by Leith and Upatnieks, is the most generally used arrangement of making a hologram and reconstructing to form the object's image [24], [25].

In general, the object, or scene, or information to be stored is illuminated by one of two components of a coherent light beam. The coherent light beam is generated by a laser and is split into two parts. One part of the light beam is directed at the object and the other part, called the "reference wave," is directed at the recording medium, usually a photographic emulsion or "plate." The component of the laser beam directed at the object is diffracted, or scattered, by the object and constitutes the "object wave." The object wave, together with the reference wave, are allowed to intersect at the recording medium. Since the object and reference waves are mutually coherent, they form a spatially and temporally stable interference pattern at the recording medium. The record thus obtained is processed, e.g. exposed and developed, and is called a "hologram." The holographic process can be described in a communication theory framework, as having three essential parts: (1) the spatial-frequency dispersion of the image, (2) the hologram recording process, a square law detection, and (3) the focusing, or reconstruction [26].

The advantages that can be gained from use of holographic storage, when compared to conventional optical storage techniques [27], are:

- Lenses are not required to project the readout pattern. Each hologram "stores" both data and the optical imaging properties of a lens of high quality.
- 2. Focus is noncritical when accessing successive holograms in the read-out process because of the large depth of field.

- 3. Image resolution can be as good as the diffraction limit imposed by the size of the hologram.
- 4. The storage medium, i.e., photographic emulsion, has large dynamic range.
- 5. Read-out of the stored data does not involve contact with the hologram, holography being essentially a projection technique. This minimizes the possibility of damage and deterioration of the master hologram.
- Input/output and storage density are not related. The data can be stored at high density, but read-out can utilize a relatively low density array of, for example, photodetectors.
- 7. Information about each part of the data is distributed over the entire hologram area. This redundancy makes the hologram relatively insensitive to dust particles or scratches. For example, scratching the hologram reduces the aperture, and reduces slightly the resolution and the read-out intensity.

The main disadvantages of holographic storage are:

- There is a limitation on the size of an electronically accessed holographic memory due to the diameter of the field lens. All systems have a field lens which must be as large as the storage medium.
- 2. Low optical efficiencies are obtained in read-out. For amplitude holograms only of the order of 1% of the incident light is diffracted into the desired image.

Most holographic information storage is "selective-access" storage.

In a digital hologram, a large number of images (each containing many bits) may be recorded on a single hologram plate. The images or "pages" can then be retrieved one at a time [10].

The two methods of recording are (1) storing the images in Physically separated parts of the hologram, which is defined as "block"

or "parallel" storage, or (2) the images are stored throughout the total hologram area, this being defined as "consecutive" storage.

With consecutive recording one hologram (the total frame) is used,
where with block recording the information is recorded as many
individual holograms. In case (1) the images are retrieved by addressing any particular hologram with the reference beam. For case (2)
the images are separated by addressing with reference beams differing
in angle of incidence to the recording medium surface, or differing in
wave length [28], [29], [18]. The method of storage is then determined
by the means of varying the reference beam.

The difference between a "holographic memory" and an "associative holographic memory" can be found in considering the type of reference beam that is utilized in the read-out process. With normal holographic storage, the same reference beam is used for reading out all information in the memory. That is, the desired information is recalled by addressing (illuminating with the reference beam) only the particular memory element where the information is to be found for block storage, method (1). For consecutive storage, or method (2), addressing is accomplished by a change in the direction of the reference beam. Recall can also be by use of these methods in combination. For associative holographic storage, in general, the total hologram is illuminated by the read-out reference beam, as in method (2) above. But, in this case the reference beam also contains information which is related to, or "associated" with, the desired information to be retrieved. The recall is then based on association, and not on reference wavefront changes obtained by illumination of a given location or with a given propagation direction.

The associative memory property of a hologram is illustrated by the storage of more than one object wavefront on a single hologram.

To obtain a one-to-one reconstruction, i.e., a retrieval of the stored information, the hologram must be illuminated either by (a) a part of the reference wavefront or (b) by a wavefront from a part of the object. The essential retrieval key is a recording wavefront that was associated with the specific wavefront desired to be reconstructed.

An associative holographic memory achieves the holography advantages of high density, high capacity storage, simpler peripheral devices, and, perhaps of most importance,—highly redundant recording. One of the major aims of the storage technique described here is also to increase read-out efficiency.

# 2.4 <u>Previous Research In Holographic Assistance For Fingerprint Identification</u>

Several experimental methods of fingerprint identification have been developed utilizing coherent light techniques. In one case, transparencies of the test and reference (stored) fingerprints are placed side-by-side, not overlapping, in the object plane of the optical system, shown in Figure 2 [30]. The Fraunhofer diffraction pattern resulting from comparison of similar prints then shows a regular pattern of parallel interference fringes in the frequency plane of the system.

If the two fingerprints are identical, regular parallel interference fringes extending to high spatial frequencies are observed. If the fingerprints are different, but similar in external contours for example, all regular structure disappears in the diffraction pattern of the comparison. Automatic evaluation is suggested by

measurement of fringe count, contrast, and regularity of spacing.

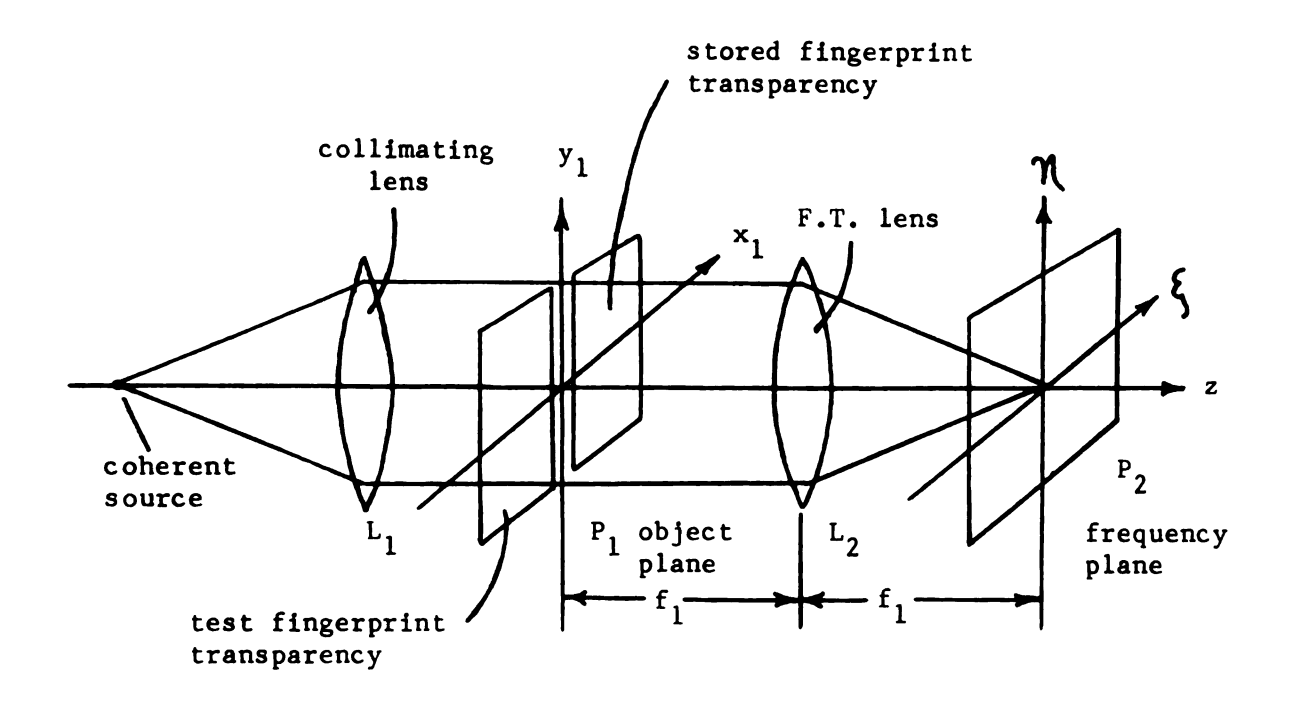


FIGURE 2. An Interference Method For Fingerprint Comparison, (after Weinberger and Ulmi [30]). (The fingerprint would be stored in transparency form.)

This method is simplified by not having a need for a hologram storage medium. The fingerprints would simply be stored as transparencies, although this in itself involves some processing and may not be an optimum storage technique (see p. 15).

Optical matched filtering correlation methods, utilizing the Fourier-transform hologram (FTH) filter, have also shown good success in fingerprint comparison experiments [31], [32]. In these techniques print identification is based on the strength of a "recognition spot," which is the field distribution in the image plane proportional to the correlation of the input print and the stored print (see the matched filter discussion, p. 51, and Figure 4). The parameters of interest

here are:

- 1. Translational positioning, x,y, and z, of the object plane print transparency is not critical. The effects of a small lateral shift (x,y positioning) and magnification (z-shift) can be compensated. Lateral shift produces a lateral shift of the bright spot image in the output plane (see p. 84, expression 4.3.1), and can be corrected for by a shift of the observing. e.g., photomultiplier, system. Magnification can be compensated by the displacement of the input plane transparency in the z-direction. This results in a defocused spot image, which has to be taken into account when checking the spot brightness, (see Section 3.7 for further discussion of reconstruction positioning tolerances).
- 2. Relative rotation between the input plane transparency and the filter need only be accurate to plus-or-minus of the order of several degrees for correlation [31].
- 3. With this spatial-filtering method the fingerprints are recognized on the basis of their
  fine details and ridge spacings, rather than
  by their general patterns. Thus, this
  technique identifies a particular print, but
  may not be able to classify it as part of a
  particular classification as with the Henry
  system discussed in Section 2.1.
- 4. A fingerprint can be identified even if the print is partly obscured or missing. A decrease in spot intensity is observed as the information content of the input print is reduced by masking. This decrease is found to be nonlinear. A rapid drop in spot intensity was observed only when the input print was 70% obscured [32].

Pointed out also were the effects of fingerprint recording pressure and noise superposed on the fingerprint. Printing pressure causes a slight deformation of the fingerprint, and correlation is very sensitive to shape deformation.

The solution to printing pressure deformation may be to record, and store, the same fingerprint with several different printing

pressures. This concept is recommended in Chapter IV, and follows that of storing several variants of an alphabetic character in character recognition. To solve the superposed noise problem, a thresholding approach, based in preprocessing, would be utilized. In this case no pre-matching processing other than a change to transparency form is required for the latent print input. However, variations on this configuration are possible, and these are discussed in the Appendix.

Most fingerprint files accumulated by law enforcement agencies are in the form of paper cards. In a holographic system, objects not in a transparency form scatter too much light to produce good diffraction images. A minimum requirement is then the transformation from paper cards to either a hologram or a transparency fingerprint file. The relative merits of holographic vs. microfilm storage were discussed in Section 2.3.

If the stored records are on microfilm there is the possibility of using an "aperture card" type of storage. The aperture card approach was one of three methods utilized in a project SEARCH experiment to determine the feasibility of holographic assistance to fingerprint identification [33]. The other two methods utilized, respectively, a microfilm, transparency or photographic slide, file and a digital data file. The digitized file was formed from measurements of the average ridge orientation at a two-dimensional array of positions on a holographic image of the fingerprint.

With the film fingerprint libraries, coherent matched filter processing is used to test for correlation. The input or "inquiry" print is processed to form the "match filter" or hologram. In the

digital case the comparison is digital, with the fingerprint library consisting of a magnetic tape. Alternatively, since the numeric ridge orientation data is extracted from holographic images for both the library and test prints, this digital method may be considered as a hologram memory technique. A parallel digitizing of the hologram library would, however, have to be incorporated for this technique to obtain an acceptable processing time level. Multiplexing in the optical comparison methods would also be necessary to increase processing speeds. The automatic processing goal is to obtain equivalent or faster received through match/no match reply response times as compared to existing manual processing systems.

The parameters of interest for the SEARCH experiment are the following:

- The file search results consisted of a set of prime candidates for each test print.
   The final identification function would be handled by skilled fingerprint technicians.
- Rolled impressions of fingerprints had more uniform inking, and were more accurately located within the allotted space on the card form, as compared to flat impressions.
- 3. Primary emphasis was placed on examining only those techniques potentially applicable to the state identification bureau function of ten-print identification. Latent fingerprint identification, as a particular law enforcement use of holography, was not considered separately.

Some conclusions reached in the SEARCH experiment are that any techniques presented should be capable of dealing with the existing files in state identification bureaus, that development of parallel processing and machine identification would increase speed and reduce costs. and substantial refinement of the proposed technical approaches

is required to improve the accuracy rates. Of major importance, it was also concluded that no system concept which relies on a final match/no match human decision can be cost-justified.

#### CHAPTER III

### THE HOLOGRAPHIC MEMORY AND TWO-DIMENSIONAL INFORMATION PROCESSING

Holographic techniques in pattern recognition generally consist of optical spatial filtering, and utilize the Fourier-transforming property of a converging lens [34]. In this chapter we examine the conditions required to form an optimum FTH filter. The filter serves as a Fourier-transform hologram memory, and may be recorded with either a point-or finite-source reference structure.

3.1 Holographic Techniques Applicable in Fingerprint Identification

Tanaka, et al., [35] classify holographic transformations of
information for the purposes of pattern recognition, in terms of the
types of recording and reconstruction signals utilized. The classi-

fications include:

- 1. Direct correlation, where the recording amplitude distributions are a  $\delta$ -function, or point source, and an amplitude distribution  $t_1$ . If the reconstructing signal is an amplitude transmittance  $t_i$  this gives for the plus and minus first order images, the convolution  $t_i \otimes t_1$ , and the correlation  $t_i \times t_1^*$ , respectively.
- 2. Coherent matched filtering (VanderLugt Filter), where the recording functions are **\S** and g, and the filter is utilized to detect the presence of a deterministic signal g, the reconstruction signal, submerged in additive, stationary noise n . This process is discussed further in the following paragraphs.
- 3. Ghost imaging, or code transformation, where the recording functions, or amplitude distributions, are  $t_1$  and  $t_2$ , and the reconstructing amplitude transmittance equals  $t_1$ . If both  $\left|T_1\right|^2$  and

 $|T_2|^2$  are independent of p,q, with  $F[t_1(x_1,y_1)] = T_1(p,q)$  and  $F[t_2(x_1,y_1)] = T_2(p,q)$ ,  $t_1$  or  $t_2$  is reconstructed when a hologram formed with  $t_1$  and  $t_2$  is illuminated with  $t_2$  or  $t_1$ .

Other examples of optical pattern recognition methods which utilize spatial-filtering techniques involve <u>inchoherent spatial</u> matched filtering [36], <u>correlation of diffraction spectra</u> [7], and <u>shadow correlation</u> (incoherent matched filtering based on geometric-optical shadowing) [37].

Optical position-invariant operations, whose effect on a point does not depend on the position of the point in the picture, can be implemented with either coherent or noncoherent light. Due to the need for general transfer functions, which are not limited to being autocorrelation functions, the "standard" optical data processing set-up is a coherent system. In coherent light techniques the pictures are usually assumed to be in the form of transparencies, located in the "object plane," with coordinates  $\mathbf{x}_1, \mathbf{y}_1$ . The light beam passes through this transparency of the object, scene, or signal to be processed, and forms the two-dimensional Fourier-transform of the signal by the use of a converging lens, in the back focal plane of the lens. This is illustrated by Figure 3.

The object transparency in plane  $P_1$  is illuminated with a monochromatic plane wave. This illumination comes from a coherent point source and is collimated by the lens  $L_1$ . A monochromatic coherent illumination of the amplitude transmission  $g(x_1,y_1)$  of the transparency in the front focal plane of the lens  $L_2$  gives a complex amplitude G(p,q) in the rear focal plane  $P_2$  such that

$$G(p,q) = \iint g(x_1,y_1) \exp[+j(px_1+qy_1)] dx_1 dy_1$$
 3.1.1

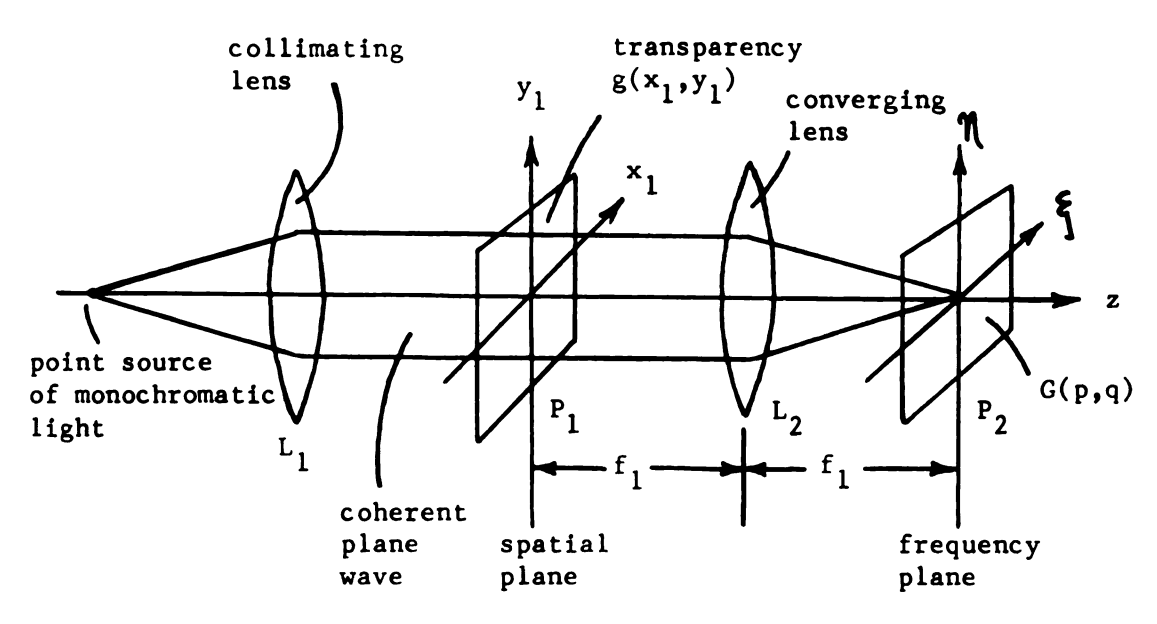


FIGURE 3. Forming the Optical Fourier Transform.

Normally, spatial filtering is accomplished by means of a filter in the common focal plane of two lenses separated by a distance equal to the sum of their focal lengths. This is shown by Figure 4. The space planes  $P_1$  and  $P_3$  and the frequency plane  $P_2$  are usually placed one focal length from the lenses to simplify mathematical analysis.

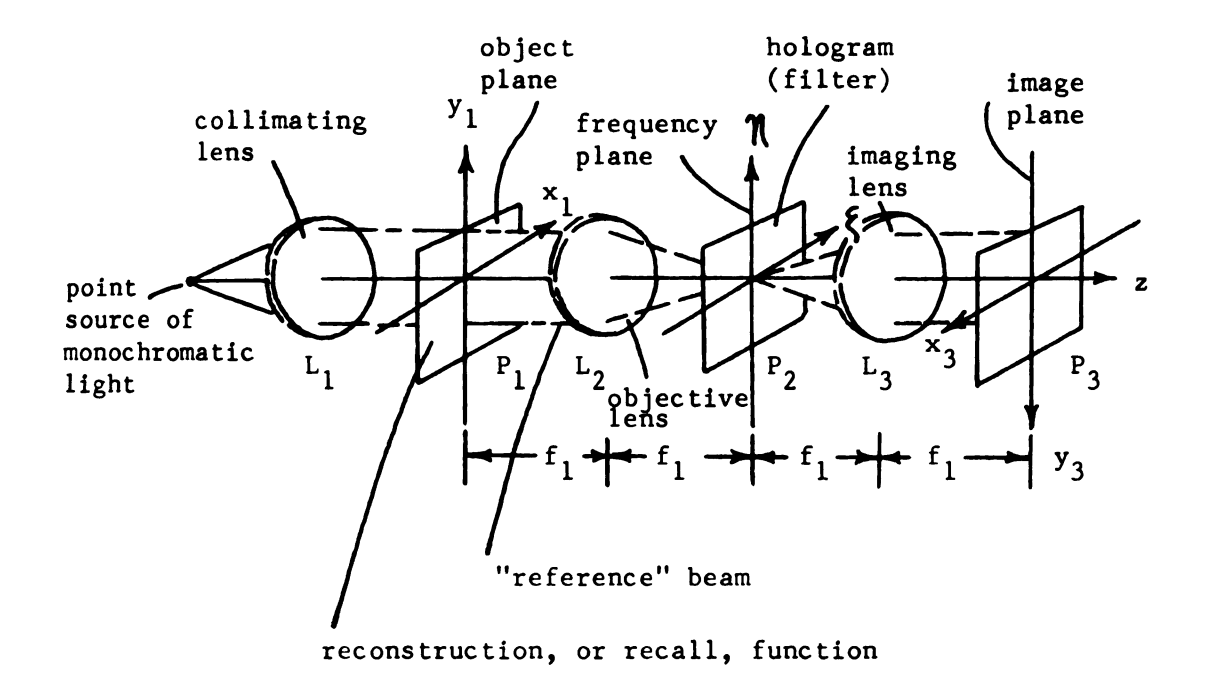


FIGURE 4. Two-Dimensional Spatial-Frequency-Plane Filtering. (This can be contrasted with the optical data processing system (---) of Figure 5, which is considered optimal in terms of utilization of the space-bandwidth product.)

A spatial filter usually having complex transmittance H(p,q) is then placed in the frequency plane to modify G(p,q). Spatial filters may be either real-valued, purely imaginary valued (phase filters,) or complex valued (spatial carrier-frequency) filters.

In the case where the unknown pattern, i.e., fingerprint to be identified, is of known size, shape, and orientation, optical template matching procedures may be applied. If the orientation or scale of the input is not known, the procedure must be repeated for every possible orientation or scale of the template relative to the input. However, optimum optical filters, such as those needed to maximize the ratio of peak signal energy to mean-square noise energy,

cannot be realized by simple templates. This ratio is maximized by matched filtering [34], which requires a complex-valued filter  $H(p,q) = A(p,q) \exp j \psi(p,q).$ 

VanderLugt extended spatial filtering to complex matched filtering for coherent optical processing [38]. It was shown that complex matched filters for coherent objects can be produced by holographic techniques—using photographic film that modifies only the amplitude of a light wave passing through it. Holographic techniques are at present the only simple method of snythesizing optimum optical complex filters.

Construction of complex filters, in the form of Fourier-transform holograms, can be accomplished by interferometric methods. The features of an interferometric complex matched filter generator are given by Figure 5.

#### 3.2 Holographic Equations and the Fourier-Transform Hologram

Light, as an electromagnetic field, requires a vector-field formalism to describe its propagation, diffraction, and interactions. However, only vector wave components parallel to one another produce interference patterns or holograms. The holographic process can therefore be analyzed by considering the interacting wave amplitudes as scalar quantities.

The object and reference waves at the hologram recording medium are regarded as having amplitudes of a single identically polarized component. Scalar diffraction theory, as opposed to vector electromagnetic theory, is then utilized, and does not take account of polarization effects. A scalar treatment is considered sufficient for

objects whose dimensions are large compared with the wavelength.

In general, the interference pattern of a hologram is considered a volume recording (Figure 6). For two coherent plane waves incident on the recording medium, planes of maximum light amplitude are generated by the interference of the two waves, and are perpendicular to the plane of Figure 6. The result is an essentially sinusoidal density variation which forms the interference pattern that is then recorded.

The type of hologram, "thick," i.e., volume, or "thin," is determined by the relationship of the recording medium thickness, s, and the period, a, of the finest interference fringes recorded. Regions of constructive and destructive interference move through the emulsion volume to form a grating structure. The fringes of this grating run at an angle that bisects the angle, 20, between the interfering incident wave vectors. The fringe period, measured normally between two fringes is given by

$$a = \frac{\lambda}{2 \sin \theta} \cdot 3.2.1$$

Written as  $\lambda$  = 2asin  $\theta$ , this shows that the grating consists of Bragg planes extending through a volume. If the angle between the interfering wavefronts is made small, the period of the interference planes (fringes) is much larger than the recording medium thickness, or a >> s. The recording can then be considered as a surface, or planar, recording. The hologram then behaves as a two-dimensional diffraction grating, and it is regarded as a thin hologram. For a discussion of volume holograms see [40]. Potentially, volume storage is the better storage method in terms of capacity when compared to planar storage [29].

Some holograms can act substantially thin, even if they are many

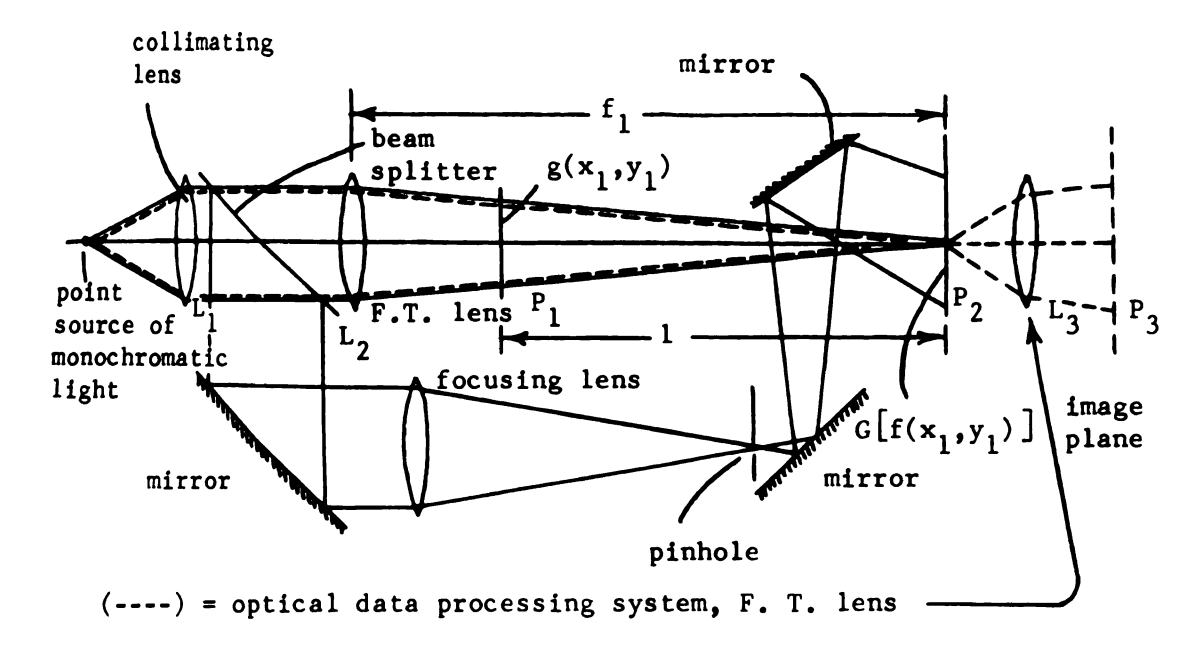


FIGURE 5. An Interferometric Matched Filter Generator, (Which Combines the Best Features of the Modified Mach-Zehnder and Rayligh Interferometers, After VanderLugt [39].) (The practical advantages of this system are that all lenses have small relative apertures and operate over small field angles. Abberations and cost are therefore minimized, and also, the offset angle can easily be increased without requiring any optical aperture increases.)

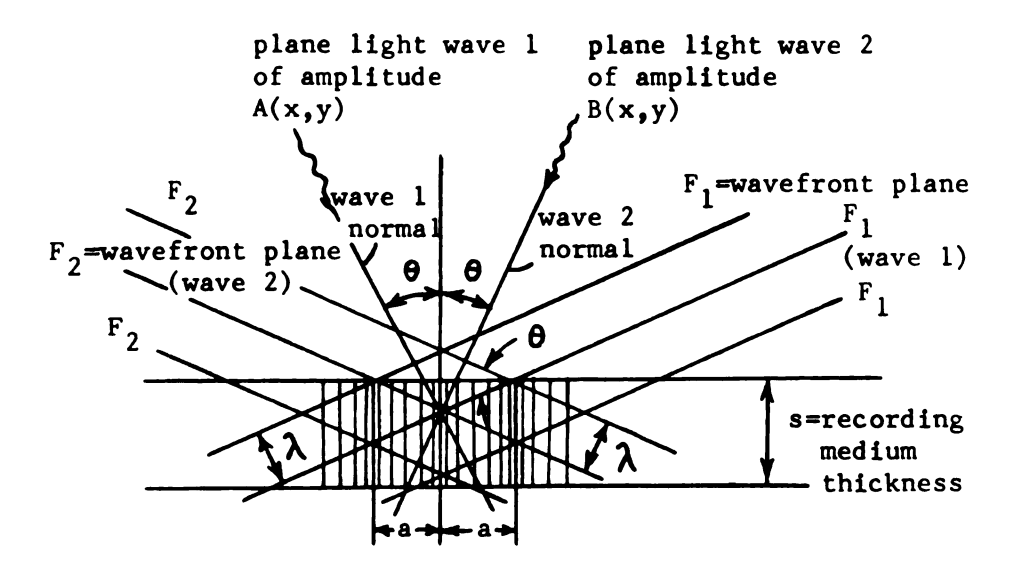


FIGURE 6. Recording of the Interference Pattern Produced by Two Plane Waves From the Same Coherent Source to Form a Hologram [23]. (Wavefront planes F<sub>1</sub> and F<sub>2</sub> represent the positive maximum amplitude fronts and are incident at equal angles to the normal of the recording medium.)

wavelengths thick. A popular hologram recording medium is Kodak 649-F plate, which has a thickness of the order of 1644 and a refractive index of the order of 1.5. The angular and wavelength sensitivity of such thick holograms becomes very low if the angle between the two interfering beams is less than 10 degrees, or, that is, the carrier frequency is less than 300-400 cycles/mm. These thick holograms then act substantially like thin ones. Only holograms obtained with very narrow signal beams, however, have the interference terms entirely within the two-dimensional recording region.

Pictorial processing deals, for the main part, with plane surfaces.

Therefore, consideration from this point on will be limited to the type of hologram storage which can be approximated as a planar recording, i.e. a thin hologram.

Consider the interference of waves of identical wavelength, representing the scalar amplitude and phase distributions of a monochromatic wave from a single source. The complex light amplitudes at any plane in the optical system are stated as complex functions of space coordinates.

Assume the existence of a thin hologram recording medium in the plane z=0, and defined by the coordinates x,y. The object wave can be represented by  $A=A(x,y)\exp j \phi_A(x,y)$  and the reference wave by  $B=B(x,y)\exp j \phi_B(x,y)$  where A(x,y) and B(x,y) are the amplitudes of the waves as functions of position and  $\phi_A(x,y)$  and  $\phi_B(x,y)$  are their spatial phases. Since the temporal factor  $\exp j \omega t$  is not observable in optical detectors, it need not be considered here.

The physically measurable quantity at the recording medium is the intensity distribution I(x,y) of the incident light. The

exposure of the hologram, with the time-averaging understood, can then be written as

$$I = ||A+B||^2 = (A+B)(A+B)^*$$

$$= AA^* + BB^* + AB^* + A^*B$$
3.2.2

where  $AA^*$  is the intensity of the light from the object,  $BB^*$  is the intensity of the light from the reference source, and  $AB^*$  and  $A^*B$  are the interference terms.

A hologram can be considered as an instantaneous recording of the state of wave propagation. The reconstruction of the object wave, i.e., retrieval of the stored information, is possible in accord with the Huygens-Fresnel principle. This principle states that propagation of the object wave after reflection, or transmission, from, or through, the object (a transparency or slide for example) depends only on the laws of diffraction. That is, the wave field beyond an aperture, which in this case is the hologram area, is essentially determined by the amplitude and phase distribution within the aperture.

When a beam of light passes through any semitransparent object the light is diffracted. In the holographic reconstruction process, the recorded wave is thus "allowed" to continue its propagation. This is accomplished by illuminating the hologram with the reference wave  $B(x,y)\exp j\phi_B(x,y)$  used in the recording. The spatial modulator, i.e., the hologram, impresses on the incident reference wave a pattern of amplitude and phase which allows duplication of the original object wavefront.

Processing of the recording medium to form a hologram is usually aimed at obtaining a linear transfer characteristic. The hologram  $amplitude \ \ transmittance \ t_A(x,y) \ is \ then \ linearly \ proportional \ to \ the$ 

intensity I(x,y) of the interference pattern in the x,y-plane of the recording medium.

In general the amplitude transmittance is of the form

$$t_{A} = f (I)$$
 3.2.3

and the light diffracted by the hologram, taking  $t_A$  to be directly proportional to I, neglecting the physical thickness of the medium, and omitting the constants, is given by

B. 
$$t_A = B (AA^* + BB^*) + BBA^* + BB^*A$$
 3.2.4

The first term is a reconstruction of a wavefront proportional to the reference wave. If B is sufficiently uniform so that  $BB^*$  is approximately constant across the hologram, the other terms are

BB\*A = reconstruction of a wavefront proportional to the original object wavefront.

BBA\* = reconstruction of a wavefront that is phase conjugate to the original object wavefront.

Separation of the reconstructed terms, to avoid degradation of the object image by interference with the conjugate image, is possible by using an "off-axis" reference beam. Consider the reference wave to be a plane wave with a y,z-plane wave vector, and incident on the recording medium at an angle  $\alpha_0$  with respect to the z-axis. The reference wave is then represented by

Bexp(
$$j2\pi\alpha(y)$$

where  $\propto = \sin \alpha_o / \lambda = \text{constant}$ . Then the interference pattern is

$$I(x,y) = A^{2}(x,y) + B^{2} + A(x,y) B \exp \left\{ j \left[ 2\pi \alpha y - \phi_{A}(x,y) \right] \right\}$$

$$+ A(x,y) B \exp \left\{ -j \left[ 2\pi \alpha y - \phi_{A}(x,y) \right] \right\}$$

$$= A^{2}(x,y) + B^{2} + 2A(x,y) B \cos \left[ 2\pi \alpha y - \phi_{A}(x,y) \right]$$

and the amplitude and phase distributions of the object wave have been encoded, respectively, as the amplitude and phase modulations of a spatial carrier of frequency &. The recorded signal is a non-negative real-valued function. In communication theory terms, a complex valued function of bandwidth W is recorded as a real-valued function on a carrier frequency 2W [26].

Fourier-transform holograms reconstruct two real image wavefronts which are mirror images of each other, rather than a real and
a virtual image wavefront as do the other types of holograms
(Figure 7). The FTH can be formed with or without a lens, and in the
far-or near-field of the object plane [2] (Figure 8). To satisfy
Fourier-transforming requirements, the reference source has to be
in the plane of the object, and the object is thus necessarily a
plane object or a transparency.

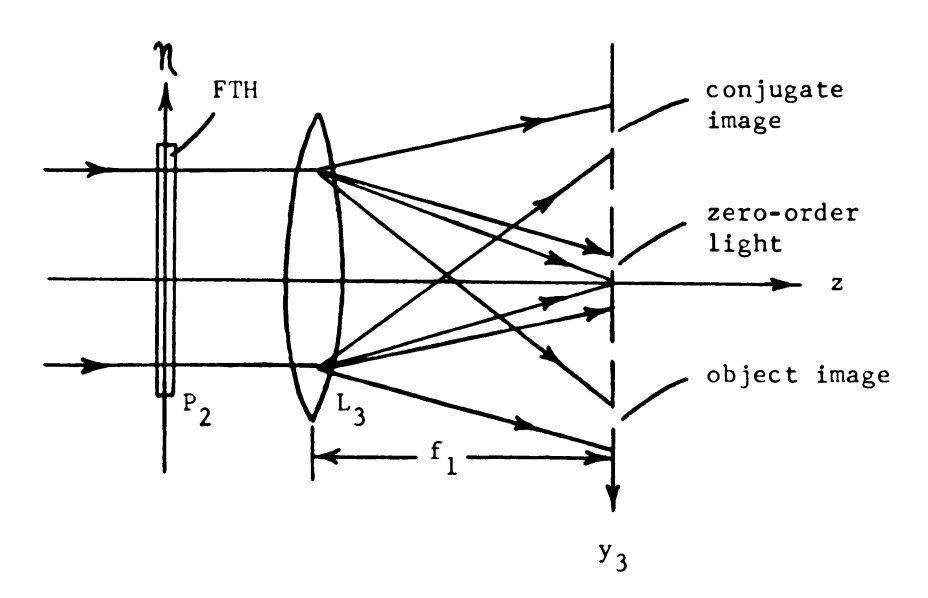


FIGURE 7. Generation of Two Real Images With a Fourier-Transform Hologram.

In Figure 7, the zero order consists of the undisturbed reconstructing beam, and is focused about the origin of the image plane. Deflected to opposite sides of the image plane are two additional images, the plus and minus first orders. The plus first order consists of the object image, and the minus first order is of equal intensity and corresponds to the "conjugate" object image. Physical separation of the three distributions in the image plane is possible by choosing a sufficiently high spatial carrier frequency  $\propto$ . Utilizing a point reference source  $\{(y_1+b,x_1) \text{ co-planar to the object } g(x_1,y_1)$ , and with image plane (output) intensity detection, the conjugate image  $g^*$  differs from the other sideband image  $g^*$  only by viewable direction inversion. Only the first diffracted orders are observed. Higher diffracted orders are generally missing or very weak for a linear recording of a two-beam interference pattern.

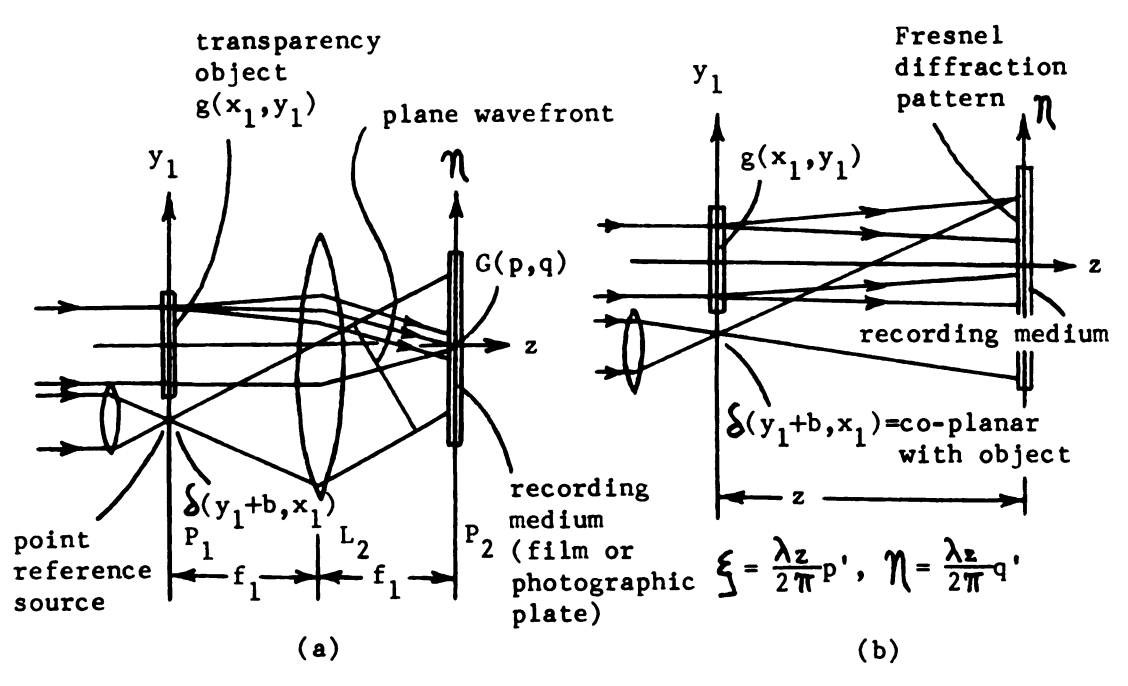


FIGURE 8. Two Arrangements for Forming a Fourier-Transform Hologram. (a) With a Lens, and (b) Without a Lens. (See, for example, [2] for mathematical analysis.)

A near-Fourier-transform approach should, however, be used when forming the FTH to overcome any dynamic range problems with the recording medium. This locates the recording medium at a plane which is slightly displaced from the Fourier-transform plane. The light distribution between the opaque and transparent points, such as found when using binary data (e.g., the fingerprint ridge pattern) is then more evenly distributed in the recording plane (see Section 4.1, Eq. 4.1.1, for the allowed displacement).

### 3.3 The Performance Establishing Properties for An Optical Fourier-Transform Hologram Associative Memory

Parameters associated with the optical holographic memory which may be studied are quite numerous [41],[27],[8]. Allowing a splitting of the holographic memory into three parts: (1) input, recording, or storing, (2) the storage medium, and (3) the output, reconstruction, or retrieval, gives a structured list of possible parameters to be investigated. A listing of some of these respective parameters is given by Tables 1, 2, and 3.

The holographic memory design parameters tend to be directly related to the recording material, and we need a choice of storage medium for their discussion. The storage medium is therefore assumed to be in the form of a photographic emulsion. The most commonly used recording medium for holographic work at present is Kodak 649-F high resolution film.

To limit to practicality the number of parameters to be considered, such parameters as involving beam deflection accuracies, read-out photodetector criteria, or storage medium types are not directly investigated. The parameters focused on are those that

tend to specify the performance bounds of the optical FTH associative memory. Operational performance of this type of system may be evaluated on the basis of (1) discrimination, (2) storage capacity, and (3) read-out speed [8]. It is the intent here to concentrate on discrimination properties, due to the high possibility for imperfect inputs.

It is assumed that the system is a diffraction limited coherent system with perfect aberration-free lenses large enough to pass all the spatial frequencies of the object. The transfer function can therefore be assumed to be a constant, with the impulse response behaving as a \$\frac{1}{2}\$-function. Use of the same wavelength for reconstruction as for recording is assumed. Thus, wavelength sensitivity effects are not considered, and distortion of the reconstructed image wave is minimized.

The basic requirements for forming and recording the interference pattern are also assumed as satisfied. These requirements are: (a) sufficient temporal and spatial coherence of the light source, (b) stability of optical path length and of components comprising the interferometer, and (c) sufficiently high resolution of the recording material to record the fine details of the interference pattern [42]. The input fingerprint data may be visualized as being in the form of 35 mm film aperture cards.

Shrinkage of the hologram recording photographic emulsion may have to be included as a consideration for high spatial frequencies. In this case the spacing of the recorded interference fringes becomes comparable to the emulsion thickness. Shrinkage during the chemical processing generally causes a spatial-frequency dependent

change in both orientation and spacing of the recorded interference fringes when the recording is composed of a range of frequencies.

Thus since simultaneous satisfaction of the Bragg relation for all spatial frequency components is not possible, response may be degraded.

TABLE 1. Holographic Memory Input Parameters

- -Stability requirements dictate use of a pulsed laser of the mode-locked or mode-dump type [43].
- -Physical dimensions and layout of optical, and electrical, components. A short exposure pulse period limits the maximum permissible path difference between the interfering rays to less than  $\lambda/2(\lambda/\lambda)$  [44].
- -Exposure time and the development process, (for example, with photographic materials).
- -The beam deflection system must have stability and positional repeatability. To be considered are light efficiencies, thermal dissipation, beam intensity range, and deflection speed. The approaches considered may be classed as electrooptic, acousto-optic, or mechanical.
- -In order to obtain identical specification object beam lens  $L_2$  and readout lens  $L_3$  the page composer diameter may be set equal to the storage medium diameter [45].
- -Also to be considered are: the axial separation between the page composer and the storage medium, tilt angle of the reference beam, and object dimensions and code pattern (self-associative holographic memory) diameter and spacing. Tilt angle, or spatial carrier frequency, range is dictated by the page composer specifications.

TABLE 2. Holographic Memory Storage Medium Parameters

- -Type of recording medium, permanent or read-write, effectively grainless for high packing density.
- -Diffraction efficiency.
- -Storage life, partially determined by the total number of read-write or rewrite cycles(material fatigue).
- -Physical dimensions; are primarily determined by the resolution of the storage material (spacebandwidth product) and the geometrical and thickness needs.
- -Resolution limit. A photographic emulsion should be capable of recording over 1500 lines/mm. See for example [27].
- -Beam power and beam wavelength for storage and retrieval; are determined by the recording medium sensitivity and holographic diffraction efficiency.
- -Sensitivity and dynamic range.
- -Linearity (nonlinearity effects) of the recording medium. Noise is present in the image due to (1) scattering by the recording material, and (2) due to nonlinearities of the recording material.
- -Noise characteristics.
- -Dimensional stability for different environment conditions. Normal environment operation.
- -Copying capabilities.
- -Beam ratio =  $k = \frac{\text{reference beam intensity}}{\text{object beam intensity}}$
- -Also to be considered are: the spatial extent of the hologram, sub-hologram diameter and spacing, spatial frequency range to be accomodated, and the number of consecutive holograms that are possible in superposed storage.

TABLE 3. Holographic Memory Recall Parameters

- -The detector array. The size of each "page" of data to be read out must be matched to the array dimensions and resolution. To maximize read-out light, the photodetector diameter must be equal to the page-composer diameter.
- -Image intensity at the detector must be sufficient for data resolution.
- -A fast access time requirement, of the order of lasec, makes selection of the retrieval beam deflection technique important. Read-out speed is a function of the laser power, photodetector sensitivity, and system losses.
- -The SNR of data to be read out must be consistent with permitted error rates.
- -Positional displacements may have to be corrected for by a pre-read positioning code (see Chapter IV).
- -Detection window size, typically 300 to 400 µm.

The problem of emulsion shrinkage is relieved by use of preprocessing stress-relieving techniques and alignment of the hologram recording surface perpendicular to the bisector of the angle between the object and reference beams. With this alignment, the recorded fringes are normal to the surface, and the shrinkage in the thickness dimension does not decrease the fringe spacing [46].

When recording holograms on film, the film can be placed in a "liquid gate," or between glass plates containing an index-matching liquid. This serves as a means for obtaining higher rigidity and to make the phase distribution more uniform from frame to frame. A

liquid gate may also be utilized for mounting of the input transparency and to compensate for unwanted phase shift due to the surface relief of the developed emulsion, or hologram. Conservation of uniform phase transmission would increase the discrimination ratio (defined on p. 55) of identical fingerprints recorded on different films of the same type. However, immersion may not be necessary for high quality photographic emulsions. Alternatively, the phase disturbing effect of the (sub-) holograms would be much weaker than that of the object transparencies because of the smallness of the hologram area. Also, liquid immersion cannot be considered in practical applications.

Lee [47] shows that the FTH memory error rate is related to the storage capacity and other recording parameters, such as film-grain noise. Two types of noise must be considered in holographic memories: intermodulation noise and film-grain noise [48].

Intermodulation noise may be considered as "background noise."

This comes from the intermodulation between the different point source terms, as in the case of the self-associative code-transformation, and from aberrations in the optical system, emulsion processing distortions, and emulsion nonlinearities. Emulsion nonlinearity is affected by total exposure, the spatial frequency of the maximum modulation, as related to the beam ratio, and the carrier frequency. Background noise can therefore be controlled by adjusting the recording parameters.

Intermodulation noise may also come from "crosstalk." Crosstalk noise is a function of the recorded pattern dimensions, the output detection window size, emulsion nonlinearity, and spectrum center

separation. An optimum spectrum center spacing must be determined to optimize capacity vs. discrimination. Crosstalk noise thus limits the storage capacity.

Film grain noise becomes a factor when a large number of absorption holograms are superposed on the same frame or plate. In this case, film grain noise is a dominating limitation [49]. As patterns are stored consecutively on one hologram with plane reference waves differing in propagation direction, the memory capacity is limited by noise due to the granularity of the photolayer, plus noise due to surface roughness, base inhomogeneity, etc. With block storage, the maximum memory storage density approaches a limit set up by the hologram resolution.

Maximum capacity of a holographic memory device is calculated by Smith [40], and also Burckhardt [50]. This parameter is very recording medium dependent, and is not considered further here.

Complex amplitude transmittance will not generally be a linear function of exposure. Nonlinear recording/reconstruction results if the input light distribution variations exceed the dynamic range of the recording medium. Nonlinearities may be divided into two classes: (1) the intrinsic nonlinearities, and (2) the material nonlinearities. The later arise from material response curves.

The most conspicious result of the former nonlinearity is found in the nonlinear response of amplitude transmittance, or reflection, to exposure by formation of higher order images in the reconstruction. The higher orders are diffracted at larger angles than the first-order waves. This, therefore, has little effect on the output image, except in high density storage considerations. A near-FTH recording

has been recommended as a solution to this problem (p.37).

#### 3.4 Hologram Efficiency

Holograms may be classified according to the type of object diffraction that is recorded [51]. Since different approximations are made for far-and near-field diffraction, a natural division is possible on the basis of phase behavior at the recording medium. A second way of designating holograms is by their effect on the reconstructing wave [44], and holograms may thus be classified as amplitude or phase types.

A photographic emulsion hologram is classified as an amplitude hologram if absorption is the primary means of reconstructing the object wavefront. An absorption hologram absorbs the reconstructing light in correspondence with exposure during recording. In a phase hologram the phase of the incident light is changed in correspondence to the exposure during recording. In practice neither a pure attenuation or a pure phase shift can be attained. A hologram is classified by its operation of primarily by attenuation or primarily by phase shift.

"Diffraction efficiency" is defined as the power diffracted into a first-order wave divided by the power illuminating the hologram. If the hologram is exposed uniformly this ratio can be one of intensities. This is generally meant as the fraction of the usable readout beam power that is diffracted into one of the reconstructed image waves. Usable power then means a normalization to take into account incidental light losses by surface reflection, by base absorption, or by other factors extraneous to the nature of the hologram. The diffraction

efficiency directly influences the power and sensitivity requirements for the (laser) light source and photodetectors.

The maximum diffraction efficiency of the thin amplitude hologram can be calculated by assuming a simple sinusoidal-amplitude grating transmittance described by

$$t_A(x,y) = 1/2 [1 - \cos 2\pi x]$$
 3.4.1

In theory, this transmittance could be obtained if a perfectly linear holographic recording medium is exposed to two interfering equalintensity plane waves. As in Section 3.2, the reference wave is considered to be an off-axis plane wave Bexp(j2774y), which then interferes with an axial unmodulated plane wave of amplitude A.

The amplitude transmittance of this linear model hologram is defined, over a limited dynamic range, as transmitted/incident light amplitude =  $t_{o}$ -KI, where a linear relationship between  $t_{A}$  and the exposure E, and therefore between  $t_{A}$  and I, is assumed,  $t_{o}$  is the uniform transmittance of the unexposed film or plate, and K is a proportionality constant. Therefore, from Eq. 3.2.5

$$t_A(x,y) = 1 - 1/2 - 1/2 \cos 2\pi dy$$
 3.4.2

where the maximum reconstruction efficiency is obtained by evaluating K to satisfy the limitation  $0 \le KI \le 1$ , since  $t_A$  swings from 0 to 1 if  $t_O = 1$ . Choosing the maximum value of A, such that the object beam intensity  $A^2$  is equal to the reference beam intensity  $B^2$ , the transmittance level of the dc term  $(A^2 + B^2)$ , which is considered as the bias or average exposure of the hologram, is then 1/2. The ac component, or intermodulation term  $2AB\cos 2\pi \le y$ , contributes 1/2.

The transmitted field, assuming that the hologram is illuminated by a reconstructing axial plane wave of unit amplitude, is given by

 $r(x,y) = 1/2 - 1/4 \exp(j2\pi x) - 1/4 \exp(-j2\pi x)$ . 3.4.3 The intensity of each first-order diffracted wave is 1/16, or only 1/16 of the incident, unit amplitude, light is received by one of the first-order reconstructed image wavefronts. The maximum theoretical diffraction efficiency of a thin amplitude hologram is then 6.25%.

A fringe modulation of 100% cannot be achieved in practice, where there is a need for reduction in the contrast of the sinusoidal grating to maintain linearity (i.e., to reconstruct a wavefront proportional to the original object wavefront). The practical diffraction efficiencies for thin amplitude holograms are in the region of 1 to 2% [40].

To increase the diffraction efficiency a phase hologram may be formed from the amplitude hologram, for example, with a silver-halide photographic emulsion, by bleaching out the silver grains. Phase hologram practical efficiency is of the order of 5 to 10% [44], but it is felt that plane hologram information storage/retrieval properties can be discussed here most simply by confining attention to plane amplitude holograms.

Growth in laser power may help to compensate for the poor diffraction efficiency of holographic recording media. However, a more attractive approach toward increasing reconstruction efficiency is the possibility of storing many associations which lead to the same object image recovery on the same hologram [52]. This possibility is the major consideration here.

Friesem, et al. [41] have obtained data on the parameters related to recording spatially modulated coherent light in

constructing holograms, by using monochromatic plane object and reference waves. Experimental results show that the diffraction efficiency is maximized when the average exposure (bias level) of a spatially varying exposure pattern has an amplitude transmittance of 0.5. The maximum value point is found to be essentially independent of the beam ratio k.

Fixing the bias point amplitude transmittance at 0.5, and utilizing a beam ratio of 50:1 to ensure linear operation, the diffraction efficiency is shown (Figure 9) to decrease with increasing offset angle  $\Theta$ . The rate of decrease is uniform up to  $\Theta$  = 50 degrees, and is reduced by 50% at  $\Theta$  = 90 degrees.

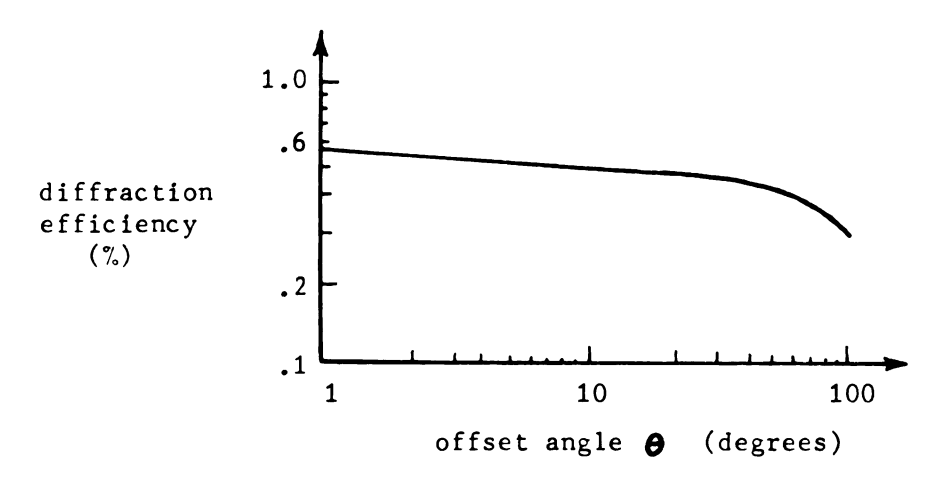


FIGURE 9. Diffraction Efficiency as a Function of Offset Angle Between Object and Reference Beams, (for  $t_A = 0.5$  and k = 50). (After Friesem, et al., [41]).

A hologram recording is most suitably characterized by its amplitude transmittance vs. exposure, or  $t_A$  - E, curve. By choosing a suitable bias point on the curve, the slope of the  $t_A$  - E curve can be utilized to predict the amount of light diffracted by the hologram for low offset angles. The  $t_A$  - E curve is

the photographic emulsion dynamic transfer function, and a linear approximation is valid, except at both large and small exposures. See for example [53] for the use of film nonlinearities in optical spatial filtering.

Friesem, et al., [54] have also shown that for a bleached absorption, i.e. phase, hologram an optimum combination of diffraction efficiency of 5% with a 16.5 db SNR can be obtained for Kodak 649-F emulsions and using the EB2 bleach process, with a beam ratio k = 1, and a density (before bleaching) of 1. It was observed that images of SNR  $\geqslant$  15 db would be required for visual display (see the satellite transmission discussion, p. 10).

The main disadvantage of holographic storage (p. 17) is the low optical efficiency in readout. Typically, only the order of 1% of the incident light is diffracted into the desired image. Thus, along with high information storage density, a requirement to be met by a proposed optical memory system must be efficient light utilization.

# 3.5 Redundant Recording As a Means of Providing Protection Against Loss of Information

Spatial redundancy in holographic recording can be obtained by utilizing a diffused-light hologram. A diffusing medium, such as a sheet of ground glass, may be inserted between the laser and the transparency, usually close to the transparency. This introduces an extremely complex phase distribution across the illuminating wave. If the light illuminating the object (or the light reflecting from the object) is diffused, light scattered by each point of the object takes the form of a spherical wave. The light from each point of the object spreads out so as to cover the entire hologram recording medium. This

results in a reduction of the required recording medium dynamic range, and the degree of spatial redundancy in the hologram is increased. If the hologram is damaged, torn, or scratched, it is still possible, with some loss in resolution, to form an image of the whole object. Another advantage is that effects of dust and scratches on the optical components are smeared over the total hologram and have negligible effect on reconstruction.

The disadvantage is that the appearance and effective resolution of the image is reduced by "speckle." Speckling results from recording a very large number of spherical wavefronts, from each point of the object, as a summation when forming the hologram. Speckle is transferred to the image in the reconstruction. The image then exhibits random light variations resulting from the interference of the diffusely scattered, or illuminating, waves.

Speckle "grain" effective dimensions are diffraction limited and proportional to the f/number of the imaging system ([7], p. 345). In direct observation where the pupil of the eye defines the resolution, speckle is prominent.

For non-visual observation, speckle is not a significant problem if the hologram is chosen large enough such that the effective speckle grain is smaller than the limit of resolution of the recording medium. Also, Pennington and Collier [55] have shown that when ghost imaging with the Fourier-transform hologram, diffuse illumination may be used to improve image quality by making the background noise more uniform. The object transparency consisted of transparent letters on an opaque background. The illumination, both in recording and in reconstruction, was by laser light passing through a diffusing ground-glass screen.

For a practical file-searching system, however, diffuse illumination has several drawbacks. The same diffusing ground-glass screen is required for the reconstruction, or retrieval, of the hologram stored information as was used in the recording, or storage, process. Duplication of the data base may be desired for several separate retrieval systems. In this case, the data have to be restored in each system, using the respective system's diffusing screen in the recording process. This is an impossibly expensive task.

Diffuse illumination also becomes unacceptable when using a binary information input. Speckle spots in this case are not distinguishable from information spots of a binary-coded page image of a page-organized store. Binary spots are of minimum resolvable dimension for high density storage.

Fourier-transform holograms solve these problems, as do holograms formed by interference of light from point-source objects and a plane reference wave. Each point of the Fourier-transform plotted in the plane of the recording medium represents the total amplitude of a particular spatial frequency. Recorded is the power spectrum of the input pattern, regarded as a superposition of spatial Fourier components. Each grain of a photographic film carries a record of the intensity of a particular Fourier component, which is a feature of the wave as a whole. Every grain records something about the object as a whole. Since each point in the hologram plane then represents information about the total object, the FTH has redundancy, analogous to diffused-light holograms.

In holographic recording with point objects, light from the point sources is spread over the entire hologram's area, and thus

ensures interference patterns over the entire recording medium surface. In this case, as well as with the FTH, any part of the hologram will reproduce the same image as any other part of the hologram. Every small area of the hologram contributes to the amplitude of every part of the image. Dust or scratches lower the total image intensity by only the ratio of the obscuring area to the total stored area of the hologram. The active area of the hologram may therefore be reduced to a point where aperture limiting reduces resolution to intolerable levels.

## 3.6 Coherent Matched Filtering: the Format for Optical Holographic Pattern Recognition

A linear space-invariant filter is a "matched filter" for a particular signal g(x,y) if its impulse response h(x,y) is given by  $h(x,y) = g^*(-x,-y)$ . The required frequency-plane transfer function then is  $H(p,q) = G^*(p,q)$ , or the frequency-plane filter should have an amplitude transmittance proportional to the complex conjugate of the Fourier spectrum of the signal  $G^*$ . Noise, denoted by n(x,y), is also present in the system. Noise is considered as anything in the input not of interest, or a hinderance to the signal identification. In latent fingerprint processing, noise takes the form of other unnecessary fingerprints and the structure imposed by the surface from which a fingerprint is obtained. The optimum filtering process maximizes the ratio of peak identification signal to rms noise [38], and is given by

$$H(p,q) = \frac{G^*(p,q)}{N(p,q)}$$
 3.6.1

The signal and noise are assumed to be additive. The noise is assumed homogeneous, and N(p,q) represents the noise spectral

density function. With linearly additive noise, 1/N(p,q) is usually considered as a proportionality constant, and is not implemented in practice [42].

Latent fingerprint processing noise transmittance is generally not expected to be additive nor uniform. However, the continued non-implementation of the 1/N(p,q) function does not seem to significantly affect fingerprint identification experimental results [33].

In complex signal detection by optical correlation filtering with matched filters, a plane reference wave acts as the carrier function. The total intensity distribution at the recording medium, in plane  $P_2$  of Figure 5, when recording to form the filter is given by  $I(p,q) = B^2 + A^2(p,q) + 2BA(p,q)\cos\left[2\pi\alpha N - \psi(p,q)\right] \qquad 3.6.2$  omitting constants, as was shown in Eq. 3.2.5. The filter transfer function is then described by the bias level  $B^2 + A^2(p,q)$ , the modulus 2BA(p,q) and the phase  $\psi(p,q)$ . Developing of the (photographic film or plate) record forms the FTH with amplitude transmittance proportional to the intensity distribution incident during exposure, or

 $t_A \sim B^2 + G^2 + BGexp(j2\pi \propto N) + BG^*exp(-j2\pi \alpha N)$  3.6.3 where  $G(p,q) = |G(p,q)| \exp j\psi(p,q)$ , with |G(p,q)| = A(p,q) in Eq. 3.6.2, and  $F[g(x_1,y_1)] = G(p,q)$ . The last term in Eq. 3.6.3 is the desired matched filter function, and includes a linear phase term  $\exp(-j2\pi\alpha N)$ . If the signal  $g(x_1,y_1)$  to which the filter is matched is presented at the input plane  $P_1$  of the processing system of Figure 4, incident on the hologram (filter) placed in plane  $P_2$  is a field distribution proportional to G. Transmitted by the hologram is a field proportional to G, which is real and given by

 $B^2G + |G|^2G + BG^2\exp(j2\pi\alpha N) + BG^*G\exp(-j2\pi\alpha N)$ . 3.6.4 Since  $GG^*$  is real, the hologram cancels all the phase curvature of the hologram transmitted wavefront, and this transmitted field distribution is a plane wave, and is brought to a focus by the final transforming lens  $L_3$ . The field strength in the image plane  $P_3$  is proportional to

$$B^{2}g(x_{3},y_{3}) + g(x_{3},y_{3}) \otimes g^{*}(-x_{3},-y_{3}) \otimes g(x_{3},y_{3})$$

$$+ B[g(x_{3},y_{3}) \otimes g(x_{3},y_{3}) \otimes (x_{3},y_{3}-\alpha \lambda f)]$$

$$+ B[g^{*}(-x_{3},-y_{3}) \otimes g(x_{3},y_{3}) \otimes (x_{3},y_{3}+\alpha \lambda f)]$$

The first and second terms are not of interest, and are centered at the origin in the  $P_{\rm q}$  plane. The fourth term may be rewritten as

$$g^{*}(-x_{3},-y_{3}) \bigotimes g(x_{3},y_{3}) \bigotimes \delta(x_{3},y_{3}+\alpha\lambda f)$$

$$= \iint_{-\infty}^{+\infty} g(u,v) g^{*}(u-x_{3},v-y_{3}-\alpha\lambda f) dudv$$
3.6.6

and is seen to be the autocorrelation  $g \not \times g$  centered at  $(0,-\alpha \lambda f)$  in the  $P_3$  plane. If  $\alpha$ , the carrier frequency, is sufficiently high, a separation of terms off-axis is effected.

In Fourier-transform processing, since the amplitude of the F.T. is translation invariant with respect to input displacement, the input registration problem is solved inherently as a part of the signal detection and identification problem. The presence of a signal  $g(x_1,y_1)$  is detected by measuring the intensity of light at a focal point of the third transforming lens corresponding to the position of the input in the object plane. The plane  $P_3$  output "spot" represents, by its brightness, the likelihood that the matched signal exists at the location of the spot. The peak of the spot is proportional to the cross-correlation between the input signal and the signal to which the filter was matched. The "spot"

is seen to be small, bright, and surrounded by nearly uniform background light. If the two signals are not identical, no spot image is formed. If a signal other than  $g(x_1,y_1)$  is present at the input for reconstruction, the hologram in general does not cancel all the curvature of the incident wavefront G, and the light is not brought to a focus by the third lens.

Autocorrelation image brightness will equal or exceed that of a cross-correlation. A filter which yields the highest cross-correlation is therefore assumed to be matched to the input. In theory, the autocorrelation coefficient  $S_k$  is larger than any cross-correlation coefficient S. This may be shown by use of the Schwartz inequality [36], [57]. Assume a normalization, by the square root of the total energy in the signal to which a filter is matched, in order to compare several filter responses to the same input. The peak output, at a photocell for example, for the correct matched filter is, from

Eq. 3.6.6: 
$$|S_k|^2 = \frac{\left| \iint g_k g_k^* \, dud\tau \right|^2}{\left| \iint |g_k|^2 \, dud\tau \right|} = \iint |g_k|^2 \, dud\tau$$
.

For an incorrectly matched filter, the response  $|S|^2$  is

$$|S|^2 = \frac{\left|\iint g_k g^* dud \boldsymbol{\gamma}\right|^2}{\iint |g|^2 dud \boldsymbol{\gamma}}$$
3.6.8

where, the input is assumed to be  $g_k(x_1,y_1) = g(x_1,y_1)$ . Using Schwartz's inequality,

$$\left| \iint g_k g^* du d\tau \right|^2 < \iint |g_k|^2 du d\tau \iint |g_k|^2 du d\tau$$
 3.6.9

where the < holds for  $g(x_3,y_3) \neq Kg_k(x_3,y_3)$  for K any arbitrary constant. Thus, the correlation coefficient, measured by a photocell

behind a pinhole, with the matched filter is larger than with any other filter or

$$S_{k} > S$$
 3.6.10

and where  $S_{\mathbf{k}}/S$  is the discrimination ratio.

Rapid automatic pattern recognition is a potential application of this type of optical correlation [58].

# 3.7 The Recall Variables: Latent Fingerprint Transparency and FTH Memory Frame, Filter, Positioning Accuracies

VanderLugt states the premise that optical data processing systems should have the capability to search the input data for location, scale, and orientation of the signal [39]. As with the usual coherent optical system frequency-plane filtering methods, the input data location problem is solved here inherently as part of the recognition problem, (see Section 4.3). VanderLugt, et al., [56] have also concluded that, although system response decreases with departure from nominal scale and orientation, the response deterioration as a function of the input quality degradation is far greater than the effects of a change in input size, or orientation.

Filter displacements which may be expected to be induced by a changing mechanism are lateral, longitudinal, and tilting. Lateral and longitudinal displacements are considered as the most likely to occur. FTH filter positioning tolerances have been studied, for the coherent optical matched filter system, for both uniform and nonuniform spectral densities [59]. The optical data processing system utilized is as shown by Figure 5, p. 31.

The SNR is based on the intensities of the light distributions in the output plane  $P_{\mathfrak{F}}$ . The performance criterion for lateral

displacement is the SNR, as a function of displacement  $\Delta p$  of the filter normal to the optical axis, normalized to unity for zero displacement.

Since the position of the signal in the input plane does not affect the maximum value of the signal in the output, the SNR may be derived by computing its value for  $\mathbf{x}_1 = \mathbf{x}_3 = 0$ . Assuming uniform spectral density, where the input plane data is given by  $f(\mathbf{x}_1) = g(\mathbf{x}_1) + n(\mathbf{x}_1)$  so the noise is homogenous and additive, the signal response at the output plane,  $P_3$ , is given by

$$r_{\text{signal}} = \frac{K}{2\pi} \int_{-\infty}^{+\infty} \frac{G(p)G^*(p+\Delta p)\exp(jpx_3)}{\left|N(p+\Delta p)\right|^2} dp \qquad 3.7.1$$

where the signal extent is assumed to be much less than the aperture of the system. Using the convolution theorem, Eq. 3.7.1 can be stated as

$$r_{\text{signal}} = \frac{K}{N_0} \int_{0}^{+\infty} g(\boldsymbol{\gamma}) g^*(\boldsymbol{\gamma} + x_3) \exp[-j \Delta p(\boldsymbol{\gamma} + x_3)] d\boldsymbol{\gamma} \quad 3.7.2$$

for uniform noise spectral density of  $N_0^2$ , and where the matched filter is in the classic form  $H(p,q) = KG^{*}(p,q) / |N(p,q)|^2$  (see Section 3.6). The mean square noise at the output is given by

$$r_{\text{noise}} = \frac{\kappa^2}{2\pi} \int_{-\infty}^{\infty} \frac{|N(p)|^2 |G(p+\Delta p)|^2}{|N(p+\Delta p)|^4} dp \qquad 3.7.3$$

which is independent of the filter displacement,  $\Delta p$ , and can be stated,

by use of Parseval's formula, as

$$r_{\text{noise}} = \frac{K^2}{N_0} \int_{-\infty}^{+\infty} |g(\boldsymbol{\gamma})|^2 d\boldsymbol{\gamma}$$
 3.7.4

The SNR is then given by

SNR = 
$$\frac{\left|\frac{r_{signal}(x_3=0,\Delta p)}{r_{noise}(\Delta p)}\right|^2}{3.7.5}$$

and

performance = 
$$\frac{\left| \int_{-\infty}^{+\infty} |g(\boldsymbol{\tau})|^2 \exp(-j\Delta p \boldsymbol{\tau}) d\boldsymbol{\tau} |^2}{\left| \int_{-\infty}^{+\infty} |g(\boldsymbol{\tau})|^2 d\boldsymbol{\tau} |^2} \right|^2}$$
3.7.6

where  $\Delta p$  = displacement of the filter, in plane  $P_2$ , and  $0 \le \tau \le L$ , with L = length of the signal.

To relate the signal to the performance of the system for small values of displacement  $\Delta p$ , a signal is needed that would cause a rapid decrease in performance with small increase in  $\Delta p$ . This signal would therefore maximize the derivative of the performance equation for small values of  $\Delta p$ . The derivative of Eq. 3.7.6 is maximized, for small  $\Delta p$ , if (from Eq. 3.7.6)  $\int_0^L \gamma |g(\gamma)|^2 d\gamma$  is maximized, and this integral is maximized if the signal is defined as

$$|g(\tau)|^2 = 1$$
;  $0 \le \tau \le L$  3.7.7  
= 0; elsewhere.

Substituting in Eq. 3.7.6 gives

performance = 
$$sinc^2 \left(\frac{\Delta pL}{2}\right)$$
 3.7.8

and the performance is observed to decrease rapidly with increasing lateral filter displacement  $\Delta \xi$ , where  $\xi = \lambda lp/2\pi$  and  $\chi = \lambda lq/2\pi$ . The performance degradation vs. increasing displacement is more pronounced as the input signal length increases. This can be related directly to the space-bandwidth product of the signal.

With nonuniform noise, for the same relative aperture of the optical system (L/1, where L = length of the signal and l = distance from plane  $P_1$  to plane  $P_2$  of Figure 5), the effect is more severe. The allowed displacement is nearly an order of magnitude less for the same loss in performance, when compared to the uniform noise case. Performance is therefore very much dependent on the form of  $\left| N(p) \right|^2$ .

To discuss filter displacement parallel to the optical axis, the system is considered as having the filter in a Fresnel diffraction plane, as opposed to the Fraunhofer, since the system is now space variant. With L  $\ll$  1, the Fourier-transform of the signal is a slowly varying function of  $\Delta z$ , the displacement of the filter from the frequency plane. The performance of the system in this case may be determined as a function of c/1, for fixed values of  $\Delta z$  and relative aperture, where c is the distance that a signal is displaced from the optical axis in the object plane (refer to Figure 10).

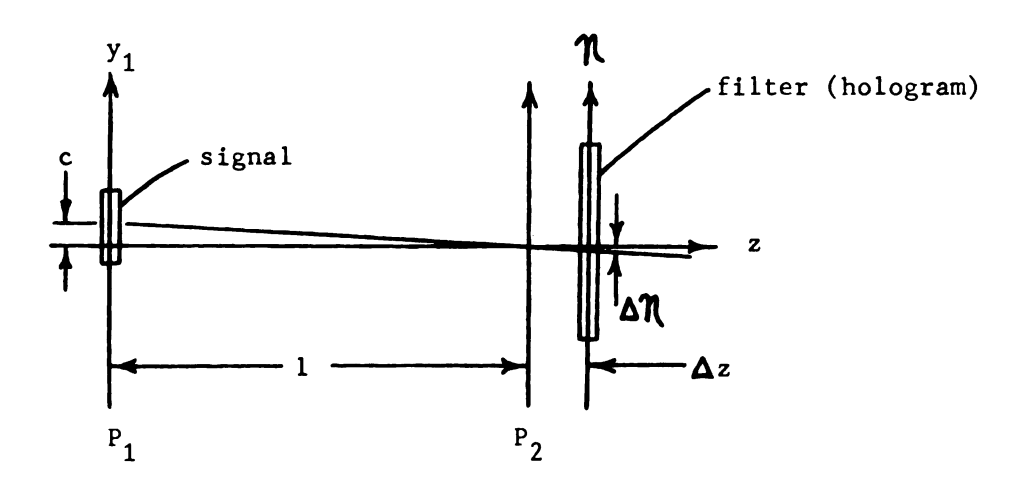


FIGURE 10. Longitudinal Filter Displacement From the Frequency Plane

The signal path from the center of the signal spectrum passes through the frequency plane at the optical axis, and is displaced a distance  $\Delta N$  from the optical axis at the  $\Delta z$  displaced filter, where

$$\Delta \mathcal{N} = \frac{c \Delta z}{1}$$
 3.7.9

and combined with the relation  $\mathcal{T} = \lambda \ln 2\pi$ , gives

$$\Delta p = \frac{2\pi c}{\lambda 1^2} \Delta z$$
 3.7.10

which is then substituted in Eq. 3.7.6 to relate the performance of the system to  $\Delta z$  and also c.

Comparing to the case of lateral displacement, for the same loss in performance vs. displacement, the longitudinal displacement required is much larger than the lateral. That is, longitudinal filter displacement has far less effect on system performance, than an equivalent length lateral displacement. This same result is obtained for uniform and nonuniform noise spectral density.

## 3.8 The Extended-Reference-Source, "Ghost Imaging," or Self-Associative Holographic Memory

From the previous discussion of fingerprint identification methods it may be concluded that it is desirable to apply FTH techniques. An expressed aim is also to utilize a holographic memory to store the fingerprint library. It is possible to realize these desirable features when using the self-associative concept, or as defined by Stroke, the "coded Fourier-transform hologram" method [2]. Also of importance, retrieval with incomplete, or fragmentary, information is achieved with this method.

In this case the object wavefront can be considered as consisting of two parts

$$O = A + B$$
 3.8.1

which overlap in the far field or Fraunhofer region. If the respective amplitudes in the plane of the recording medium are then given by  $\mathrm{O}_{\mathrm{A}}$  and  $\mathrm{O}_{\mathrm{B}}$ , the intensity recorded is

$$I = |O|^{2} = |O_{A} + O_{B}|^{2} = |O_{A}|^{2} + |O_{B}|^{2} + O_{A}O_{B}^{*} + O_{A}^{*}O_{B}.$$
 3.8.2

The recording of this diffraction pattern thus forms a hologram (see

Section 3.2), and the phase is recorded without using a separate reference beam. If the B wavefront is now considered as being the reference wave, the analysis here involves the use of a source other than a point source, i.e., the source is of finite extent as indicated in Figure 11. In place of the point source, a spatially coherent extended source is used for the reference beam.

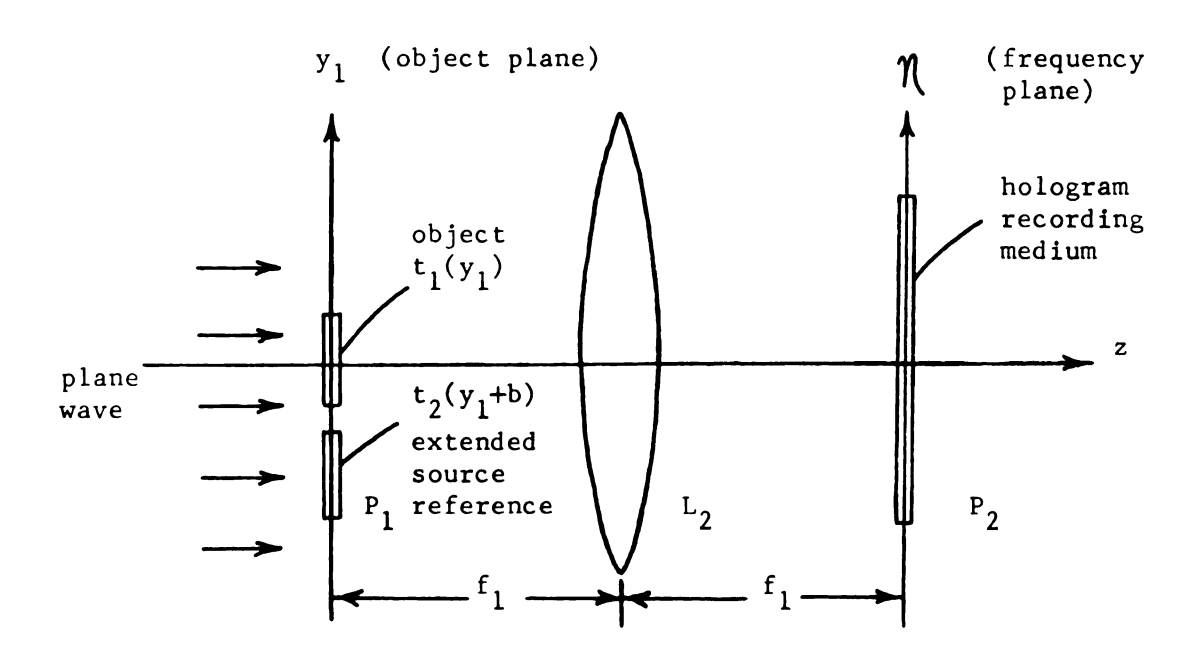


FIGURE 11. Forming the Extended-Reference-Source Fourier-Transform Hologram.

It has been proven that a finite source in Fourier holography is compensated for if the reconstructing source is identical to the source used to obtain the hologram, and this source has certain symmetry properties [60]. This may be shown by considering the complex amplitude at the hologram recording plane for both the object and reference waves as being spatially modulated. That is, the object and reference waves,

A and B, are both given by illuminating transparencies with amplitude transmissions  $t_1(y_1)$  and  $t_2(y_1+b)$ , respectively, with collimated light. In the following, only the spatial variation in the y-direction is considered, to simplify notation.

The transmitted light complex amplitude, from a unit amplitude plane wave illumination, immediately behind the object plane  $(x_1,y_1)$  is given by

$$t_1(y_1) + t_2(y_1 + b)$$
 . 3.8.3

Lens  $L_2$  performs a Fourier-transformation to give, in the frequency plane  $P_2$ , the complex amplitude

$$T_1(q) + T_2(q) \exp(-jqb)$$
 3.8.4

where  $T_1(q) = F[t_1(y_1)]$  and  $T_2(q) = F[t_2(y_1)]$  with p,q chosen to be positive. Correct exposure and development of the photographic plate or film inserted into plane  $P_2$  records the interference of the Fourier-transforms of  $t_1$  and  $t_2$  to give the Fourier-transform hologram. The intensity recorded is

$$I(q) = |T_{1}(q) + T_{2}(q) \exp(-jqb)|^{2}$$

$$= [|T_{1}|^{2} + |T_{2}|^{2}] + T_{1}T_{2}^{*} \exp(+jqb) + T_{1}^{*}T_{2} \exp(-jqb).$$
3.8.5

This hologram then has a transmittance, t, proportional to I(q).

The hologram is now replaced in its original, or recording, position in plane  $P_2$  and the transparency  $t_2$  is removed from the object plane. Illuminating the transparency  $t_1$  by a plane wave (Figure 4), the complex amplitude of the wavefront at the  $P_2$  plane is the Fourier-transform of  $t_1$ . The complex amplitude transmitted by the hologram is then  $T_1$  • t. The third term of Eq. 3.8.5 then yields

a reconstructed wave in the output plane, the upper sideband image, which is due to taking the inverse Fourier-transform of the complex amplitude distribution in the  $P_2$  plane by lens  $L_3$ , and which is proportional (note Eq. 3.2.4) to

$$F^{-1}[T_1T_1^*T_2\exp(-jqb)].$$
 3.8.6

This may be written as

$$F^{-1}\left\{F[t_1(y_3) \times t_1^*(y_3)]T_2\exp(-jqb)\right\}$$
 3.8.7

and since  $T_2 \exp(-jqb) = F[t_2(y_3+b)]$  this image amplitude is given by

$$A(y_3) \sim F^{-1} \left\{ F[t_1(y_3) \times t_1^*(y_3)] F[t_2(y_3+b)] \right\}$$

$$\sim [t_1(y_3) \times t_1^*(y_3)] \otimes t_2(y_3+b).$$
3.8.8

Thus, the complex amplitude in the output plane is the convolution of  $t_2(y_3+b)$  with the autocorrelation of  $t_1(y_3)$ . This image is centered at the coordinate  $y_3 = -b$  (noting the reflected coordinate system of plane  $P_3$  in Figure 4.) If the autocorrelation of  $t_1$  is a **S**-function, this yields an image of the transmittance  $t_2(y_1+b)$ . If this condition is satisfied, the autocorrelation function shows a single sharp peak.

A very narrow peak of the autocorrelation function

where  $t_1$  reconstructing =  $t_1$  recording, approaching a  $\delta$ -function, is possible if  $t_1$  has a very broad spectrum of spatial frequencies. An example is the regular-sized complex-structured fingerprint. The natural size fingerprint has a binary structure with a relatively high and limited spatial frequency content of 2-10 lines/mm. This leads to recording fringes of the higher spatial frequencies essential to high selectivity. The result is a high autocorrelation spot

intensity, or high matched filtering discrimination ratio between identical fingerprints with respect to noise level (Figure 12).

A peak autocorrelation intensity for identical fingerprints of 175 times noise level has been reported by Horvath, et al., [31].

The second term of Eq. 3.8.5 yields a reconstructed wave in the output plane whose image amplitude is given by

$$A(y_3) \leftarrow [t_1(y_3) \oplus t_1(y_3)] \times t_2^*(-y_3+b)$$
 3.8.10

This complex amplitude in the output plane is the cross-correlation of  $t_2^*(-y+b)$  with the convolution  $[t_1(y_3) \bigotimes t_1(y_3)]$ . This convolution is not, in general, a  $\delta$ -function, except for sources with twofold rotational symmetry about the optical axis. An uncompensated, or "smeared," reconstruction then results, centered at  $y_3 = +b$ , as the extended-reference-source method lower sideband image.

## 3.9 Summary of Theoretical Considerations

Photographic emulsion, plane amplitude, near-Fourier-transform holograms, with recorded fringes normal to the surface, are assumed as the memory medium. The FTH provides redundant recording, and separation of reconstruction images is possible by choosing a sufficiently high spatial carrier frequency. However, diffraction efficiency decreases with increasing offset angle. In the reconstruction, hologram (filter) lateral displacement from the recording position is critical in determining performance. The allowed displacement is very dependent on the form of  $\left| N(p,q) \right|^2$ . In matched filtering, a bright output plane spot image is formed only if the recording and reconstruction signals are identical. Recording and retrieval with an extended-reference source is possible if the autocorrelation of the reconstructing wave front has a single sharp peak.



FIGURE 12. Output Plane Light Distribution From a Coherent Optical Matched-Filter Correlator Showing the Autocorrelation of an Oily Fingerprint. (Courtesy C. E. Thomas, KMS Industries).

#### CHAPTER IV

## THE SELF-ASSOCIATIVE HOLOGRAPHIC MEMORY AND RECORDING/RETRIEVAL OF FINGERPRINT DATA

In this chapter we synthesize a system for latent fingerprint identification, based on self-associative holographic fingerprint storage, and retrieval by FTH detection filtering. It is proposed to utilize (1) extended-reference-source coding, in the form of light-source code patterns from an array of point sources, to associatively record the fingerprint library, (2) storage of fingerprint variants which can be used to "confirm" the identification, and (3) superposition recording of the different fingerprints utilizing a change in propagation direction of the reference beam, or spatial frequency multiplexing. The change in reference wavefront direction increases discrimination in the output, with the recall actually being based on association.

## 4.1 <u>Description of the Proposed Self-Associative Holographic</u> Memory

The data is divided into two parts. One set of data consists of the fingerprints. The other set of data consists of point-source code words. Illumination of a photographic plate by the interference pattern of a fingerprint beam and a code beam is used to form a Fourier-transform hologram.

Several fingerprint variants are recorded in association with one code word. Each fingerprint would be stored together with several rotation, printing pressure, and different size variants, as indicated by Figures 13 and 14. Recording of the variants

might be performed by use of computer generated patterns, by fingerprint ridge tracing on the original print card.

Block and consecutive recording are combined, as indicated by

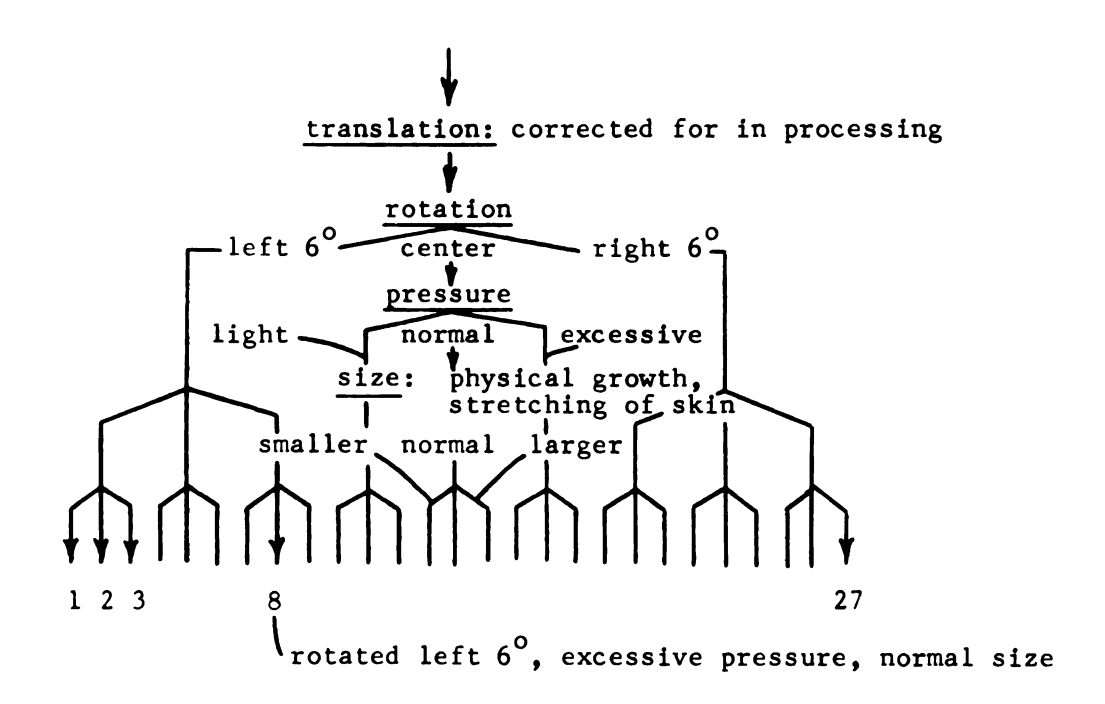


FIGURE 13. Twenty-seven Variants/Fingerprint, Ten-Finger File.

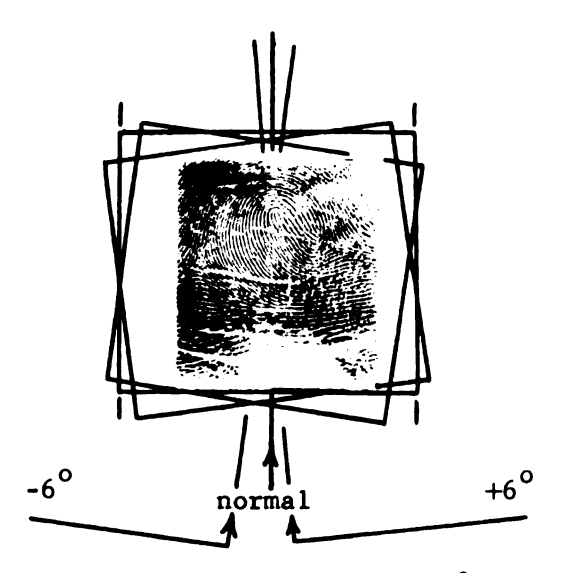


FIGURE 14. The Rotation Variants. (Up to  $\pm 3^{\circ}$  Relative Rotation Gives Little or No Effect in Matched Filtering Methods, as noted on p. 21).

Figure 15. Each hologram frame contains a number of blocks, or sub-holograms. The subholograms, (filters) consisting of a fingerprint or variant recording, are formed in non-overlapping fashion over a photographic plate and designated as a "layer." The different prints and variants are then recorded on the same hologram in superposition as consecutive layers. A layer equals one print plus all its variants. The layers are not physically separable, and are differentiated from each other by recording with different code words, and by spatial frequency multiplexing, or recording with different carrier frequencies.

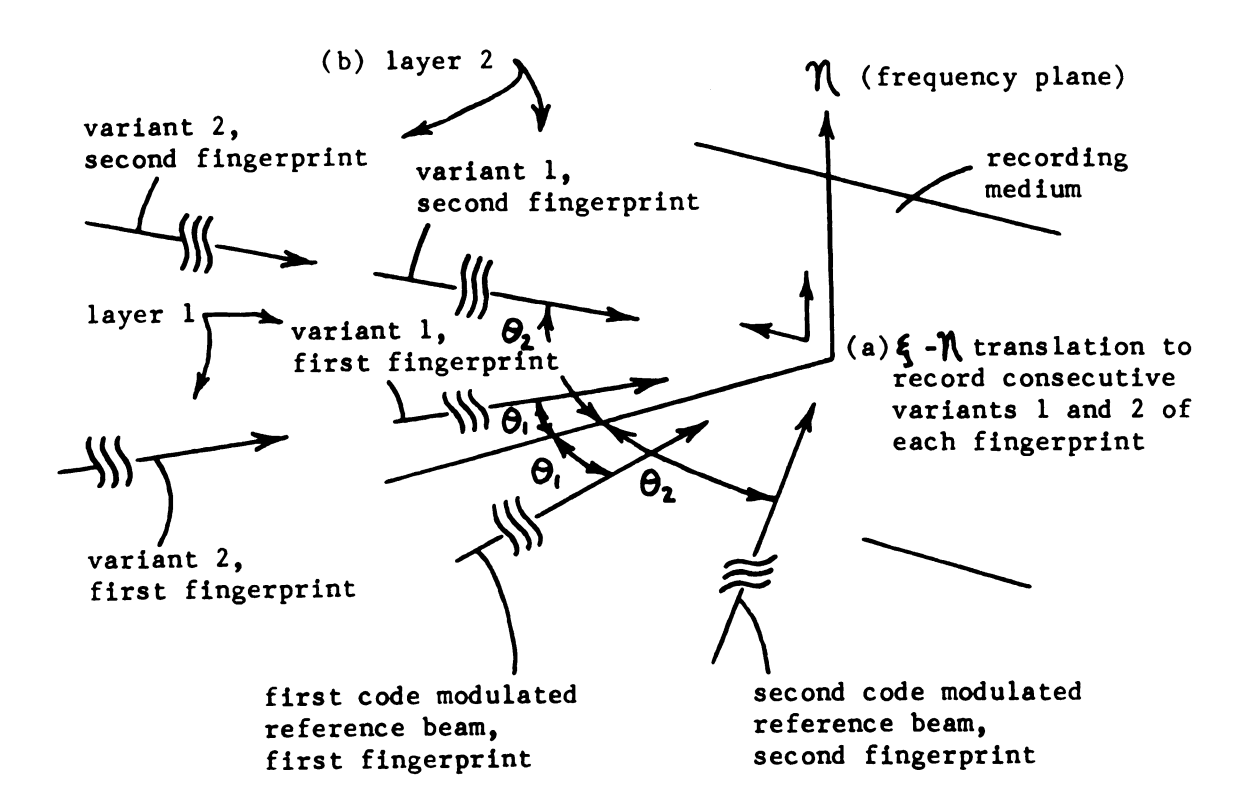


FIGURE 15. Consecutive Recording of (a) Fingerprint Variants and (b) Different Fingerprints in Superposition.

Two collimated beams originating from a laser are used for recording each subhologram. One beam is coded by passing it through a transparency of the fingerprint or its variant. The other beam passes through a code mask consisting essentially of an array of holes in a plate, forming a matrix of point sources of light.

The two-dimensional code plate consists of (a) an array of small, simple, glass lenses of short focal length mounted in a plate, and (b) a shutter, or light valve, matrix plate mask. The lens array is used to produce an array of point sources, or focused spots of light, at the shutter plate. This provides uniform, spatially coherent, illumination of the shutter plate. The shutter matrix plate is then used to vary the code by opening or closing the shutters or valves. This geometry is indicated by Figure 16. Note also Figure 8(a).

The multiple waves of the array code interfere with a fingerprint variant wavefront at the frequency plane P<sub>2</sub> and are recorded to form a Fourier-transform subhologram. A fly's-eye lens array [61], [62] is used to image the object beam onto the storage medium. The fly's-eye lens array, together with the x,y deflection of the laser beam, produces an array of point sources. Each point source provides a different propagation angle for the object beam, and illuminates a different subhologram recording area. A page composer mask is utilized at the recording medium to limit the exposed area for each detection filter recording, in order to maximize storage density.

A random phase plate, of 0 degree or 180 degree phase shift, may also be included with the shutter plate mask to ensure a sufficiently uniform spatial distribution of reference illumination of the sub-

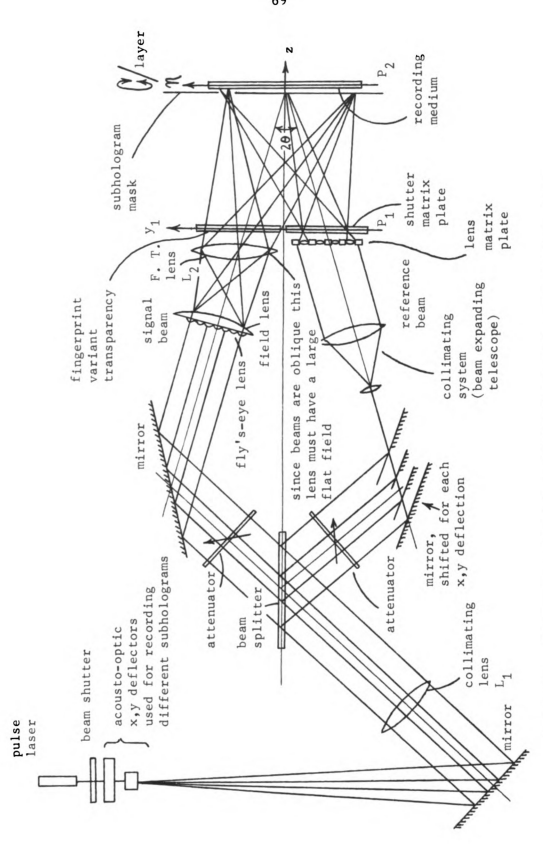


FIGURE 16. Recording the Self-Associative Hologram: Functional Diagram

holograms [63]. The phase would here be shifted according to a computer-generated pseudo-random sequence. For the present consideration the phase mask is omitted. A near-Fourier-transform plane recording (p. 37) is assumed, where the displacement distance from the exact Fourier-transform plane is given by [62]

± 1**λ**/wD 4.1.1

where l = the distance between the object plane and the exact F. T. plane, w = the code point spacing, and D = the code plate aperture.

In the recall, or search, process the hologram developed from the above recording procedure is placed at the identical position it occupied during recording. A search mask consisting of a latent print transparency (or light modulator presentation) is placed in the input plane. It occupies the same position as that occupied by the recording fingerprint variants.

A hololens [64] is used to illuminate all the subholograms on one hologram plate simultaneously with the latent fingerprint beam f. The hololens is essentially a holographic fly's-eye lens and consists of an array of point-source phase holograms, one for each subhologram of page capacity. The hololens provides a method of beam deflection with efficient light utilization.

A real ghost image of the code array associated with the stored fingerprint F ( $f \simeq F$ ) is obtained, together with the stored print image, in some measure from each subhologram of the layer containing F and its variants. The code array images from each layer appear in

Reconstruction positioning accuracies were discussed in Section 3.7 and are discussed further in Sections 4.3 and 4.5.

superposition. The superposition of the code images results in a confirmation by the variant subholograms.

To isolate the upper sideband image containing the desired code, a mask in the output plane may be used to eliminate the undiffracted light and the lower sideband image. All recordings of different fingerprints, of up to the order of 10 to 10<sup>2</sup> in superposition, on one hologram can be searched simultaneously, as shown by Figure 17.

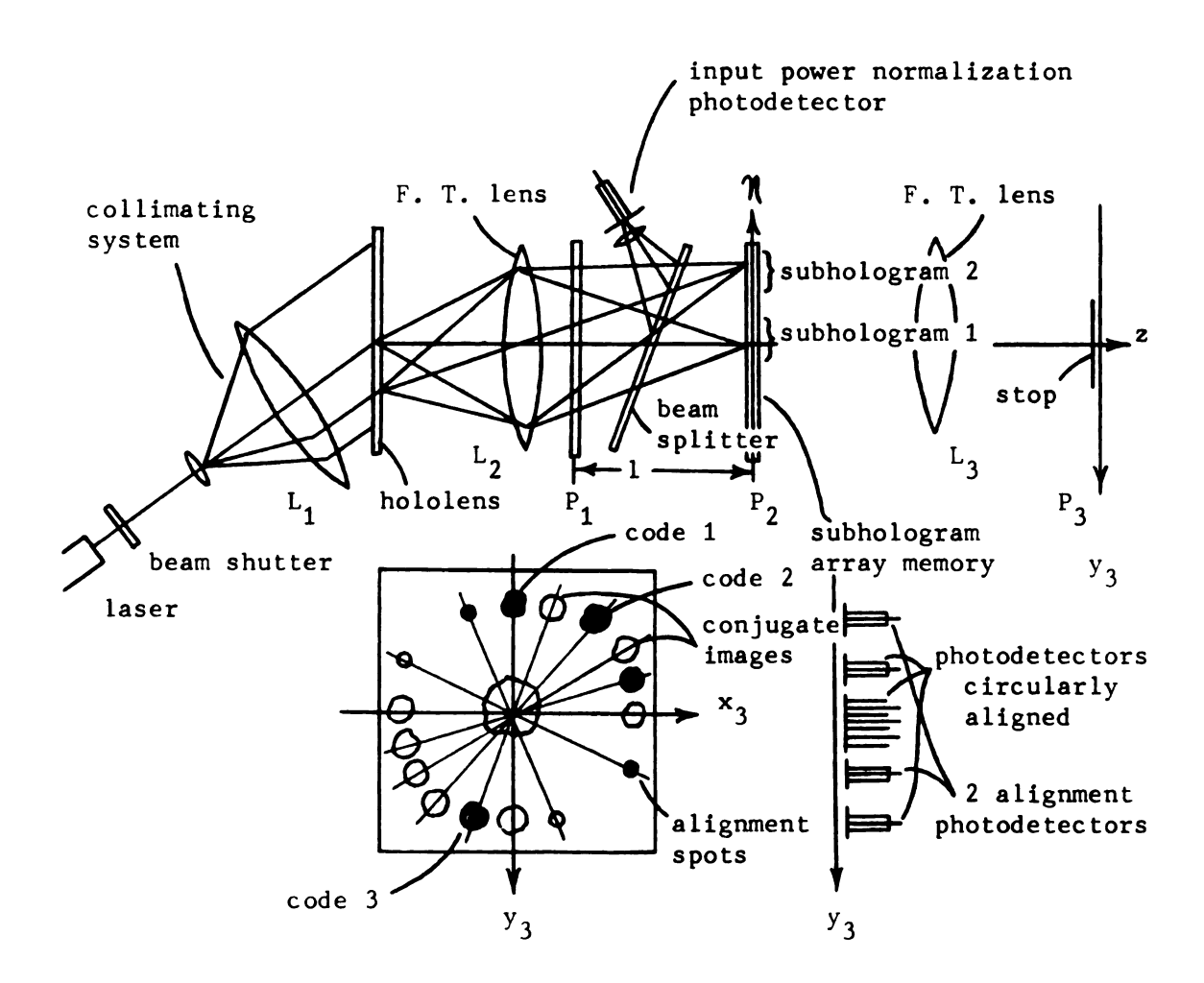


FIGURE 17. Hololens Search for a Fingerprint Match With a Latent Fingerprint Input: Functional Diagram.

The latent print input can also be routed to search several pages (filters) in parallel in order to increase search speed, Figure 18.

The plane wavefront of a laser beam can be decomposed by lenses and modulator elements into sub-beams. For intermediate optical distances the lens system can be iterated by several successive reimaging stages without suffering diffraction, loss, and scattering.

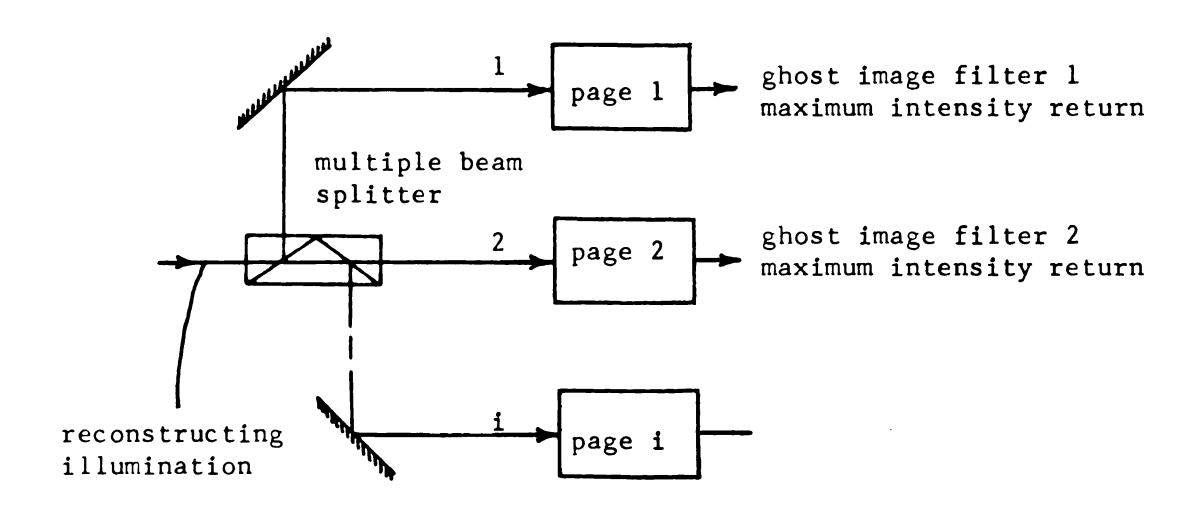


FIGURE 18. Searching Several Pages in Parallel by Use of a Compound Structure of Beam Splitters.

This technique, instead of maximizing the ratio of peak signal to mean noise for one spot image, as in coherent matched filtering, performs the signal-to-noise maximization on an array of spots, in the form of a code. The code is then detected by an electronic system. The proposed self-associative holographic storage technique design is thus aimed at increasing accuracy over the previously considered methods discussed in Section 2.4.

Accuracy requirements which should be satisfied by an automatic fingerprint identification system include: the ability to process a large number of prints against a secure stored-data library, a probability of correct identification of 99% or higher, and a probability of false identification of 2% or lower. Absolute negative response is therefore also needed.

It is believed that a human being will, in the final analysis, always have to inspect visually a claimed match. Thus, the false match is considered to be the least serious error. False dismissal, however, provides no opportunity for correction, and is a serious error.

## 4.2 <u>Capabilities of the Self-Associative Holographic Memory In</u> Automatic Fingerprint Identification

A pre-processing step may be utilized to produce an enhanced representation of the latent fingerprint before its conversion to transparency form. A flying-spot scanner reader with detectors that are sensitive to white (uninked), black (inked), and gray (partially inked) areas would scan the fingerprint and pass its information to the pre-processor. The pre-processor can then apply continuity logic to locate fingerprint ridges to reinforce their structure by eliminating inking imperfections such as small breaks, pore holes, and separation of blurred ridges [65].

The basic retrieval aim is to transform a latent print input into its associated code output. A full fingerprint image corresponding to the latent (partial) input would also be recalled, but the requirements for resolution of the fingerprint image are not considered at this time.

A negative of the fingerprint (white ridges on a black back-ground) is preferred for the object wavefront. A positive has too much white area in common which results in undiffracted light.

Assume a fingerprint variant "negative ridge" transparency in the input (object) plane, with transmittance

$$F(y_1)$$
 4.2.1

and, further, assume the reference wavefront is derived from a one-dimensional array of point sources (Figure 19). Assume the transmittance of one of the point reference sources of the array, located at  $y_1 = -b_i$ , is given by

$$(y_1 + b_i)$$
 4.2.2

with the total point-source array transmittance then expressed as

$$\sum_{i=1}^{N} A_{i} = \sum_{i=1}^{N} \delta(y_{1} + b_{i})$$
 4.2.3

for N point sources.

If the point source array is represented by the complex amplitudes of light arriving at the hologram plane as

$$A_1 + A_2 + \dots$$
 4.2.4

and if the fingerprint light complex amplitude arriving at the hologram is represented by B, then the intensity in the frequency plane is (Eq. 3.2.2)

$$I = (A_{1} + A_{2} + ... + B) (A_{1}^{*} + A_{2}^{*} + ... + B^{*})$$

$$= A_{1}A_{1}^{*} + A_{2}A_{2}^{*} + ... + BB^{*} + ... + (A_{1}A_{2}^{*} + A_{2}A_{1}^{*} + ...)$$

$$+ B(A_{1}^{*} + A_{2}^{*} + ...) + B^{*}(A_{1} + A_{2} + ...).$$

The intermodulation terms  $(A_1A_2^* + A_2A_1^* + ...)$  indicate the interference among the point source terms.

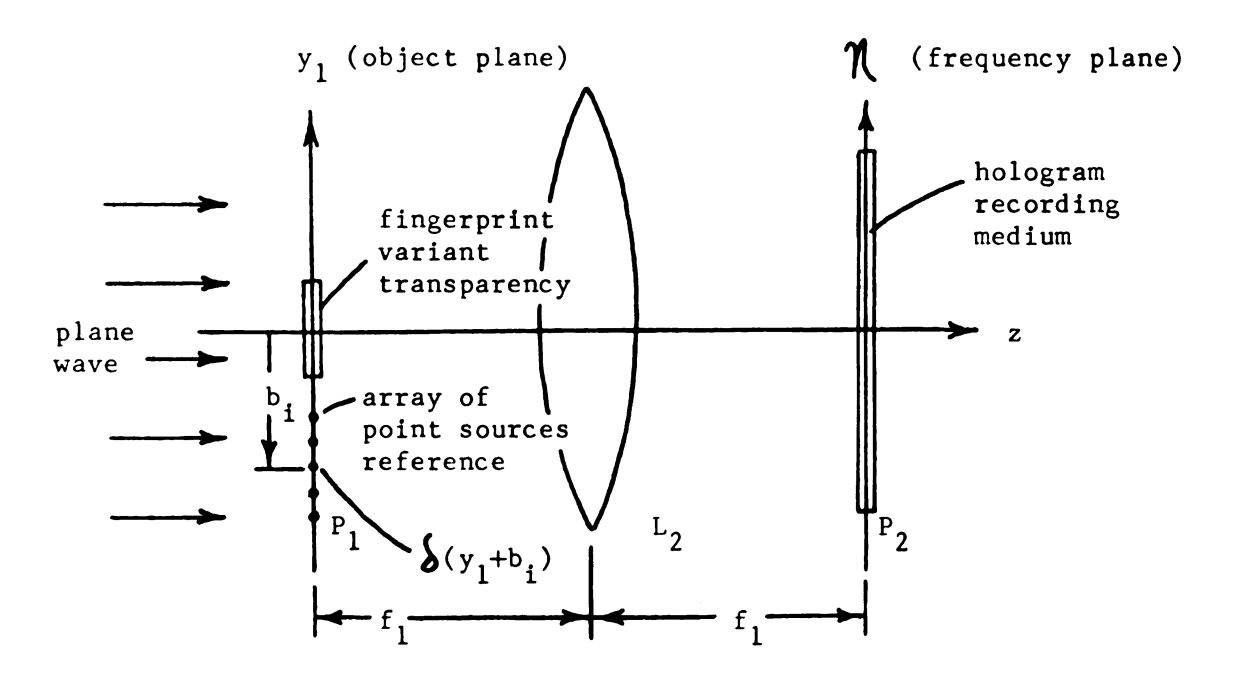


FIGURE 19. Recording the Self-Associative Hologram. (From Figure 11).

A two-dimensional array code, consisting of  $^{M}$  row  $^{x}$   $^{N}$  column point sources appropriately spaced, may be assumed (Eq. 4.2.3) to be represented by

$$\sum_{e,i=1}^{M,N} \alpha_{e,i} \delta^{(x_1+b_e,y_1+b_i)}$$
 4.2.6

where  $\mathcal{A}_{e,i} = 0$  or 1, and  $(b_e,b_i) = coordinates$  of the array code point.

The intensity in the frequency plane at one of the illuminated subholograms (Figure 20) is given, from Eq. 4.2.5,

$$I_{mn}(p,q) = F_{mn}(p,q)F_{mn}^{*}(p,q) + \sum_{e,i=1}^{M,N} \mathcal{Q}_{e,i}^{2}$$

$$+ \sum_{e,i=1}^{M-1,N-1} \sum_{ee,i=2}^{M,N} \mathcal{Q}_{e,i} \mathcal{Q}_{ee,i}^{*} e^{\exp \left\{-j\left[p(b_{e}-b_{ee})+q(b_{i}-b_{ii})\right]\right\}}$$

$$+ \sum_{e,i=1}^{M-1,N-1} \sum_{ee,i=2}^{M,N} \mathcal{Q}_{e,i}^{*} \mathcal{Q}_{ee,ii}^{*} e^{\exp \left\{+j\left[p(b_{e}-b_{ee})+q(b_{i}-b_{ii})\right]\right\}}$$

$$+ F_{mn}(p,q) \sum_{e,i=1}^{M,N} \mathcal{Q}_{e,i}^{*} e^{\exp \left[+j(pb_{e}+qb_{i})\right]}$$

$$+ F_{mn}^{*}(p,q) \sum_{e,i=1}^{M,N} \mathcal{Q}_{e,i}^{*} e^{\exp \left[-j(pb_{e}+b_{i})\right]}$$

$$+ (2.7)$$

where  $F_{mn}(p,q) = F[F_{mn}(x_1,y_1)]$ , and  $F_{mn}(x_1,y_1)$  corresponds to the fingerprint variant defined in Eq. 4.2.1. In an absorption hologram, therefore, the recording consists of a summation of terms.

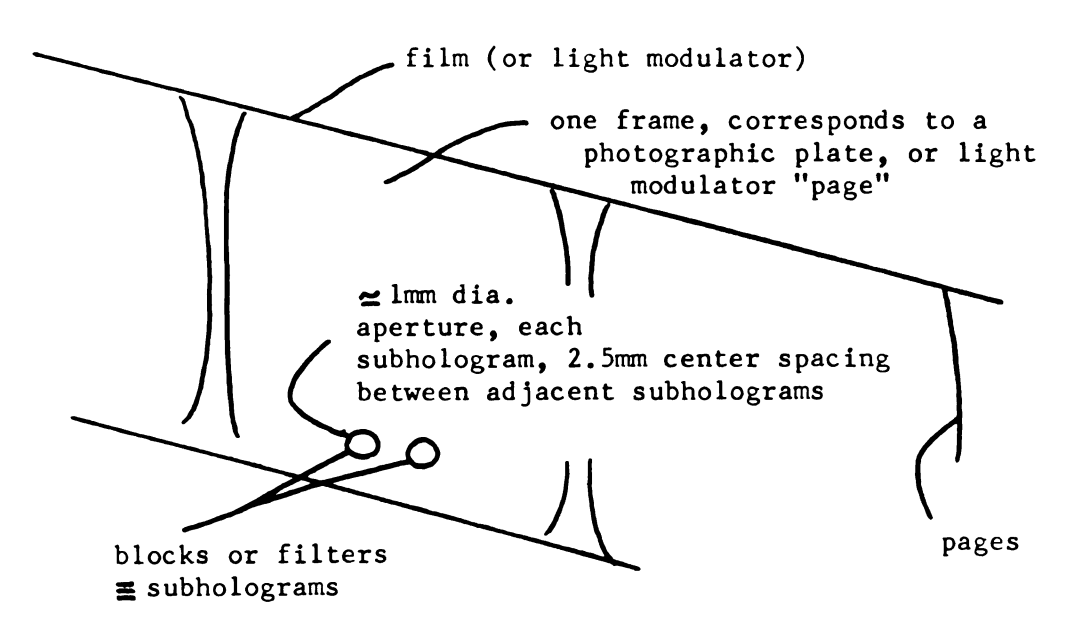


FIGURE 20. The Self-Associative Hologram Physical Geometry.

If the angle between the object (print variant) and reference (point-source array) is chosen large enough to separate the image waves in the output plane  $P_3$  from the waves diffracted by the intermodulation terms (Eq. 3.6.6), the effect of these terms can be neglected. The intermodulation waves propagate in directions close to the direction of the reconstruction illumination (latent print) beam.

The other terms of Eq. 4.2.7 show that the point sources behave independently. Analysis can therefore be restricted to a single point. The analysis for an array of points follows immediately from superposition.

If the hologram is now assumed to be formed by recording the fingerprint-variant object wave interfering with a point reference source, at  $y_1 = -b$ , and described by

$$(y_1+b)$$
 4.2.8

the hologram transmittance, assuming linear recording (Eq. 3.8.5), is given by

t ~  $F(q)F^*(q) + 1 + F(q)exp(+jqb) + F^*(q)exp(-jqb)$  4.2.9 where F(q) = the Fourier-transform of the input object signal, using the relation  $F[S(y_1+b)] = exp(-jqb)$ .

Illuminating the hologram now by the light beam passed through a transparency (or light modulator) of a latent fingerprint, as indicated by Figure 21, whose transmittance is given by

$$f(y_1-c)$$
 4.2.10

the hologram will generate a diffracted wavefront which gives the ghost image of the point source. The complex amplitude transmitted

tsee definition of F[] in nomenclature.

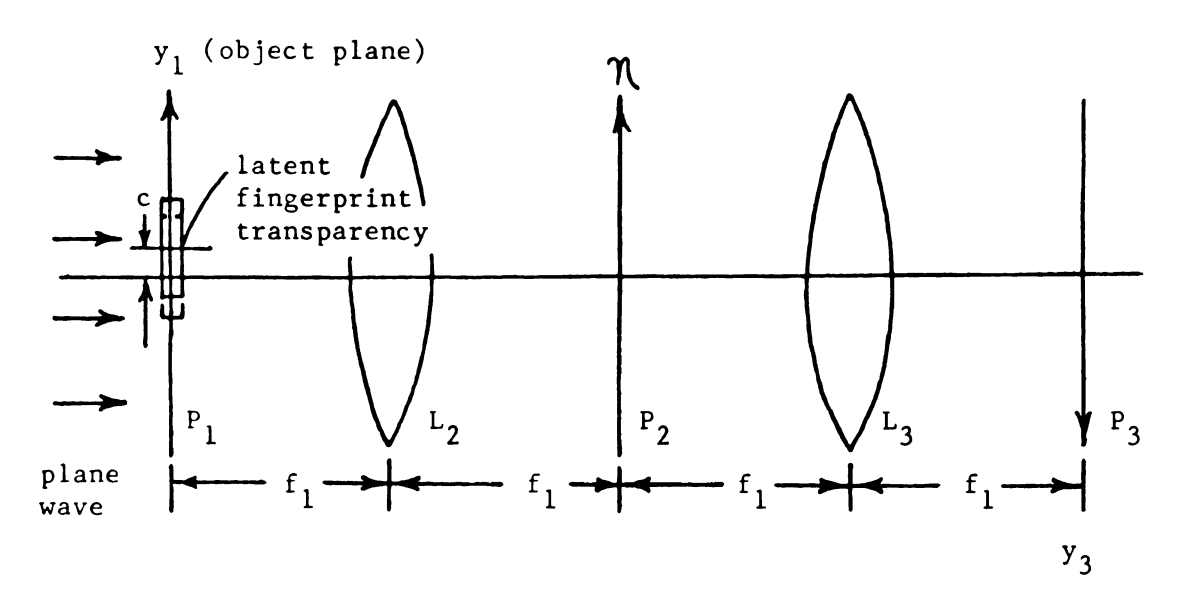


FIGURE 21. Recall With the Self-Associative Hologram.

by the hologram is  $f(q)\exp(+jqc) \cdot t$ , where  $f(q) = F[f(y_1-c)]$ , or

$$r = F(q)F^{*}(q)exp(+jqc) + f(q)exp(+jqc) + F(q)f(q)exp[+jq(c+b)] + F^{*}(q)f(q)exp[-jq(b-c)]$$
4.2.11

or, in terms of the total array code, the complex light amplitude transmitted by the hologram is

$$F_{mn}(p,q)F_{mn}^{*}(p,q)f_{m'n'}(p,q)\exp(+jqc) \qquad 4.2.12$$

$$+ f_{m'n'}(p,q) \sum_{e,i=1}^{M,N} Q_{e,i}^{2} \exp(+jqc)$$

$$+ F_{mn}(p,q)f_{m'n'}(p,q) \sum_{e,i=1}^{M,N} Q_{e,i}^{*} \exp\left\{+j\left[pb_{e}+q(c+b_{i})\right]\right\}$$

$$+ F_{mn}^{*}(p,q)f_{m'n'}(p,q) \sum_{e,i=1}^{M,N} Q_{e,i}^{*} \exp\left\{-j\left[pb_{e}+q(b_{i}-c)\right]\right\}$$

$$+ (see next page)$$

$$(4.2.12 \text{ continued})$$
+  $f_{m'n'}(p,q) = \sum_{e,i=1}^{M-1} \sum_{ee,i=1}^{M-N} \alpha_{e,i} \alpha_{ee,ii}^* \exp \left\{ -j \left[ p(b_e - b_{ee}) + q(c + b_i - b_{ii}) \right] \right\}$ 
+  $f_{m'n'}(p,q) = \sum_{e,i=1}^{M-1} \sum_{ee,i=1}^{M-N} \alpha_{e,i}^* \alpha_{ee,ii}^* \exp \left\{ +j \left[ p(b_e - b_{ee}) + q(c + b_i - b_{ii}) \right] \right\}$ 

where  $f_{m'n'}(y_1-c)$  is, in this case, a latent fingerprint transmittance corresponding to the  $n^{th}$  variant of the  $m^{th}$  stored print, and the last two terms are the intermodulation terms and represent the background noise.

If the holographic recording is nonlinear, as indicated by quadratic and higher order diffraction, the presence of the intermodulation terms may result in the generation of false images at the primary image locations of other code image points. However, intermodulation term noise is not a factor in Fourier-transform absorption holograms if the recording is linear. In this case, the reconstructed wave amplitude is proportional to the object wave amplitude used in recording the hologram. Not exceeding the dynamic range of the recording medium, which would produce a recorded nonlinearity, then becomes important.

As noted previously (p.77), with linear reconstruction, the intermodulation terms scatter light only in the vicinity of the reconstructing beam and will not affect the desired image quality. Intermodulation noise is therefore a problem only at low carrier frequencies.

Taking the inverse Fourier transformation of Eq. 4.2.11 by lens  $L_3$  gives the complex amplitude distribution in the output plane (Eqs. 4.1.8 and 4.1.10) in Eq. 4.2.13.

$$A(y_3) \sim [F(y_3) \times F^*(y_3)] \oplus f(y_3-c) + f(y_3-c)$$
  
+  $F(y_3) \oplus f(y_3-c-b)$   
+  $F^*(y_3) \times f(y_3+b-c)$  4.2.13

The first term, for a sharply peaked autocorrelation of F, can be considered as an image of  $f(y_1)$ , centered at  $y_3 = c$ , and is coincident with the undiffracted light image of the latent print, centered at  $y_3 = c$ , as given by the second term. The third term is the lower sideband image, centered in the output plane at  $y_3 = b+c$ . It consists of the convolution of the stored print  $\equiv F$  and the latent print  $\equiv f$ . The fourth term is of importance here, as it contains a ghost image of the point source, centered at  $y_3 = -b$ , if f is considered as a partial of F. The fourth term of Eq. 4.2.13 can be rewritten as

$$F^{-1}\left\{F^{*}(q)f(q)\exp[-jq(b-c)]\right\}$$

$$= F^{-1}\left\{F^{*}(q)f(q)\exp(jqc)\exp(-jqb)\right\}$$

$$= F^{-1}\left\{f^{*}(q)f(q)\exp(-jqb) + \left[F^{*}(q)-f^{*}(q)\right]f(q)\exp[-jq(b-c)]\right\}$$

$$= \left[f^{*}(y_{3})Xf(y_{3})\right] (y_{3}+b) + \left[(F^{*}(y_{3})-f^{*}(y_{3}))Xf(y_{3})\right] (y_{3}+b-c)$$

The first term of Eq. 4.2.14 represents the autocorrelation of f evaluated at  $y_3 = -b$ . The total recorded information, 0 of Eq. 3.8.1, can be assumed to consist of the stored fingerprint variant plus its array code (point source), with f being a fragment of this total. For a sharply peaked autocorrelation of f this gives a ghost image of the point source, or  $(y_3+b)$  located at  $y_3 = -b$ . This results in the familiar spot image observed in the classical character recognition VanderLugt matched filter technique. However, instead of one spot, a matrix of spots is

found in the output plane. The quality of this image is dependent on how nearly the autocorrelation of the fragment approaches a 6-function. The image has the same form as in the recording, or is essentially realized as

$$\left| \sum_{e,i=1}^{M,N} (x_i + b_e, y_3 + b_i) \right|^2 .$$
 4.2.15

The second term of Eq. 4.2.14 consists of the cross-correlation of the latent print f with the portion of the stored print missing in f, i.e.,  $F^*-f^*$ , evaluated at  $y_3 = -b+c$ . That is, the broad cross-correlation function is found in the vicinity of the peaked autocorrelation, with center displacement from  $y_3 = -b$  depending on the area of the stored print, such as center or edge, given by the latent print. (This is discussed further in Section 4.4)

This result satisfies the matched filter concept expressed in Section 3.6. The terms derived are essentially the same as for complex spatial filtering, where the optimum filtering process is given by

$$H(p,q) = \frac{G^{*}(p,q)}{N(p,q)}$$
 4.2.16

For recognizing an input latent fingerprint pattern given by  $F(y_1-c)$ ,  $G^*(p,q)$  must be set equal to

$$F^{*}(q)\exp(-jqc) \qquad 4.2.17$$

where N(p,q) represents the Wiener spectrum of the autocorrelation of the complex input noise transmittance in the plane  $(x_1,y_1)$ .

In a fingerprint identification system, noise is in the form of smudges, dirt, and other degradations. Under these conditions, N(p,q) is none-white and non-Gaussian, and is a function of spatial

frequency. However, in practical applications 1/N(p,q) may still be assumed to be a proportionality constant, as noted, in Section 3.6.

The degree of scale or rotation difference, for example, between the input (latent) print and any subhologram stored print determines the extent of recall, or confirmation, of the print code by each respective subhologram. Noise sources of this type are suppressed in each layer in terms of how much the noise affects each variant subhologram in that layer. Noise sources that influence only a few subholograms can therefore be highly suppressed.

A processing method which is designed to suppress noise due to signal size change is given by VanderLugt [39], and a variation is also discussed by Lee and Gossen [66]. However, this method involves mechanical adjustment in the form of axial movement, from Figure 5, of the plane  $P_1$ , lens  $L_3$ , and plane  $P_2$ , and is not amenable to highspeed processing.

The answer to the search, i.e., a match or no match to a stored fingerprint, is obtained by utilizing a thresholding device. All ghost images of the point-source code array are compared to detect the code with the highest intensity for a maximum number of array points.

One of the problems with the standard optical correlation matched filter scheme is that the brightness of the autocorrelation spot may be equal, or above the threshold, for several fingerprints. This problem is minimized by utilizing a self-correcting code, consisting of an array of point sources, instead of one point source.

Using one-dimensional notation, the code is accepted only if all n out of a total of N points are above threshold. Further, each code word has the same number of code array points. Thus, the same number, n  $(n \le N)$ , of points are checked between different finger-prints for intensity. The intensity of a code-image point-source response reflects the degree of match between the content of the search mask (latent print) and the stored data (stored print).

# 4.3 Provisions for Accurate Latent Fingerprint Transparency and FTH Filter Positioning In the Recall, or Search, Process

As in other holographic optical memory configurations [17], the successful operation of this system depends on close angular tolerances. The reconstruction (code) from all subholograms of each layer must be superimposed on a common readout matrix. Due to emulsion shrinkage some slight distortion and non-overlap is to be expected, but may not be observable in practice.

Rapid movement of the holograms through the system is envisioned during the search. The identical placement requirement, as expressed in Section 3.7, therefore presents a problem. Automatic alignment of each hologram, or page, before it is searched, with either continuous movement or "paging," is necessary. This can be accomplished by utilizing an auxiliary point source interference recorded on the hologram. Maximum brightness, or the exceeding of a threshold, of the output plane spot of this source (see Section 3.6) is used as an indication of accurate alignment. A narrow-band detector of a few photocells would be required to sense any displacement.

In the search process the input latent print could also be displaced when converting to transparency form, in a lateral translation, for example, from the original print recording position. With techniques such as vidicon scanning, the position of the input object to be identified can be very critical in determining the correct autocorrelation peak. In spatial filtering, the input position is not critical, and in the present case the result is that the ghost image of the corresponding code will appear displaced by the same input displacement distance in the output plane.

From Figure 21, the input latent fingerprint transparency  $f(y_1-c)$  could be displaced from its original position (see Figure 19) by d units in the  $+y_1$  direction, with its transmittance then given by  $f(y_1-c-d)$ . From Eq. 4.2.14, the first term becomes

$$[f^*(y_3) \star f(y_3)] \otimes \delta(y_3 + b - d)$$
 4.3.1

where the point-source image is displaced from  $y_3 = -b$  by d units in the  $+y_3$  direction.

Output sensing compensation for this latent print displacement is accomplished by an automatic check of the output plane auxiliary point source position. It is assumed that a minimum size for a partial latent print is necessary, such as 1/3 or 1/2 of the finger-print, in order to determine reasonable recording positional accuracy such as right-side-up, etc.

### 4.4 Requirements When Addressing With Fragmentary Information

A fragment of the object can be used to illuminate a Fourier-transform hologram to generate a "ghost image" of the remainder.

This ghost image will, however, be noisier as the fragment decreases

in size (and changes position). This point of view is basic to the fingerprint identification method described here, and is shown by Figure 22. Also, if the input information is smeared or noisy in some other respect, besides "too small" a fragment, some light may show up in the code for other fingerprints.

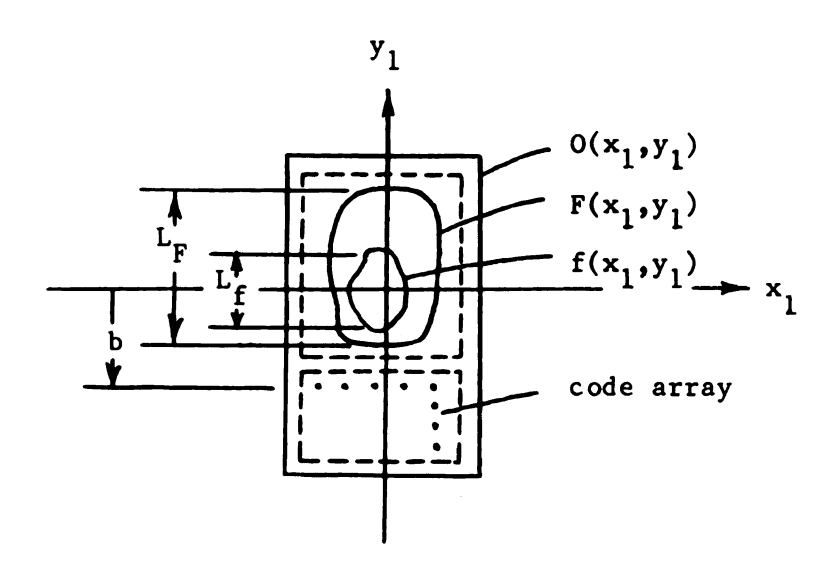


FIGURE 22. Total Object Transmittance 0 = Fingerprint Variant Transmittance F + Its Array Code Transmittance, (Where f May be Considered as a Partial of F, and Where f is a Fragment of 0).

Spurious signals below a given level can be rejected as discussed in Section 4.2. A further check can be made to see that all points of a code are above the threshold, and a final computer decision is made on giving a "more than one possible match" answer vs. "final answer" by use of increasingly higher thresholds.

As pointed out previously, if a planar FTH is illuminated with a fragment f of the original object waveform laterally displaced in the input plane, not only is the fragment image displaced in the output plane but the entire object ghost image is displaced to

remain in register with the fragment image. Ghost image experiments have verified this result by showing reconstruction of ghost images through a displacement of the illuminating fragment, in steps, through a total distance of 0.5 in. [55].

In the usual case, it is assumed that the spatial carrier frequency  $\propto$  (Eq. 3.2.5) is high enough to prevent overlap of the three terms in the output plane. These three terms are obtained by combining the first and second terms of Eq. 4.2.13 as

$$A(y_3) \sim \left\{ [F(y_3) \times F^*(y_3)] \otimes f(y_3 - c) + f(y_3 - c) \right\}$$

$$+ [F(y_3) \otimes f(y_3 - c - b)]$$

$$+ [F^*(y_3) \times f(y_3 + b - c)].$$
4.4.1

From Eq. 4.4.1, the minimum center-to-center spacing between the fingerprint variant  $F(y_1)$  and its code array in the input plane, to avoid overlap in the output plane, can be calculated.

If the latent print, or fragment  $f(y_1-c)$  is assumed to be from the center of the print F then  $c \rightarrow 0$ , and the first term of Eq. 4.4.1 is centered at  $y_3 = 0$ . Denoting the maximum length, in the y-direction of the input plane, of the fingerprint variant by  $L_F$ , and that of the latent print by  $L_f$ , the first term length is  $2L_F+L_f$ . That is, in plane  $P_3$ 

$$\left\{ \left[ F(y_3) \star F^*(y_3) \right] \otimes f(y_3) + f(y_3) \right\} \longrightarrow 2L_F + L_f$$
4.4.2

where  $f(y_3)$  is the image of the latent print and is of length  $L_f$ , and since the autocorrelation of F has length  $2L_f$ ,  $[F(y_3) \not \times F^*(y_3)] \not \otimes f(y_3)$  has a total length of  $2L_F + L_f$ , cocentric with the  $f(y_3)$  length. The length of each sideband is  $L_F + L_f$ , since the stored print of length  $L_F$ 

is convolved and correlated, respectively, with the latent print of length  $L_{\rm f}$ . That is, in plane  $P_{\rm g}$ 

$$[F(y_3) \otimes f(y_3-b)] \longrightarrow L_F+L_f$$

and

$$[F^*(y_3) \times f(y_3+b)] \rightarrow L_F + L_f$$
 4.4.3

This is shown by Figure 23 for minimum separation between the output plane terms. As was shown by Eq. 4.2.14, the code array image complex amplitude in the output plane is produced as a convolution of the code array waveform with the autocorrelation of the reconstructing fragment waveform.

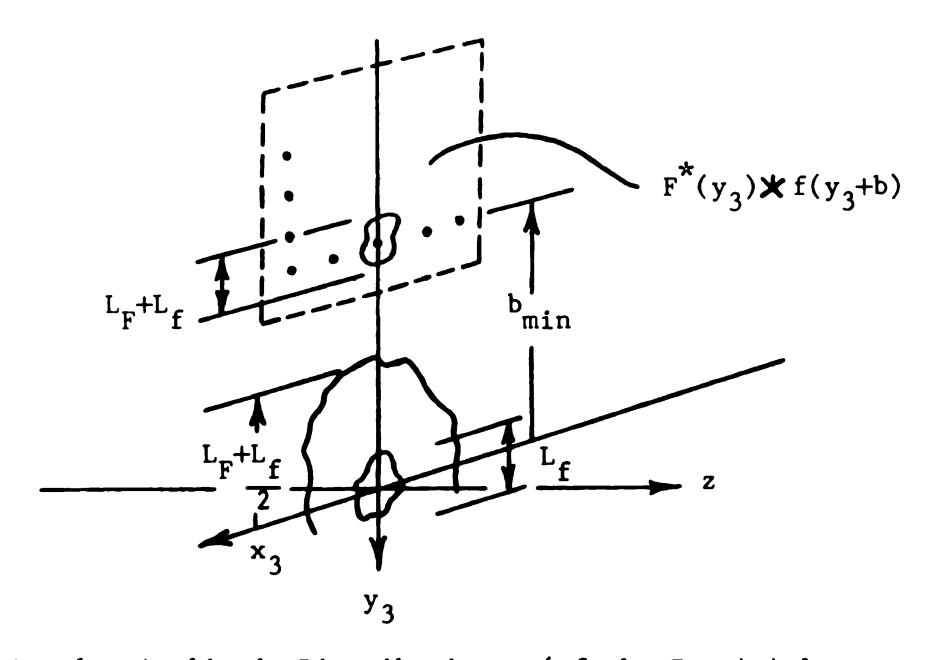


FIGURE 23. Complex Amplitude Distributions, (of the Eq. 4.4.1 terms), in the Output Plane P<sub>3</sub>. (The spatial carrier frequency has to be high enough to avoid overlap of the output terms.)

Therefore, to avoid overlap of the three output terms, the minimum spacing between the center of a fingerprint variant and its nearest array-code point source in the input plane, in the y-direction, is given by

$$b_{min} \ge \frac{3}{2} L_F + L_f$$
 4.4.4

or, since  $\alpha = \sin \alpha / \lambda$  and  $\sin \alpha = b/f_1$ , this requires

or, using the small angle approximation  $\sin \alpha_0 \simeq \alpha_0$ , complete separation is achieved if the tilt of the reference wave is such that

If the latent print size  $L_f$  approaches the stored print size  $L_F$  a higher carrier frequency is required, and is approximately equal to 5/2 ( $L_F/\lambda f_1$ ). It is thus of interest to define the system parameters related to the size, location, and intensity of the fragment, or latent fingerprint input.

The latent fingerprint input is assumed to be located essentially (by eye-measurement) in the same position as the portion of the original fingerprint it represents occupied in the recording of the hologram. This positioning would be performed as part of the input transparency-forming process. Also, as noted on p. 77, the minimum reference beam offset  $b_{\min}$ , in practice, would have to take into account the area surrounding the reconstructing beam direction occupied by the intermodulation term image field.

The relative amount of light in the output varies as a function of the latent fingerprint size. This is clearly illustrated by the output variation between symbols such as 1 and 8. This may result in a cross-correlation coefficient S being larger than the autocorrelation coefficient  $S_k$  for different size fragment inputs. To obtain clear discrimination, normalization of the form indicated by Eq. 3.6.8 may be utilized. From Eq. 4.2.12, this would correspond

to the normalization

$$f_{m'n}(p,q)F_{mn}(p,q)/f_{m'n}(p,q)/2$$
 4.4.7

This compensation can be introduced electronically, after the output code detection. The photodetectors, or the filter itself, can be then biased to compensate for such inequalities of signal energy.

# 4.5 Requirements On the Parameters of a Fourier-Transform Hologram Self-Associative Memory for Successful Retrieval of Stored Data

When considering the practical aspects of applying the FTH self-associative memory as a storage medium for a fingerprint data file, two major problems, other than the basic storage material requirements, are presented: reconstruction positioning tolerances and low diffraction efficiency.

For real-time operation, the frequency plane must be time-shared by a fast change of hologram plates, or filters. Any errors introduced in the placement of the filter then cause the filter to be displaced from its optimum, highest SNR, position (see Section 3.7). The main reconstruction registration concern is accurate placement of the filter (hologram) in the normal direction, or lateral to the optical axis. The permissible static lateral displacement for a performance loss of less than 3 db, assuming uniform N(p,q) , is of the order of  $30\mu$  [59].

The latent fingerprint may also be displaced, in the object plane, from the original print recording position. Registration problems for the latent print input, as well as with the hologram, are solved by automatic alignment. An auxiliary point reference source subhologram is recorded for use in placement error corrections, as pointed out

in Section 4.3.

Another parameter to be considered is that less light flux is diffracted by the later exposure gratings as the number of superposed subholograms increases. The output intensity is found to decrease monotonically with exposure order [67].

The reconstructed beam intensities are not uniform from the superposed subholograms, although constant exposure may be used in recording each layer subhologram. Recording with larger exposure values proportional to increasing order in the recording sequence for each successive subhologram should be utilized to give uniform diffraction efficiency. Prebiasing with uniform light intensity is used to increase the time of the first exposure since the value of the first exposure is small. In a sequence of m superposed exposures, the individual exposure time  $\tau$  is then made proportional to  $\tau$ /<sub>m</sub>. The intensities of the individual exposures are added by the emulsion.

A very small shift in the spectrum centers when recording superposed subholograms is also recommended [8], as a method to alleviate saturation of the photographic emulsion by the low frequency information. This would decrease the noise due to emulsion nonlinearity.

Addressing the uniquely coded superposed subholograms with a latent print allows reconstruction of only one of the subholograms, while the unaddressed subholograms contribute incoherent noise. The SNR degradation for each code point in the image takes the form of a "halo" of noise, produced by (1) cross-correlation between the recalled reference code and the codes representing all other subholograms recorded on the same illumination area, and (2) from the

autocorrelation of the recalled code (Eq. 4.2.14).

To increase discrimination in the face of crosstalk noise in the output among adjacent spatial frequency recorded fingerprints, each fingerprint would be coded using an array of point light sources selected on the basis of Hamming's distance  $D(\beta_1, \beta_2)$  [68]. If it is assumed the code strings, (row) x (column), are of the same length and are expressed as

$$\beta_1 = x_{11}, x_{12}, x_{1N}, x_{21}, \dots, x_{M\times N}, \beta_2 = y_{11}, y_{12}, \dots, y_{1N}, y_{21}, \dots, y_{M\times N}$$

D 
$$(\beta_1, \beta_2) = \sum_{i=1}^{M \times N} \sum_{j=1}^{M \times N} |x_{ij} - y_{ij}| = \text{maximum}$$
 4.5.1

and the Hamming distance is defined as the number of places in which two binary sequences  $m{\beta}_1$  and  $m{\beta}_2$  differ.

As shown by Eq. 4.2.14, the object wave need not be planar or spherical. The only conditions on it are that (1) its Fourier-transform must correlate sharply with itself, where since the Fourier-transform of a plane wave is a point, a plane wave is ideal, and (2) it must extend over the whole subhologram.

For a hologram recording of a plane object wave with a point reference (at an angle  $2\theta$  to one another, Figure 6) the fringe spacing is given by Eq. 3.2.1 as  $a = \frac{\lambda}{2} \sin \theta$ . The recording medium resolution required to record a wave at an angle  $2\theta$  with respect to the reference beam is thus 1/a. To record a hologram at  $6328\text{\AA}$  of a fingerprint variant whose greatest extent  $L_F$  is 10 degrees away from the reference beam requires a resolution of

Holograms at larger angles require a resolution of 2000 to 3000 lines/mm. The Kodak 649-F photographic plate, for example, has a limiting resolution of better than 2000 lines/mm. The hologram resolving power should be twice as large as the limiting resolution for reasonable uniformity of the brightness of the image. With the reference source considered to be at the center of the edge of the object field (Figure 22), permissible print and code beam separation angles of up to 40 degrees are possible. However, as noted previously (p. 32), in order to consider the holograms as plane diffraction gratings the angle between the print beam and the code beam must be of the order of 10 degrees or less. A compromise must be reached between use of the highest separation angle allowed and still have true plane holograms, but large enough to enable discounting of intermodulation noise.

In character recognition, a broadband FTH matched filter can, in general, tolerate a  $\pm$  15% change in scale and a  $\pm$  16 degree change in rotation and still produce an autocorrelation spot response distinguishable from noise [56]. However, performance decreases with increasing departure from nominal, and cross-correlation peak intensities approach that of the autocorrelation.

Since for objects of the same size the low frequencies of the Fourier-transform are approximately the same, it is advantageous for the filter to contain only the higher spatial-frequency components of the object. High selectivity of this type of filter has been demonstrated for continuous-tone photographic objects [69].

<sup>†</sup> See b<sub>min</sub> calculation on p. 87.

A high pass filter, or one that emphasizes the higher spatial frequencies, can be obtained by overexposure of the optical axis area of the hologram recording medium. The central area, which records the low spatial frequencies, is then highly absorbing and diffracts little light in the reconstruction. Very low spatial frequencies represent undiffracted light passing through the open areas of the patterns. This makes up the largest part of the reconstruction transmission, and is not essential for discrimination.

Although the high-pass spatial filter emphasizes edges and corners of an input object, it would have limited use in a finger-print identification system. In this case, there are no relatively large, similar, open unmodulated transparent areas between different print inputs, such as in alphabetic characters. Fingerprints, by virtue of their almost constant-width line structure have a very narrow band-width. Only a very small central region may be considered for overexposure for a fingerprint processing system.

A scale search, which may be necessary in a character recognition application, is simplified here by a predictable range of scale changes. Thus included, in the form of fingerprint variants (Figure 13), are two size changes: smaller and larger, respectively, from "normal."

It is also apparent that optimum image quality must occur within a limited range of reference-to-signal beam power. The choice of the beam ratio k is made on the basis of linearity of recording and hologram efficiency.

For the conventional hologram (see p. 47) the reference wave is two to three times larger in amplitude than the object wave. This is so that the fringe contrast does not extend beyond the linear region of the  $t_A$ -E curve of the photographic emulsion. However, an optimum complex spatial filter can be synthesized beyond the recording emulsion linear region. If the phase spectrum is preserved, a small variation of the amplitude spectrum will not change the first-order impulse response, although emulsion nonlinearity contributes to the background noise.

Nonlinear holograms can be utilized to increase the discrimination ratio (defined by Eq. 3.6.10) [53]. Output autocorrelation intensity measurements, alternatively, indicate a sharp decrease in peak intensity with increasing input pattern rotation angle (relative to the frequency plane) for a nonlinear hologram. The decrease is especially evident after the angle becomes more than 3 degrees, for a given window size in the input movement direction [8].

As recognition selectivity is increased, tolerance to scale changes, or rotations, decreases; therefore, included in the present system are rotational print variants of +6 degrees and -6 degrees as shown in Figure 13. With +6 degree variants, it may be assumed that the latent print orientation will be within +3 degrees of any recorded orientation.

The several (27) subholograms of one fingerprint and its variants are recorded in association with a specific code word in consecutive exposures. This scheme is utilized to obtain a beam ratio of kel, or about equal recording illumination on any subhologram for the print variant and its code word.

Exposure with the normal (center) fingerprint variant of more than one subhologram, to give identical randomly spaced out

subholograms, may also prove useful in achieving higher reconstruction efficiency (see Figure 15).

Over 1000 single point-source objects have been successfully stored in superposition and retrieved, one at a time, with diffuse reference beam addressing [70]. (The reference wave was coded by moving the diffuser between exposures.)

The recording in superposition of a minimum of 10 fingerprints or variants by the use of a point-source array coded reference wave is visualized here for each hologram frame. Diffraction efficiency fluctuates as a function of external vibration, changes in coherence, and emulsion occupation of fringes depending on the order of exposure in the superposition recording. The exact number of possible superpositions would therefore be determined by operational testing.

The power per code bit, or spot, in the output image is given by the total power into the hologram times the hologram efficiency, and is divided by the number of bits (spots) in the code word, or

I each code point in the image = 
$$\frac{I_0 \epsilon}{MxN}$$
 4.5.3

where  $\boldsymbol{\xi}$  = subhologram efficiency,  $I_o$  = reconstruction irradiance, and there are MxN code points.

To find the diffraction efficiency, Eq. 4.2.9 which gives the subhologram amplitude transmittance, is represented as

$$I_{mn} = \left| B + \sum_{i=1}^{N} A_{i} \right|^{2}$$

$$= \left| B \right|^{2} + \sum_{i=1}^{N} \left| A_{i} \right|^{2} + \sum_{i=1}^{N} \left( BA_{i}^{*} + B^{*}A_{i} \right)$$

$$+ \sum_{i=1}^{N} \sum_{v=1}^{N} \left( A^{*}_{v} A_{v} + A_{u} A^{*}_{v} \right)$$

$$(4.5.4)$$

using one-dimensional notation. For superposition of m exposures the intensity is given by

$$I = \sum_{1}^{m} I_{mn}$$
 . 4.5.5

The light diffracted into the image depends directly on the variance of the amplitude transmittance of each subhologram. For linear recording the amplitude transmittance is dependent on the slope of the  $t_A$ -E curve, the average exposure, and the beam ratio [40]. The geometry of the object does not affect the amount of flux diffracted, unless this influences the beam ratio. B in this case is then assumed to represent the average intensity  $\langle B^2 \rangle$  at the subhologram plane due to a fingerprint variant. Each subhologram recording is then represented as a linear multiple exposure hologram.

Regarding each subhologram as the recording of the interference pattern of a digital data beam, i.e., the code word since this is the "data" which is recalled, and a plane reference beam, this being the fingerprint variant beam, the beam ratio is defined by

$$k = \frac{|B|^2}{\sum_{i=1}^{N} |A_i|^2}$$
 4.5.6

The modulation or visibility of the  $N^{th}$  fringe pattern is defined as  $\begin{bmatrix} 40 \end{bmatrix}$ 

$$V_{N} = \frac{I_{max} - I_{min}}{2 \overline{I}}$$
 4.5.7

where  $I_{max}$  and  $I_{min}$  are, respectively the values of the intensity at the maxima and minima of the fringe pattern, and the bias point

is defined as

$$\overline{I} = \frac{I_{\text{max}} + I_{\text{min}}}{2} . 4.5.8$$

From Eq. 3.2.5, it is observed that  $I_{max}$  is obtained when cos[] = +1, and  $I_{min}$  is obtained when cos[] = -1.

Assume that the average exposure is equal to N times the exposure required to record each of the N code points sequentially. The visibility of the  $N^{\mbox{th}}$  fringe pattern is then given by

$$V_{N} = \frac{2K \sqrt{N} |B| |A|}{N |B|^{2} + \sum_{i=1}^{N} |A_{i}|^{2}}$$
4.5.9

neglecting the fourth term of Eq. 4.5.4, and where K is a constant that includes the slope of the  $t_A$ -E curve as well as the optical transfer function of the recording medium, and each of the N code beams has the same intensity  $|A|^2$ , (see p. 83, and also [71]). In terms of the beam ratio, omitting constants, the visibility is expressed as

$$V_{N} = \frac{2 \sqrt{k}}{(1+k) \sqrt{N}}$$
 4.5.10

at an average exposure of  $(1+k)N|A|^2$ .

The diffraction efficiency of the N<sup>th</sup> point of the code word, for fixed average exposure is  $\sim$   $V_N^2$  [41]. Assuming a unit amplitude latent fingerprint reconstruction beam, paralleling Eq. 4.5.3, the first-order intensity of any code point in the output plane codeword image is then, from Eqs. 4.5.10 and 3.4.3, equal to 1/16NM.

If m gratings, each consisting of N single-point gratings, are superposed in consecutive recording on each subhologram the total number of gratings is mN. The visibility of the N $^{\rm th}$  fringe pattern is

now given by

$$V_{N}$$
 for m superpositions = 
$$\frac{2 J k}{(1+k) J N m}$$
 4.5.11

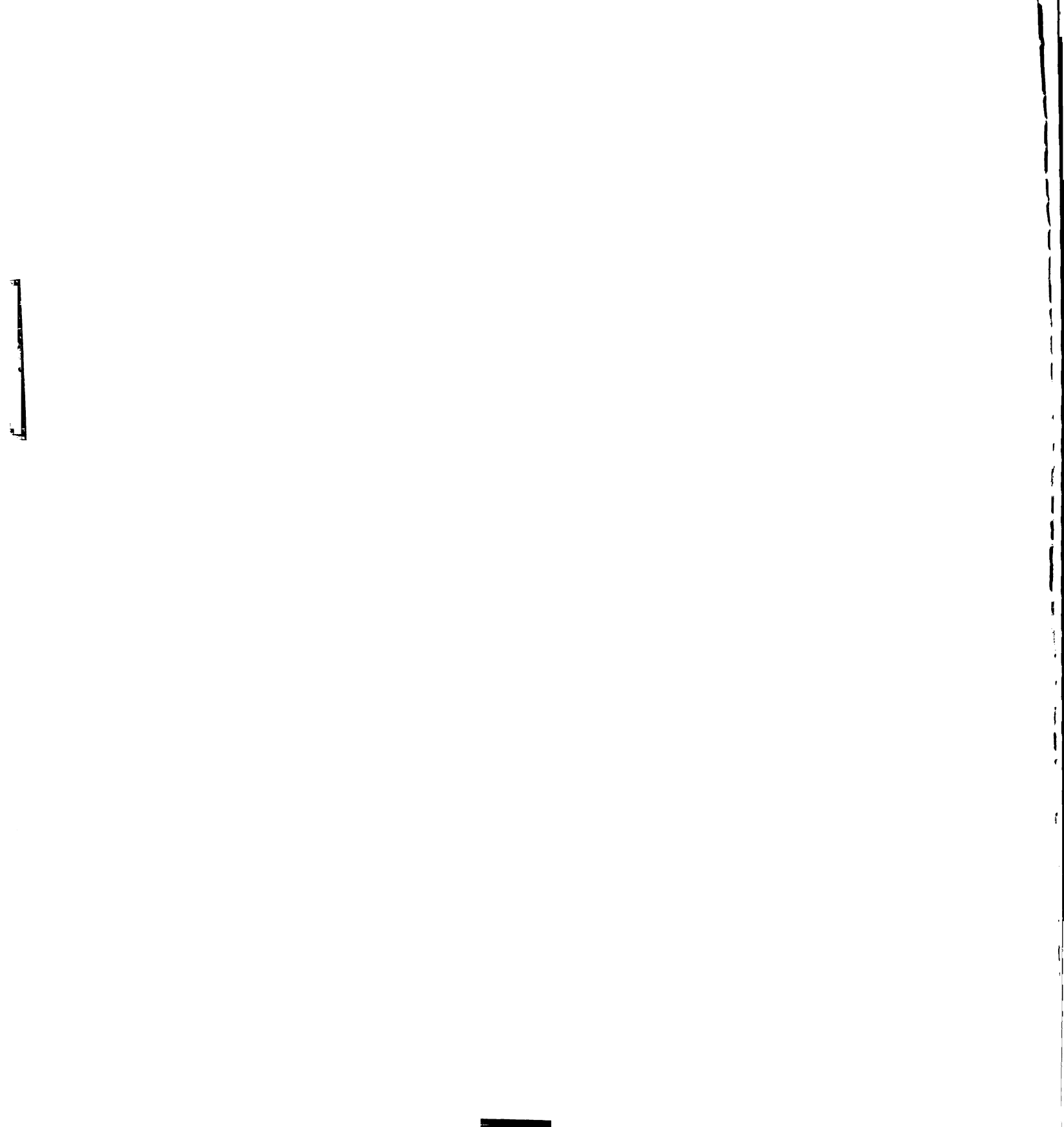
and the first-order intensity of any code point is now equal to  $1/16 \text{ NMm}^2$ .

The maximum diffraction efficiency available from one individual subhologram is reduced by the square of the number of exposures.

This gives low signal intensity in any spot or point image. With an extended array of point sources the limiting noise is due to crosstalk since the noise terms associated with various points overlap.

Forms of image intensification are available [72]. In the present application more than one detection filter is placed on every page (see p. 71). From the above results it is observed that, due to low diffraction efficiency, the readout signal may be submerged in detector noise or scattered by the hologram medium. Image intensification by about a factor of m would be accomplished by the confirmation of a code word from the recording of several identical scattered and variant subholograms for each fingerprint. The summation of contributions by variants of a fingerprint should especially increase processing accuracy with imperfect inputs.

The hololens diffracts about 80% of the incident readout illumination in the desired direction. Based on the hologram diffraction efficiency, and taking into account the efficiency of the optical system, for 10<sup>2</sup> different fingerprints recorded on one hologram in superposition, each of 10<sup>2</sup> code points receives about 10<sup>-7</sup> of the original beam intensity. Photodetector array sensitivity is typically 10<sup>-11</sup> J/code point. The required readout energy of 10<sup>3</sup> ergs



can then be supplied by various laser sources, depending on the readout rate desired. Compensation must also be provided for laser power fluctuations and for fluctuations in diffraction efficiency between different hologram page stores.

The detection window size in the output plane for each code point would be rectangular 3mm x 0.5 mm, consistent with possible input translational displacements, and with detector active area dimensions. Hologram and input positioning errors would be sensed in the output plane by utilization of a coherent fiber optics bundle, to cover the auxiliary spot zone with a diameter of 3mm, and one fiber diameter of 10  $\mu$ .

## 4.6 Summary of Design Considerations

Negative ridge fingerprint size, rotation, and pressure variants are recorded in the form of near-Fourier-transform subholograms. The self-associative holographic memory is formed by fly's-eye lens point-source array extended-reference coding, and superposition storage of different fingerprints by spatial frequency multiplexing. Code differentiation is optimized by use of Hamming's distance. The spatial carrier frequency is selected on the basis of obtaining planar recording as well as noninterference with the intermodulation terms. Prebiasing of the photographic film memory medium, and longer exposure times for successive superposed recording gives uniform diffraction efficiency. The diffraction efficiency is found to be inversely proportional to the square of the number of superpositions. A small shift of the spectrum centers is used to avoid overexposure of the low frequency area of each subhologram.

A code (ghost) image is recalled from the self-associative holographic memory by spatial-frequency-plane filtering with a test (latent) fingerprint input. The match/no match decision result of a fingerprint file search is then realized by intensity thresholding of the code images. A hololens is utilized to provide simultaneous reconstruction illumination of all subholograms in one memory frame. Together with the recording geometry, this gives output plane superposition of the variant subhologram diffracted code images. In the search process, automatic alignment of the holograms (filters), in the frequency plane of the spatial filtering system, is accomplished by utilizing an auxiliary point-reference recording. Maximum brightness of the reconstruction image of this point source indicates correct filter positioning. Compensation for any input, latent fingerprint, translational position changes is accomplished by observing the corresponding displacement of the auxiliary point image in the output plane.

#### CHAPTER V

## GENERAL SUMMARY, CONCLUSIONS, AND FUTURE RESEARCH

This dissertation has described a digital computer-controlled, real-time, coherent optical processor. Latent fingerprints would be identified by matching against a card-changeable, self-associative, holographic memory fingerprint file. The memory is termed as "self-associative" and is a memory in which recall is by ghost imaging, or code transformation. The technique utilizes extended-reference-source coding, and subhologram storage of fingerprints and their variants. Spatial frequency multiplexing is used to maximize output discrimination with superposed consecutive-exposure recording.

It is assumed that the input to the system, the latent print, is in transparency form. The stored prints would be in the form of near-Fourier-transform holograms. The described technique is based on optical spatial filtering, and a standard FTH processor is basic to the concept. Projection of the latent print image into the input plane and the holograms, or filters, into the frequency plane would be accomplished by use of light modulation devices. Rapid access to the file, possibly by means of a fingerprint reader, is considered a primary requirement.

The method discussed is intended to be effective independent of the particular holographic memory medium utilized. Parameters examined can be transferred to other materials as required. For purposes of discussion, however, photographic film storage in the form of plane amplitude holograms is assumed. Also, an array of spatially separate

plane holograms, as considered here, has the advantage over more elegant volume storage in that it can be realized with currently available recording materials.

Several pressing problems exist in holographic memory design.

Among them is the need for a read/write storage medium, a storage medium with high hologram diffraction efficiency, and techniques for mass production of holograms. In general, it is concluded that for a fingerprint identification application, higher efficiency should be the primary research area.

It is pointed out that the system-defining parameters are closely related. The important parameters are shown to be the beam offset angle, the beam ratio, reconstruction positioning accuracies, and diffraction efficiency.

It is concluded that an offset angle of the order of 10 degrees and a beam ratio of  $k \approx 1$  are optimum for self-associative recording. In the reconstruction process, hologram lateral positioning accuracies are very critical. However, automatic alignment is possible by use of auxiliary point reference sources.

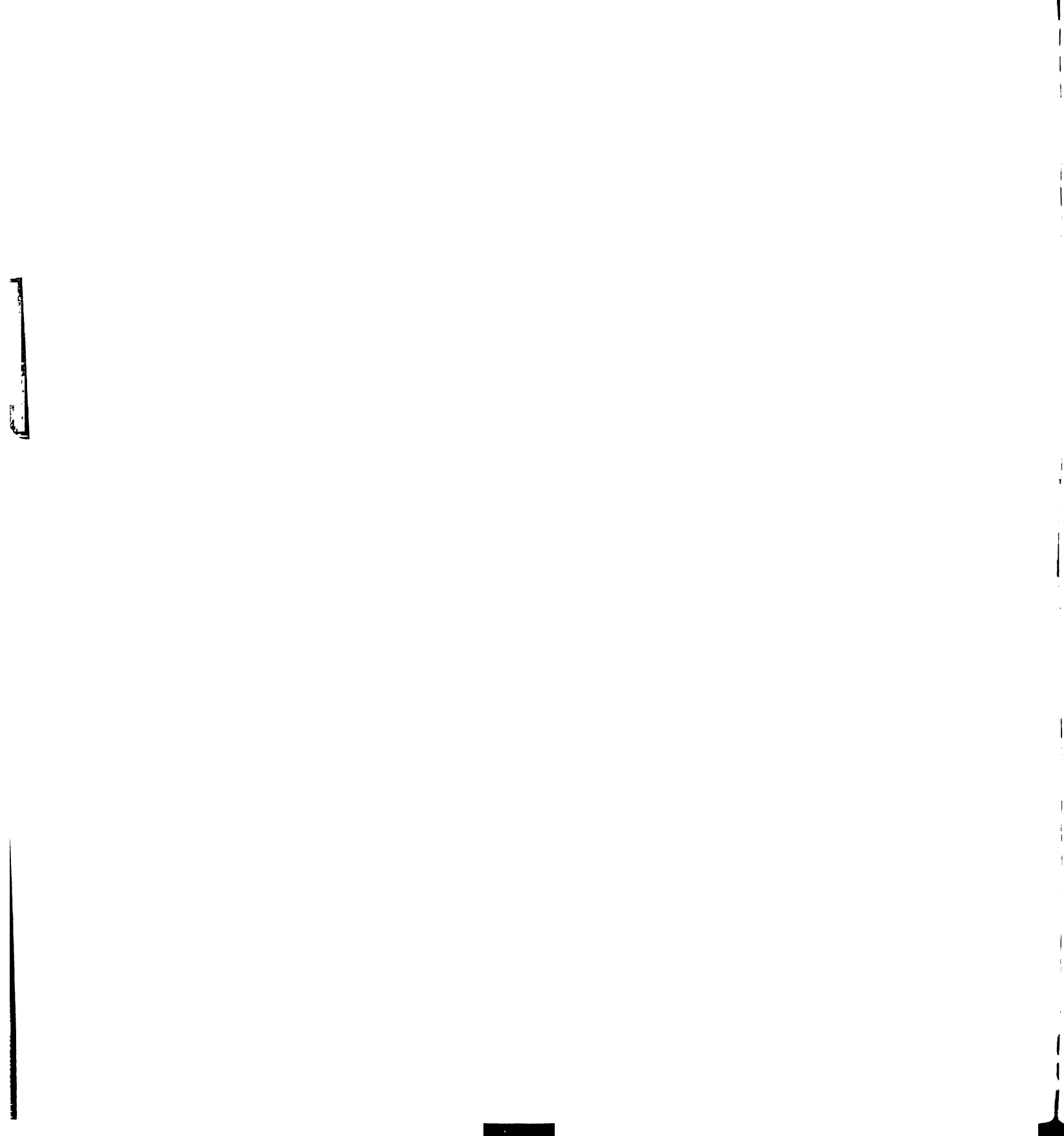
Diffraction efficiency is found to be equal to 1/16MNm<sup>2</sup>, with some output intensification taking place due to the superposition of code images contributed by the recorded fingerprint variants. Also, compensation has to be introduced to provide for the different amounts of energy due to variations in latent print size.

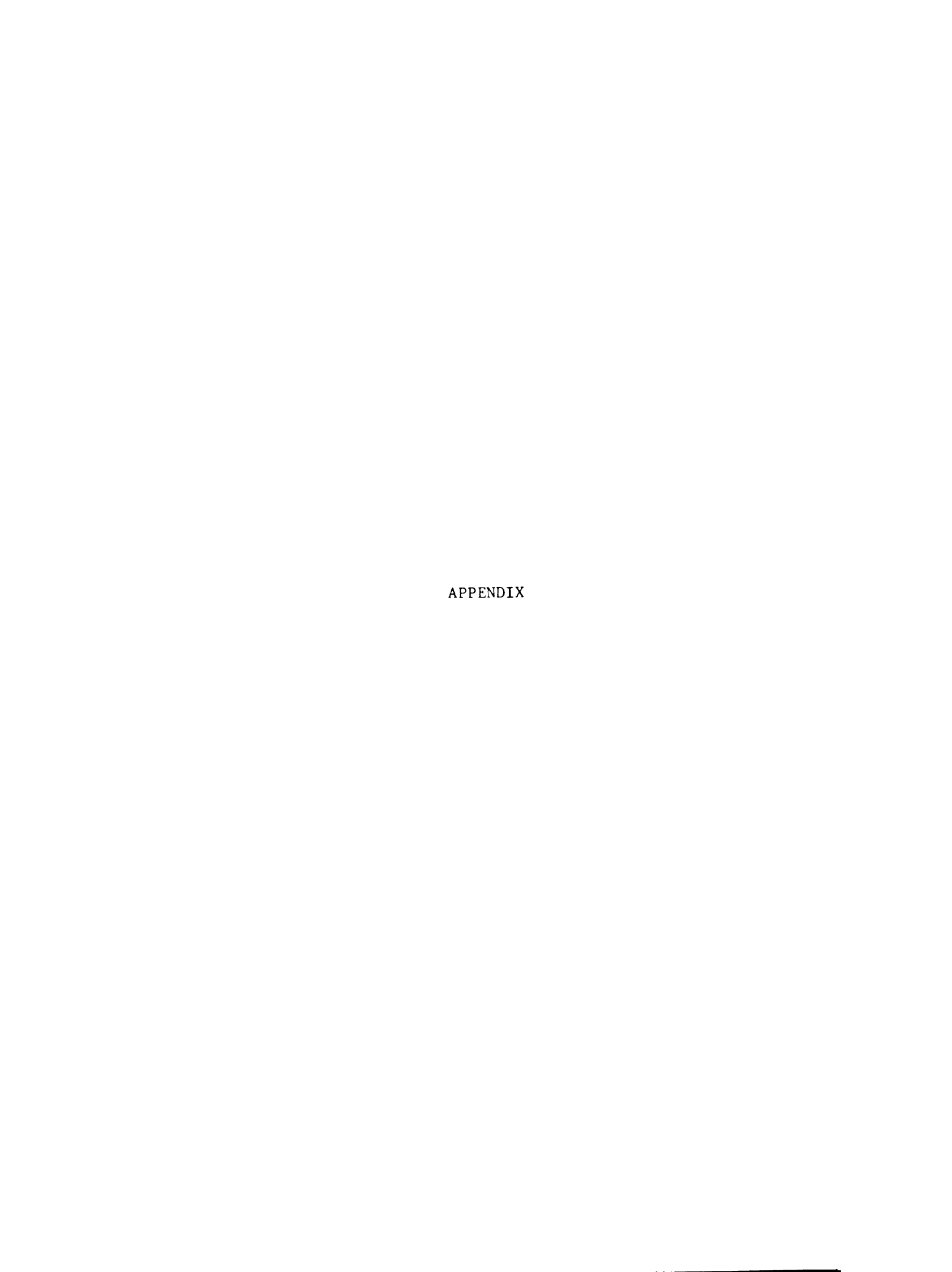
The proposed self-associative holographic storage technique has the capability to increase file-search result accuracy, in terms of such criteria as correct match or correct dismissal, when compared to previously considered methods of holographic fingerprint identification.

Identification is possible even if the input, the latent print, is imperfect, or if only a partial latent print is available. High discrimination ratios may be obtained by utilizing multiple discriminant functions based on (1) the use of multiple detection filters formed by storage of fingerprint variants, (2) spatial-frequency multiplexed output discrimination, (3) error-correcting coding, (4) image intensity, and (5) a maximum number of code points above threshold.

Future research would involve experimental development and operational testing. The possibility of translating the code for each print from binary to Henry classification code might be considered. Digital computer work could also be performed to arrive at an automated method for obtaining fingerprint pressure variants, from scanning a basic fingerprint.

Other application areas for this technique are in biological specimen identification for pathological diagnosis, and for automating white blood cell identification. Inputs in these cases would be compared against a library of microscope-slide standards.







#### APPENDIX

#### VARIATIONS ON THE DESCRIBED SYSTEM

No two fingerprints from the same finger ever turn out exactly the same. Peak correlation voltages that are found in the output of fingerprint matching systems are actually cross-correlation voltage peaks, not autocorrelation peaks. As expressed in Chapter 2, p. 21, size, rotation, and pressure variants (see Figure 13) of each fingerprint are therefore stored along with the fingerprint.

In the described system no pre-processing of the latent fingerprint (transparency) before the matching step is required in the identification procedure. A disadvantage is that some storage density is sacrificed, when compared to storing fingerprints without variants.

At least two variations are possible on the latent fingerprint identification scheme presented here. One variation involves processing the latent print to give rotations, stretchings, etc. All the latent derived variants would be recorded on one transparency. This transparency is then placed in the input, and all variants are processed simultaneously. The other variation deals with normalizing the stored as well as the latent prints to some given standard.

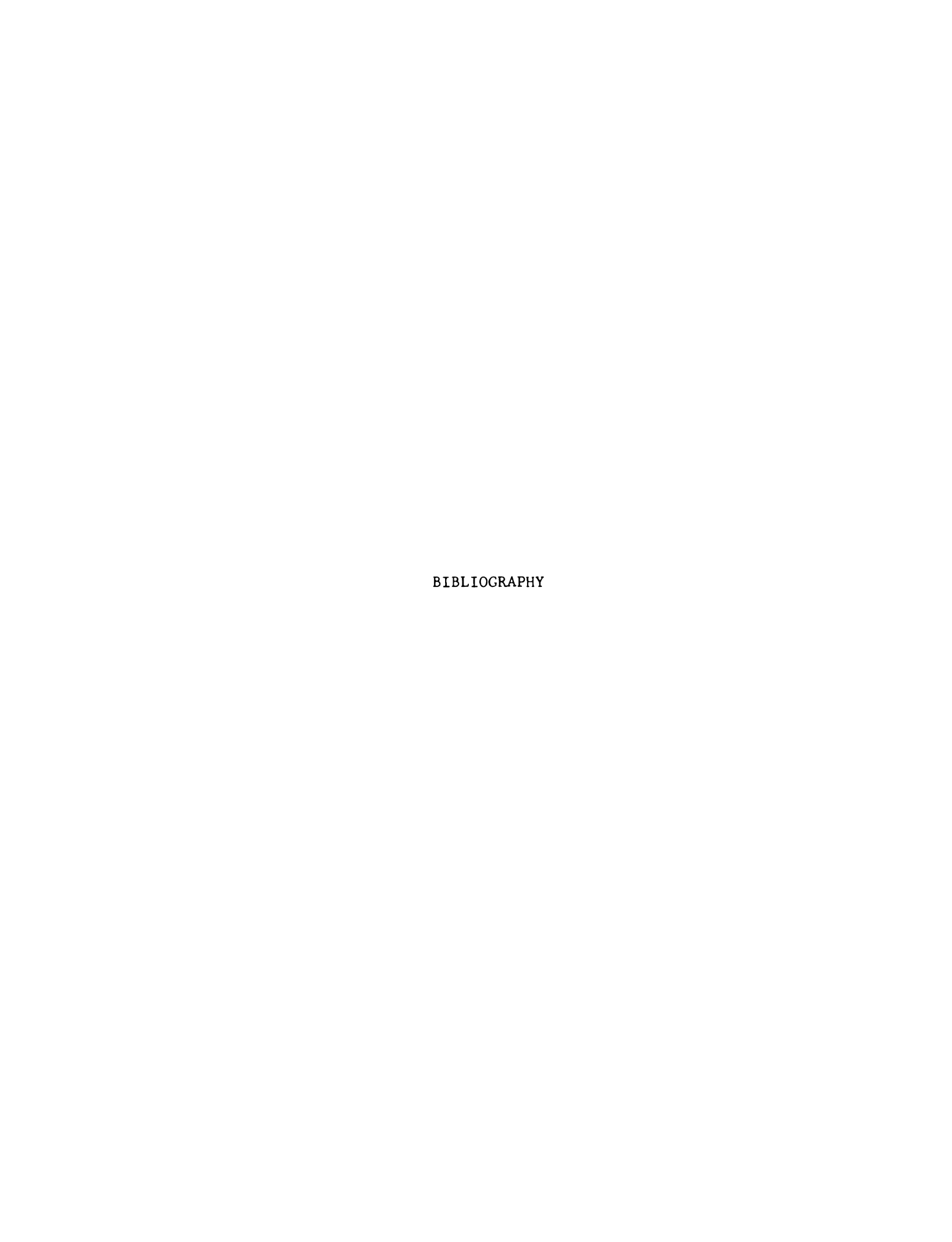
Alphabetic characters have to be recognized before full normalization can take place. A fingerprint, on the other hand, has a unique pattern which can be processed to eliminate most of the undesirable noise. The fingerprint may be interpreted to correct for imperfections (see p. 73) and to generate idealized ridge widths and spacings by ridge tracing. Topological features would remain

unchanged.

It must be determined if an interpretation system can be produced to distinguish the latent print from other superimposed prints, and from the background noise due to the surface structure from which the latent print was "lifted." Also, coherent optical correlation utilizes the whole shape of the ridges, and not just the detailed characteristic points. Normalization effects must be determined on the ratio of true correlation voltage to the maximum false correlation voltage.

Latent fingerprints may not be readable by automatic fingerprint reader equipment for purposes of classification, due to their
frequently poor quality. Two questions are to be answered when
proposing to form variants from the latent print: first, can the
latent print be processed to form variants considering the probable
fragmentary nature of the latent print, and second, can a real-time
fingerprint identification system tolerate the possibly extensive
pre-processing required to form the latent print variants?

The described latent fingerprint processing technique utilizing stored variants allows the use of variants without appreciable loss in total system efficiency. The contributions of all variants to the identification are summed, resulting in image intensification, and in increased identification accuracy with imperfect inputs.



### **BIBLIOGRAPHY**

- vanHeerden, P. J., "A New Optical Method of Storing and Retrieving Information," and "Theory of Optical Information Storage in Solids," <u>Applied Optics</u>, Vol. 2, pp. 387-392, and pp. 393-397, April, 1963.
- 2. Stroke, G. W., "An Introduction to Coherent Optics and Holography," Chapters 5, 6, 2nd Ed., Academic Press, New York, 1969.
- 3. Collier, R. J., and Pennington, K. S., "Ghost Imaging By Holograms Formed in the Near Field," Applied Physics Letters, Vol. 8, No. 1, pp. 44-46, January, 1966.
- 4. Kohonen, T., "Correlation Matrix Memories," submitted to <u>IEEE</u>
  <u>Trans. on Computers</u> on November 23, 1970.
- 5. Nakajima, M., Morikawa, T., and Sakurai, K., "Automatic Character Reading Using a Holographic Data Processing Technique," Applied Optics, Vol. 11, No. 2, pp. 362-371, February, 1972.
- 6. Gabor, D. and Stroke, G. W., "Holography and Its Applications," Science Journal, pp. 40-47, June, 1965.
- 7. Gabor, D., "Character Recognition by Holography," Nature, Vol. 208, pp. 422-423, October 30, 1965.
- 8. Collier, R. J., Burckhardt, C. B., and Lin, L. H., "Optical Holography," Chapter 14, Academic Press, New York, 1971.
- 9. Damon, R. W., McMahon, D. H., and Thaxter, J. B., "Materials for Optical Memories," <u>Electro-Optical Systems Design</u>, pp. 68-77, August, 1970.
- 10. Caulfield, H. J., and Lu, S., "The Applications of Holography," John Wiley & Sons, New York, 1970.
- 11. Bordogna, J., Keneman, S. A., and Amodei, J. I., "Recyclable Holographic Storage Media," <u>RCA Review</u>, Vol. 33, pp. 227-247, March, 1972.
- 12. Nisenson, P., and Iwasa, S., "Real Time Optical Processing With Bi<sub>12</sub>SiO<sub>20</sub> PROM," Applied Optics, Vol. 11, pp. 2760-2767, December, 1972.

- 13. Bridges, C. B., "Practical Fingerprinting," Funk and Wagnalls Company, Inc., New York, 1942.
- 14. Hankley, W. J., and Tou, J. T., "Automatic Fingerprint Interpretation and Classification Via Contextual Analysis and Topological Coding, in "Pictorial Pattern Recognition," (Cheng, G. C., Ledley, R. S., Pollock, D. K., and Rosenfeld, A., Eds.) pp. 411-456, Thompson, 1968.
- 15. Technical Report No. 7, "Satellite Transmission of Fingerprint Images-The Results of a Feasibility Experiment," Project SEARCH Technology Committee, California Crime Technological Research Foundation, June, 1972.
- 16. DeWolf, N., "Speed Kills," EEE, August, 1970.
- 17. Anderson, L. K., "Holographic Optical Memory For Bulk Data Storage," Bell Laboratories Record, pp. 319-325, November, 1968.
- 18. Anderson, L. K., "High Capacity Holographic Optical Memory," Microwaves, pp. 60-66, March, 1970.
- 19. Rajchman, J. A., "An Optical Read-Write Mass Memory," Applied Optics, Vol. 9, No. 10, pp. 2269-2271, October, 1970.
- 20. Ramberg, E. G., "Holographic Information Storage," RCA Review, Vol. 33, pp. 5-53, March, 1972.
- 21. Thompson, B. J., and Parrent, Jr., G. B., "Holography," <u>Science Journal</u>, pp. 3-10, January, 1967.
- 22. Metherell, A. F., "Holography With Sound," Science Journal, pp. 57-62, November, 1968.
- 23. Collier, R. J., "Some Current Views on Holography," <u>IEEE Spectrum</u>, pp. 67-73, July, 1966.
- 24. Leith, E. N., and Upatnieks, J., "Wavefront Reconstruction With Diffused Illumination and Three-Dimensional Objects," <u>J. Opt. Soc. Am.</u>, Vol. 54, No. 11, November, 1964.
- 25. Leith, E. N., Kozma, A., Upatnieks, J., Marks, J., and Massey, N., "Holographic Data Storage in Three-Dimensional Media," Applied Optics, Vol. 5, No. 8, August, 1966.
- 26. Leith, E. N., and Upatnieks, J., "Reconstructed Wavefronts and Communication Theory," <u>J. Opt. Soc. Am.</u>, Vol. 52, pp. 1123-1130 October, 1962.
- 27. Friesem, A. A., and Roberts, H. N., "Investigation of Optical Memory Techniques," Paper presented at NASA Conf. Holographic Instrumentation Applications, NASA Ames Research Center, January, 1970.

- Vilkomerson, D. H. R., Mezrich, R. S., and Bostwick, D. I., "Holographic Read-Only Memories Accessed by Light-Emitting Diodes," <u>Proc. Fall Joint Computer Conference</u> 33, pp. 1197-1204, 1968.
- 29. Sakaguchi, M., Nisida, N., and Nemoto, T., "A New Associative Memory System Utilizing Holography," <u>IEEE Trans. on Computers</u>, C-19, pp. 1174-1181, December, 1970.
- 30. Weinberger, H. and Almi, V., "Interference Method for Pattern Recognition," Applied Optics, Vol. 10, No. 11, pp. 2482-2487, November, 1971.
- 31. Horvath, V. V., Holeman, J. M., and Lemmond, C. Q., "Holographic Technique Recognizes Fingerprints," <u>Laser Focus</u>, pp. 18-23, June, 1967.
- 32. Tsujiuchi, J., Matsuda, K., and Takeya, N., "Correlation Techniques By Holography and its Application to Fingerprint Identification," in "Applications of Holography," (Barrekette, E. S., Kock, W. E., Ose, T., Tsujiuchi, J., and Stroke, G. W., Eds.), pp. 247-258, Plenum Press, New York, 1971.
- 33. Technical Report No. 6, "An Experiment To Determine The Feasibility of Holographic Assistance To Fingerprint Identification," Project SEARCH Technology Committee, California Crime Technological Research Foundation, June, 1972.
- 34. Goodman, J. W., "Introduction to Fourier Optics," McGraw-Hill, New York, 1968.
- 35. Tanaka, S., Kato, H., Ishihara, S., and Yatagai, T., "Pattern Classification Using Correlation With Random Masks-An Optical Papa Device," ibid [32], pp. 229-245.
- Armitage, J. D., and Lohman, A. W., "Character Recognition by Incoherent Spatial Filtering," <u>Applied Optics</u>, Vol. 4, No. 4, pp. 461-467, April, 1965.
- 37. Trabka, E. A., and Roetling, P. G., "Image Transformations for Pattern Recognition Using Incoherent Illumination and Bipolar Aperture Masks," J. Opt. Soc. Am., Vol. 54, No. 10, pp. 1242-1252, October, 1964.
- 38. VanderLugt, A., "Signal Detection By Complex Spatial Filtering,"
  IEEE Trans. on Information Theory, IT-10, pp. 139-145, April, 1964.
- 39. VanderLugt, A., "Practical Considerations for the Use of Spatial Carrier-Frequency Filters," <u>Applied Optics</u>, Vol. 5, No. 11, pp. 1760-1765, November, 1966.
- 40. Smith, H. M., "Principles of Holography," John Wiley and Sons, Inc., 1969.

- 41. Friesem, A. A., Kozma, A., and Adams, G. F., "Recording Parameters of Spatially Modulated Coherent Wavefronts," Applied Optics, Vol. 6, No. 5, pp. 851-856, May, 1967.
- 42. The U. of Michigan Engineering Summer Conferences, "Fundamentals and Applications of Optical Data Processing and Holography," Vol. 1, July 20-31, 1970.
- 43. Tufte, O. N., and Chen, D., "Optical Memories: Controlling the Beam," <u>IEEE Spectrum</u>, pp. 48-53, March, 1973.
- 44. Ramberg, E. G., "The Hologram-Properties and Applications," <u>RCA</u> Review, pp. 467-499, December, 1966.
- 45. Stewart, W. C., Mezrich, R. S., Cosentino, L. S., Nagle, E. M., Wendt, F. S., and Lohman, R. D., "An Experimental Read-Write Holographic Memory," RCA Review, Vol. 34, pp. 3-44, March, 1973.
- 46. Friesem, A. A., and Walker, J. L., "Experimental Investigation of Some Anomalies in Photographic Plates," Applied Optics, Vol. 8, No. 7, pp. 1504-1506, July, 1969.
- 47. Lee, Wai-Hon, "Effect of Film-Grain Noise on the Performance of Holographic Memory," J. Opt. Soc. Am., Vol. 62, No. 6, pp. 797-801, June, 1972.
- 48. Lee, Wai-Hon, and Greer, M. O., "Noise Characteristics of Photographic Emulsions Used for Holography," <u>J. Opt. Soc. Am.</u>, Vol. 61, pp. 402-409, March, 1971.
- 49. Mikaeliane, A. L., Bobrinev, V. I., Naumov, S. M., and Sokolova, L. Z., "Design Principles of Holographic Memory Devices," <u>IEEE</u>

  <u>Journal of Quantum Electronics</u>, Vol. QE-6, No. 4, pp. 193-198,

  <u>April</u>, 1970.
- 50. Burckhardt, C. B., "Storage Capacity of an Optically Formed Spatial Filter for Character Recognition," Applied Optics, Vol. 6, No. 8, pp. 1359-1366, August, 1967.
- 51. Brandt, G. B., "Techniques and Applications of Holography," Electro-Technology, pp. 53-72, April, 1968.
- 52. Longuet-Higgins, H. C., Willshaw, D. J., and Buneman, O. P.,
  "Theories of Associative Recall," Quarterly Review of Biophysics,
  (Printed in Great Britain), Vol. 3, No. 2, pp. 223-244, 1970.
- 53. VanderLugt, A., and Rotz, F. B., "The Use of Film Nonlinearities In Optical Spatial Filtering," Applied Optics, Vol. 9, No. 1, pp. 215-222, January, 1970.
- 54. Friesem, A. A., Tompkins, E. N., and Hoffman, G. E., "Holographic Application In High Density Document Storage and Retrieval," SPIE Annual Technical Symposium Proceedings, Vol. 3, 1971.

- 55. Pennington, K. S., and Collier, R. J., "Hologram-Generated Ghost Image Experiments," <u>Applied Physics Letters</u>, Vol. 8, No. 1, pp. 14-16, January, 1966.
- 56. VanderLugt, A., Rotz, F. B., and Klooster, A., Jr., "Character-Reading By Optical Spatial Filtering," in "Optical and Electro-Optical Information Processing," (J. T. Tippett, et al., Eds.) pp. 125-141, Mass. Inst. Technology Press, Cambridge, Mass., 1965.
- 57. Lange, F. H., "Correlation Techniques," p. 15, p. 19, D. Van Nostrand Co., Inc., Princeton, New Jersey, 1966.
- 58. Horner, J. L., "Do Computations At the Speed of Light," <u>Electronic</u> Design, Vol. 16, No. 23, pp. 60-68, November, 1968.
- 59. VanderLugt, A., "The Effects of Small Displacement of Spatial Filters," Applied Optics, Vol. 6, No. 7, pp. 1221-1225, July, 1967.
- 60. Stroke, G. W., Restrick, R., Funkhouser, A. and Brum, D., "Resolution-Retrieving Compensation of Source Effects By Correlative Reconstruction In High-Resolution Holography," pp. 274-275, Physics Letters, Vol. 18, No. 3, September, 1965.
- 61. Lee, T. C., and Zook, J. D., "Cascade Operation of Light Beam Deflectors by Fly's Eye Lenses," Applied Optics, Vol. 10, No. 8, pp. 1965-1966, August, 1971.
- 62. Lee, T. C., "MuBi Films as Potential Storage Media in Holographic Optical Memories, Applied Optics, Vol. 11, No. 2, pp. 384-389, February, 1972.
- 63. Takeda, Y., Oshida, Y., and Miyamura, Y., "Random Phase Shifters for Fourier Transformed Holograms," Applied Optics, Vol. 11, No. 4, pp. 818-822, April, 1972.
- 64. Groh, G., "Multiple Imaging by Means of Point Holograms," Applied Optics, Vol. 7, No. 8, pp. 1643-1644, August, 1968.
- 65. Banner, C. S., "The State of Development of the FBI's Automatic Fingerprint Identification System," <u>Proceedings of the International Symposium on Criminal Justice Information and Statistics Systems</u>, pp. 407-422, New Orleans, Louisiana, October 3-5, 1972.
- 66. Lee, T. C., and Gossen, D., "Generalized Fourier-Transform Holography and Its Applications," <u>Applied Optics</u>, Vol. 10, No. 4, pp. 961-963, April, 1971.
- 67. Akahori, H., and Sakurai, K., "Information Search Using Holography," Applied Optics, Vol. 11, No. 2, pp. 413-415, February, 1972.
- 68. Abramson, N., "Information Theory and Coding," p. 163, McGraw-Hill, New York, 1963.

- 69. Raso, D. J., "Simplified Method to Make Hologram Filters for Target Recognition," <u>J. Opt. Soc. Am.</u>, Vol. 58, pp. 432-433, March, 1968.
- 70. LaMacchia, J. T., and White, D. L., "Coded Multiple Exposure Holograms," Applied Optics, Vol. 7, No. 1, pp. 91-94, January, 1968.
- 71. LaMacchia, J. T., and Vincelette, C. J., "Comparison of the Diffraction Efficiency of Multiple Exposure and Single Exposure Holograms," Applied Optics, Vol. 7, No. 9, September, 1968.
- 72. Blackmer, L. L., VanKerkhove, A. P., Baldwin, R. E., and Stultz, K. F., "Some Aspects of Multiple-Beam Interference Techniques in Digital Data Recording," <u>Applied Optics</u>, Vol. 9, No. 12, December, 1970.

#### REFERENCES

Brown, B. R., and Lohman, A. W., "Complex Spatial Filtering With Binary Masks," <u>Applied Optics</u>, Vol. 5, No. 6, pp. 967-969, June, 1966.

Brown, B. R., and Lohman, A. W., "Computer-generated Binary Holograms," IBM J. Res. Develop., pp. 160-168, March, 1969.

Crofut, W. A., "Design Techniques of a Delay-Line Content-Addressed Memory," <u>IEEE Trans.</u> on <u>Electronic Computers</u>, Vol. EC-15, No. 4, August, 1966.

DeBitetto, D. J., and Dalisa, A. L., "Holographic Image Intensification by Superposition of Holograms," <u>Applied Optics</u>, Vol. 9, No. 11, pp. 2588-2590, November, 1970.

Goodman, J. W., "An Introduction to the Principles and Applications of Holography," Proc. of the IEEE, Vol. 59, No. 9, pp. 1292-1304, September, 1971.

Hanlon, A. G., "Content-Addressable and Associative Memory Systems," IEEE Trans. on Electronic Computers, Vol. EC-15, No. 4, August, 1966.

Hobbs, L. C., "Present and Future State-of-the-Art In Computer Memories," <u>IEEE Trans.</u> on <u>Electronic Computers</u>, Vol. EC-15, No. 4, August, 1966.

Lee, W. H., "Sampled Fourier Transform Hologram Generated by Computer," Applied Optics, Vol. 9, No. 3, pp. 639-643, March, 1970.

Lohman, A. W., and Paris, D. P., "Computer Generated Spatial Filters for Coherent Optical Data Processing," <u>Applied Optics</u>, Vol. 7, No. 4, pp. 651-655, April, 1968.

Lohman, A. W., Paris, D. P., and Werlich, H. W., "A Computer Generated Spatial Filter, Applied to Code Translation," The U. of Michigan Engineering Summer Conferences "Fundamentals and Applications of Optical Data Processing and Holography," Vol. 2, July 20-31, 1970.

McCoy, M. R., "MOS Read-Only Memories," EEE, August, 1970.

Nishida, N., and Sakaguchi, M., "Improvement of Nonuniformity of the Reconstructed Beam Intensity from a Multiple-Exposure Hologram," Applied Optics, Vol. 10, No. 2, pp. 439-440, February, 1971.

Preston, K., Jr., "A Comparison of Analog and Digital Techniques for Pattern Recognition," <u>Proc. IEEE</u>, Vol. 60, No. 10, pp. 1216-1231, October, 1972.

Rosenfeld, A., "Picture Processing by Computer," Academic Press, 1969.

VanderLugt, A., "Design Relationships for Holographic Memories," Applied Optics, Vol. 12, No. 7, pp. 1675-1685, July, 1973.

Yu, F. T. S., and Kung, G. C., "Synthesis of Optimum Complex Spatial Filters," J. Opt. Soc. Am., Vol. 62, pp. 147-149, January, 1972.

